Muritala Oluwaseun Arowolo

Numerical Modelling of Natural Fibres Reinforced Thermoplastic Composites

Master Dissertation
European Master Advanced Structural Analysis and Design using Composite Materials

Work developed under the supervision of
Doctor Wiyao-Leleng Azoti

Funded by the European Union

July 2023

DECLARATION

Name: Muritala Oluwaseun Arowolo

Email: oluwaseunarowolo9@gmail.com **Phone number:** +34-697 239 858

Citizen Card Number: XXXXXXXXXXXXXXXXXXXXX

Title of the Thesis: Numerical Modelling of Natural Fibres Reinforced Thermoplastic Composites

Supervisor:

Doctor Wiyao-Leleng Azoti

Year of Conclusion: 2023

Master Course in Advanced Structural Analysis and Design using Composite Materials

University of Toulouse III Paul Sabatier, 17/07/2023

Signature:

ACKNOWLEDGEMENTS

It feels surreal that the rough, patchy, and intensive study journey that began in Girona has finally come to an end in Toulouse. Apparently, this would not have been possible without Almighty God, my family, my friends, my indefatigable professors, and the MSc-FRP scholarship board.

I want to thank God for bringing me this far by blessing me with strength, resilience, and faith to push through. Alhamdulillah!! I also thank my family for their support, particularly my dad, Marouf Arowolo; uncle Prof. Toyin Arowolo; my aunt and her loving husband, Wale & Bola Senbore; my siblings and my amazing sisters Titilayo Bisiolu, Bola Adesanya, and Opeyemi Arowolo for their unwavering support. I cannot but thank my friends, Charles Adeshina, Abdulmaliq Alawode, and Ajiboye Bello for their brotherly support. Without you guys, obviously, the journey would have been more difficult. I thank you. Mahmoud Abdulhak, Atef Sawalmeh, Dagmawi, Fatemeh, Sarath Das, Radouan, Renan, and others, it was really great meeting and learning with you. Thank you. Special shout-out to my sweet friends Idowu Bisiriyu and Belinda Kejeh, thank you for being a family. I miss you guys!! I also appreciate my mentors Engr. Muibat Adeshina and Prof. Muyideen Abdulkareem for their all-time supports.

I appreciate Prof. Jose Sena Cruz, Prof. Cristina Barris, and the entire distinguished professors in AMADE. Thank you all for the help and impacting us with world-class knowledge. I appreciate Prof. Bruno Castanie for all the support. I also thank all the distinguished professors from INSA, UMINHO, and UNINA. Lastly, I thank the entire MSc-FRP scholarship board for the scholarship awarded to me. I do not take it for granted.

I specially thank Professor Wiyao Azoti, my thesis supervisor. I appreciate the uncommon guidance, support, and patience throughout the period of this work. You are more than a professor to me. Thank you so much for all you did. Without you, this work would not have been possible. I would not be able to thank you enough, and I pray God Almighty to rewards you abundantly.

I dedicate this work to my late mother, Fausat Arowolo. Thank you for helping me build the good foundation that has seen me through life up until this moment and beyond. Resilience to take up any challenge, stand shoulder to shoulder with peers across the world. May your soul continue to rest. I miss you, and I love you!

Thèse Modélisation numérique des composites thermoplastiques renforcés de fibres naturelles

RESUME

La demande mondiale croissante de durabilité dans toutes les sphères de l'activité humaine s'est considérablement infiltrée dans l'industrie des composites. Cette aspiration a conduit à la recherche de fibres bio-sourcées comme alternative aux fibres synthétiques. En outre, la recyclabilité et la gestion de la fin de vie des composites sont à l'origine de l'intensification des recherches sur les composites thermoplastiques renforcés par des fibres naturelles. Afin d'améliorer l'adoption industrielle des biocomposites, des approches de modélisation micromécanique et multi-échelle ont été utilisées pour caractériser le comportement thermomécanique des composites thermoplastiques (matrice en polypropylène) renforcés par quatre fibres naturelles différentes : lin, végétal-technique, bois-force et un hybride de lin et végétal-technique, pour une fraction volumique de fibre (V_f) de 0,2 et des rapports d'aspect de 37,5, 9,1, 17,5 et 18,5 respectivement pour des orientations de fibres aléatoires et alignées.

La microstructure de chaque composite a été modélisée à l'aide de DIGIMAT, un logiciel commercial de micromécanique, et les analyses numériques ont été effectuées à l'aide du logiciel Abaqus (Dassault System). Pour valider les résultats numériques, une modélisation analytique basée sur le schéma d'homogénéisation Mori-Tanaka a été utilisée. Les résultats thermomécaniques obtenus ont montré une bonne concordance entre les approches numériques et analytiques pour les orientations aléatoires et alignées des fibres. En outre, les résultats mécaniques obtenus pour l'orientation aléatoire des fibres étaient en bon accord avec les résultats expérimentaux rapportés dans la littérature, et le coefficient de dilatation thermique s'est avéré isotrope.

En outre, un composite thermoplastique renforcé par du lin a été appliqué à la conception numérique d'un quadcopter afin de déterminer son comportement élastoplastique sous des charges variables de 1 MN et 10 MN. Un matériau utilisateur (UMAT) a été implémenté dans le logiciel Abaqus pour déterminer l'influence des variations de V_f de 0,1, 0,2, 0,3, 0,4 et 0,5. Il est apparu que, lorsque le V_f augmente de 0,1 à 0,5, la résistance du composite fibre-PP augmente jusqu'à 0,5. En outre, la déformation plastique accumulée augmente lorsque le

V_f passe de 0,1 à 0,5, ce qui confirme la stabilité du composite lin-PP sous une charge importante.

MOTS-CLES: Bio-composite; micromécanique; modélisation multi-échelle; homogénéisation; élastoplastique.

Numerical Modelling of Natural Fibres Reinforced Thermoplastic Composites

ABSTRACT

The growing global demand for sustainability in all spheres of significant human endeavour has considerably crept into the composite industry. This yearning has led to research to identify bio-sourced fibres as an alternative to synthetic fibres. Further, the recyclability and end-of-life management of composites are responsible for the increasing research on thermoplastic composites reinforced with natural fibres. To further enhance industrial adoption of bio-composite, micromechanical and multi-scale modelling approaches were used to characterise the thermo-mechanical behaviour of thermoplastic (poly-propylene matrix) composites reinforced with four different natural fibres: flax, vegetal-technic, wood-force, and a hybrid of flax and vegetal-technic, for a fibre volume fraction (V_f) of 0.2 and aspect ratios of 37.5, 9.1, 17.5, and 18.5 respectively for random and aligned fibre orientations.

The microstructure of each composite was modelled using Digimat, a commercial micromechanics software, and the numerical analyses were performed on Abaqus software (Dassault System). To validate the numerical results, analytical modelling based on the Mori-Tanaka homogenization scheme was used. The thermomechanical results obtained showed good agreement between the numerical and analytical approaches for both random and aligned fibre orientations. In addition, the mechanical results obtained for the random fibre orientation were in good agreement with the experimental results reported in the literature, and the coefficient of thermal expansion was found to be isotropic.

Further, a thermoplastic composite reinforced with flax was applied to the numerical design of a quadcopter to determine its elastoplastic behaviour under varying loads of 1 MN and 10 MN. A user material (UMAT) was implemented on Abaqus software to determine the influence of varying V_f of 0.1, 0.2, 0.3, 0.4, and 0.5. It was apparent that, as the V_f increases from 0.1 to 0.5, the strength of the fibre-PP composite increases up to 0.5. In addition, the accumulated plastic strain increases as the V_f increases from 0.1 to 0.5, which confirms the stability of the flax-PP composite under a high magnitude of load.

KEYWORDS: Bio-composite; Micromechanical; Multi-scale Modelling; Homogenization; Elastoplastic.

TABLE OF CONTENTS

1. CONTENTS

Acknowledgements III

Résumé IV

Abstract VI

Table of Contents VII

List of Figures VIII

List of Tables XI

List of Plates XIII

List of Abbreviations and Symbols XIV

1. Introduction 1

2. Literature review 9
   - 2.1. Overview of thermoplastic composite reinforced with natural fibres 9
   - 2.2. Reinforcement: Natural Fibre Review 9
   - 2.3. Polymer Matrix - Review 23
   - 2.4. Micromechanics Modelling Framework 25

3. Materials and Methods 33
   - 3.1. Boundary condition 36
   - 3.2. Post-processing 37
   - 3.3. Application of material properties 44

4. Results and Discussions 47
   - 4.1. Flax – PP Composite Engineering Properties 47
   - 4.2. Vegetal Technic - PP Composite Engineering Properties 51
   - 4.3. Wood-Force Composite Engineering Properties 55
   - 4.4. Hybrid of Flax- Vegetal-Technic-PP Composite Engineering Properties 58
   - 4.5. Comparative Analysis of the Thermomechanical Properties of the Four Materials Studied 61
   - 4.6. Flax – Polypropylene Reinforced Composite: Application 62

5. Conclusion 66

Reference 67

LIST OF FIGURES

Figure 1-1:. Natural reinforcement: (a) vegetables resources; (b) animals' resources. Source [1]. 3
Figure 1-2:Different natural fibres used in composites [8] 4
Figure 1-3:The resultant of Voigt and Reuss approximation of effective properties. Source: [10] 6
Figure 1-4: Rule of mixture model s- Voigt (a) and the Reuss (b) models. Source [1]. 6
Figure 1-5: Micromechanical model classified. Source [1]. 7
Figure 2-1: Classification of constituent of composite. Source [1] 10
Figure 2-2: Plant internal structures. Source: [16] 11
Figure 2-3:Mechanical performance of biofibres and their corresponding composites. Source: [22] 14
Figure 2-4: Gradient hybrid composite. Source: [23] 15
Figure 2-5: Type of composites. Source: [11] 24
Figure 2-6:Thermo-mechanical properties of different classes of composite. Source: [37] 25
Figure 2-7: Illustration of the major multiscale approaches of composite. Source[40] 27
Figure 2-8: Summary of homogenization process. Source [39] 28
Figure 2-9: Scanning electron microscopy (SEM) of WoodForce (A, D), Vegetal Technic (B, E) and Flax fibres (C, F). Source [2] 28
Figure 3-1: Isolated long aligned flax fibre from the thermoplastic composite RVE. 34
Figure 3-2: Isolated long random flax fibre from the thermoplastic composite RVE. 34
Figure 3-3: Isolated short random vegetal-technic fibre from the thermoplastic composite RVE. 35
Figure 3-4: Isolated long aligned wood-force fibre from the thermoplastic composite RVE. 35
Figure 3-5:Typical contribution of matrix only (isolated) to the total stress of a RVE 40
Figure 3-6: Typical contribution of fibres only (isolated) for an aligned orientation to the global stress of a RVE 40
Figure 3-7: Typical total stress of an RVE (fibre + matrix) 41
Figure 3-8: Typical contribution of fibres only (isolated) for a random orientation to the global stress of a RVE 41
Figure 3-9:Typical contribution of matrix only (isolated) in a random composite to the total stress of a RVE 42

Figure 3-10: Typical contribution of matrix only (isolated) at a 45 orientation to the total stress of a RVE 42
Figure 3-11: Typical contribution of fibres only (isolated) for a 45 degree orientation to the global stress of a RVE 43
Figure 3-12: Typical total stress of an RVE (fibre + matrix) for a 45 degree oriented fibre 43
Figure 3-13:Quadcopter CAD model 44
Figure 3-14:The meshed quadcopter 45
Figure 3-15: Multi-scale modelling 45
Figure 4-1: Histogram of elastic modulus of random short flax fibre reinforced thermoplastic composite with VF=0.2 & AR = 37.5 48
Figure 4-2: Histogram display of elastic modulus of aligned flax fibre reinforced thermoplastic composite with VF=0.2 & AR = 37.5 49
Figure 4-3: Histogram of shear modulus of aligned flax fibre reinforced thermoplastic composite with VF=0.2 & AR =37.5 50
Figure 4-4: Histogram of Poisson ratio for long flax fibre reinforced thermoplastic composite with VF=0.2 & AR = 37.5 51
Figure 4-5: Histogram of elastic modulus of random short vegetal-technic reinforced thermoplastic composite with VF=0.2 & AR = 9.1 52
Figure 4-6: Histogram of elastic modulus of long vegetal-technic fibre reinforced thermoplastic composite with VF=0.2 & AR = 9.1 53
Figure 4-7: Histogram of shear modulus of long wood-force fibre reinforced thermoplastic composite with VF=0.2 & AR = 9.1 54
Figure 4-8:Histogram of Poisson ratio result of PP composite reinforced with aligned vegetal-technic fibre with VF=0.2 & AR = 9.1 55
Figure 4-9: Histogram of elastic modulus of random short vegetal-technic fibre reinforced thermoplastic composite with VF=0.2 & AR = 17.5 56
Figure 4-10: Histogram of elastic modulus of long wood-force fibre reinforced thermoplastic composite with VF=0.2 & AR = 17.5 56
Figure 4-11: Histogram of shear modulus of long wood-force fibre reinforced thermoplastic composite with VF=0.2 & AR = 17.5 57
Figure 4-12:Graphical display of Poisson ratio result of PP composite reinforced with aligned wood-force fibre with VF=0.2 & AR = 17.5 58
Figure 4-13: Elastic modulus result of PP composite reinforced with aligned hybrid of flax and vegetal-technic with VF=0.2 & AR = 18.5 59

Figure 4-14:Histogram of shear modulus of aligned hybrid of flax and vegetal-technic fibre reinforced thermoplastic composite with VF=0.2 & AR = 18.5 60
Figure 4-15: Histogram of Poisson ratio for PP composite reinforced with aligned hybrid of flax and vegetal-technic fibre with VF=0.2 & AR = 18.5 60
Figure 4-16: Histogram of elastic modulus of random hybrid of flax and vegetal-technic fibre reinforced thermoplastic composite with VF=0.2 & AR = 18.5 61
Figure 4-17: Accumulated plastic strain result 63
Figure 4-18: Element of interest 63
Figure 4-19: Stress - strain curve 64
Figure 4-20: Accumulated plastic strain - stress curve 65
Figure 4-21:Accumulated plastic strain – strain curve 65

LIST OF TABLES

Table 2-1: Morphological, mechanical properties and biochemical composition of flax and wood single fibres. Source [2] 13
Table 2-2: Chemical Composition of Some Common Natural Plant Fibres. Source [18] 14
Table 2-3: Recent papers on natural fibres published in 2023. 17
Table 2-3: Recent papers on natural fibres published in 2023 (cont''d) 18
Table 2-3: Recent papers on natural fibres published in 2023 (cont''d) 19
Table 2-3: Recent papers on natural fibres published in 2023 (cont''d) 20
Table 2-3: Recent papers on natural fibres published in 2023 (cont''d) 21
Table 2-3: Recent papers on natural fibres published in 2023 (cont''d) 22
Table 3-1: Equivalent fibres length LEFI, equivalent fibres diameter DIFI and aspect ratio of three not injected samples (Virgin WF, virgin VT, virgin Flax) and four samples after the first injection cycle (PP-Flax, PP-VT, PP-WF, PP-VT/Flax. Source [2] 33
Table 3-2: Flax and polypropylene (PP) matrix properties. Source (1) 33
Table 3-3:Summary of boundary conditions applied - Traction XX – direction on Abaqus 36
Table 3-4:Summary of boundary conditions applied - Traction YY – direction on Abaqus 36
Table 3-5: Summary of boundary conditions applied - traction ZZ – direction on Abaqus 36
Table 3-6:Summary of boundary conditions applied - shear XY – direction on Abaqus 37
Table 3-7: Summary of boundary conditions applied - shear YZ – direction on Abaqus 37
Table 3-8: Summary of boundary conditions applied - shear XZ – direction on Abaqus 37
Table 3-9: Flax and polypropylene (PP) matrix properties. Source (1) 46
Table 4-1: Elastic modulus result of PP composite reinforced with random flax fibre with VF=0.2 & AR = 37.5 48
Table 4-2:Elastic modulus result of PP composite reinforced with aligned flax fibre with VF=0.2 & AR = 37.5 49
Table 4-3:Shear modulus result of PP composite reinforced with aligned flax fibre with VF=0.2 & AR = 37.5 50
Table 4-4:Poisson ratio result of PP composite reinforced with aligned flax fibre with VF=0.2 & AR = 37.5 51
Table 4-5:Elastic modulus result of PP composite reinforced with random vegetal-technic fibre with VF=0.2 & AR = 9.1 52
Table 4-6:Elastic modulus result of PP composite reinforced with aligned vegetal-technic fibre with VF=0.2 & AR = 9.1 52

Table 4-7:Shear modulus result of PP composite reinforced with aligned vegetal-technic fibre with VF=0.2 & AR = 9.1 53
Table 4-8:Poisson ratio result of PP composite reinforced with aligned vegetal-technic fibre with VF=0.2 & AR = 9.1 54
Table 4-9:Elastic modulus result of PP composite reinforced with random wood-force fibre with VF=0.2 & AR = 17.5 55
Table 4-10:Elastic modulus result of PP composite reinforced with aligned wood-force fibre with VF=0.2 & AR = 17.5 56
Table 4-11:Shear modulus result of PP composite reinforced with aligned wood-force fibre with VF=0.2 & AR = 17.5 57
Table 4-12:Poisson ratio result of PP composite reinforced with aligned wood-force fibre with VF=0.2 & AR = 17.5 58
Table 4-13:Elastic modulus result of PP composite reinforced with a hybrid of flax and vegetal-technic fibre with VF=0.2 & AR = 18.5 59
Table 4-14:Shear modulus result of PP composite reinforced with aligned hybrid of flax and vegetal-technic fibre with VF=0.2 & AR = 18.5 59
Table 4-15:Poisson ratio result of PP composite reinforced with aligned hybrid of flax and vegetal-technic with VF=0.2 & AR = 18.5 60
Table 4-16:Elastic modulus result of PP composite reinforced with random hybrid of flax and vegetal-technic with VF=0.2 & AR = 18.5 61

LIST OF PLATES

Plate 3-1:Typical RVE model with boundary condion and load 35

LIST OF ABBREVIATIONS AND SYMBOLS

Abbreviations

AWJM	Abrasive Water Jet Machining
CAE	Computer Aided Engineering
CMC	Ceramic Matrix Composite
CTE	Coefficient of Thermal Expansion
MFH	Mean Field Homogenization
MFA	Microfibrillar Angle
LDF	Linear Distribution Function
PC	Polycarbonate
PE	Polyethylene
PEEK	Polyetheretherketone
PMC	Polymer Matrix Composite
PLA	Poly-lactic Acid
PP	Polypropylene
PPS	Polyphenylene Sulphide
RVE	Representative Element Volume
SEM	Scanning Electron Microscopy
UMAT	User Material

Symbols

E	Elastic modulus
G	Shear modulus
ν	Poisson ratio in plane 1-2

THIS PAGE WAS INTENTIONALLY LEFT BLANK

1. INTRODUCTION

Environmental pollution is a concern across all fields of human endeavour in the 21st century. Across different fields of endeavour, conscious efforts are being invested to limit the impact of environmental pollution, particularly the carbon pollution that seeps into the environment through different man-made actions such as construction, agriculture, manufacturing, and transportation, amongst many others. The construction, manufacturing, and transportation sectors have been acknowledged to contribute the most significantly to the carbon emissions bedevilling our environment. Hence, the diverse actions—research and innovation to reduce the carbon footprint in the said sectors The use of biomaterials and waste has been repeatedly acknowledged as a viable solution to achieve net-zero carbon in the world.

It is no longer news that composite materials have played a recognisable role in attaining the current state of development being experienced in varying fields of practise. Modern composite materials may exhibit qualities that are not easily measurable using conventional methods employed for metals. Its mechanical performance rivals that of metal, and, in fact, it became preferred over metal because of its inherent high strength-to-weight ratio. This is undoubtedly responsible for its growing adoption in varying fields such as aeronautics and Aerospace, Civil Engineering Construction, Wind engineering, and Biomedical engineering, amongst others. Initially, synthetic fibres were the fundamental materials, coupled with matrixes of different kinds (thermoset or thermoplastic). The management of end-of-life waste from synthetic composites is a current challenge bedevilling the composite industry, and this has forced an increase in research on thermoplastic matrix. Thermoplastic is known to be vulnerable to reshapeability at high temperatures, which may not guarantee its structural resilience and tolerance under intense structural load. The ceramic matrix found favour at this elevated temperature. This singular characteristic of thermoplastic explains the dominance of thermoset over time. However, sustainability demand is gradually causing a paradigm shift, forcing thermoplastics and natural fibres to gain traction. The growth and adoption of the ideas of green chemistry and the green industrial revolution have yielded increased demand for natural fibres and bio-composites[1]. Due to environmental concerns, in the composite world, a wide range of research is being carried out to use natural fibres as an alternative to synthetic fibres.

However, bio-composite has been recognised to have a better end-of-life performance because of its amenability to decompose freely with less environmental pollution. In fact, it has been reported that biocomposite can be degraded into ecological compost [1]. Natural fibres are considered advantageous because of its low cost, biodegradability and abundance of the material [2]. It is worth noting that there has been a significant rise in the utilization of renewable natural resources for the production of biomaterials in recent years. It's worth noting that there has been a significant rise in the utilisation of renewable natural resources for the production of biomaterials in recent years. In 2004, only 5% of these resources were used, but by 2010, that number had increased to 13%, and by 2020, it had reached 18%. Experts predicted that by 2030, this figure would rise to 25% [3]. The common reinforcements or fibres are linen, hemp, wood, alfa, clay, coconut, jute, and cotton hulls. Their attractive characteristics, including but not limited to resistance to corrosion and fatigue, low weight, high durability, and excellent electrical insulation, position them as a superior substitute for conventional materials like carbon, aramid, and glass [4]. Further, the preparation process of natural fibres was reported to be easy and could require less complicated equipment [2] Natural fibres are obtained from different sources - agricultural plants and animals as shown in figure 1-1 and figure 1-2.

Despite the advantages of natural fibres, they still remain constricted for applications in structures or components of low structural significance because of the evident inherent defects such as fibre non-alignment, moisture content, high moisture absorption and subsequent swelling and degradation, poor chemical and fire resistance, high variability of mechanical properties, poor interfacial interactions with polymeric or cementitious matrices, etc. [4] which are all responsible for their low structural reliance. In order to reduce the effects of the limiting properties of natural fibre, different research efforts have been dedicated to finding a solution. Researchers have sought to address the limitations of natural fibres by exploring alternatives with superior properties. Bio-hybrid composites with diverse reinforcing components offer a wide range of alternating inorganic and organic properties, allowing for new behaviours and expanded applications[5]. Numerous studies have explored the use of natural fibres in various matrices, such as thermoplastics (e.g., PP, PE) and thermosets (e.g., polyester, epoxy), to evaluate the mechanical and ultimate properties of bio-composites and bio-hybrid composites. The consensus among these studies is that the interfacial adhesion between the matrix and fibres plays a crucial role in determining the effectiveness of reinforcement [6]. This suggests that, for bio-hybrid comosite, one-site micromodelling would not be sufficient to predict its material properties with accuracy but would require multi-site micromodelling for its prediction.

The increased demand for cheap, fast, and reliable virtual analyses and designs of structural elements has forced numerical simulation to a high level of technological readiness. The advancement of the finite element approach has aided long time confidence in its adoption for analyses and design. Since it is an established fact that numerical simulation offers a cheap and time effective means to study complex engineering problems, including composite structures, it was adopted to carry out this multiscale analysis on long fibres and also numerically validate the results obtained for the random fibres through the experimental and analytical analysis of bio-composites consisting of four different natural fibres (flax, vegetal-technic, wood-force, and a hybrid of flax and vegetal-technic) and a thermoplastic matrix (polypropylene).

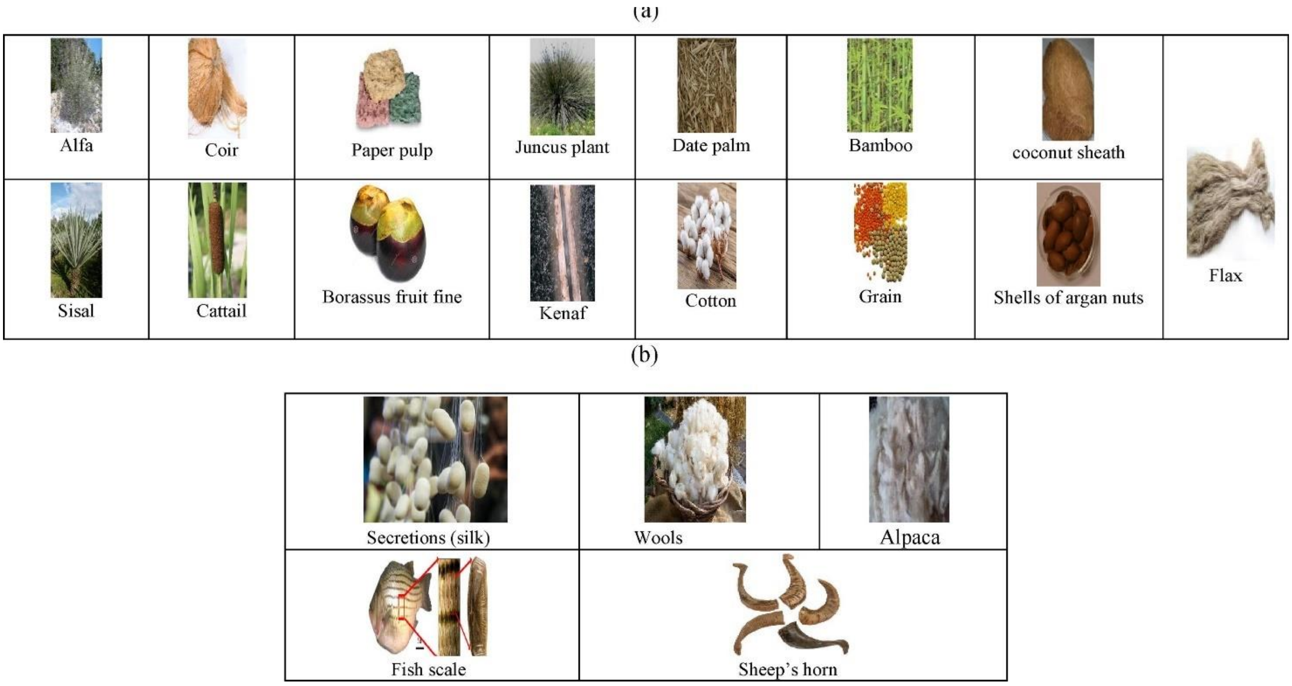

Figure 1-1:. Natural reinforcement: (a) vegetables resources; (b) animals' resources. Source [1].

Modelling using homogenization techniques enables the determination of a heterogeneous material's macroscopic properties by analysing the microscopic properties of its components. The Eshelby inclusion [7] problem and selection of a representative elementary volume (RVE) are fundamental to homogenization modelling techniques.

Various micro-mechanical models, such as Voigt-Reuss, Hashin, Halpin-Tsai, Self-coherent, and Mori-Tanaka, amongst other have been proposed to aid in this process [1]. Voigt-Reuss models (law of mixtures ROM- Inverse Rule of Mixture IROM) have been established to give the upper and lower bound results of all the existing models, figure 1-3 shows that. As shown in fig 1-4a and fig 1-4b that Voigst and Reuss models predict well properties of composite in the longitudinally and transversely respectively. The Voigt and Reuss models predict with low accuracy because it relies on simplified microstructural descriptors, such as phase volume fraction and shape in their approximations. While effective-medium approximations and mixture rules based on these descriptors provide accurate predictions for materials with low-contrast properties, they become less accurate for materials with high-contrast properties and complex phase interactions, such as those involving phase percolation [4]. In fact, Chichane et al [1] has classified different micromechanical models (shown in figure 1-5) based on the domain in terms of physical characteristics of the fibres which these models yield good results.

Figure 1-2:Different natural fibres used in composites [8]

This research work uses a multiscale modelling approach to study bio-composites consisting of natural fibres embedded within a thermoplastic matrix (poly-propylene). The microstructure was used to characterized the thermo-mechanical properties of four natural fibres which are Flax, Vegetal-technic, Wood-force and a hybrid of Flax and Vegetal-technic. Regards to the numerical approach, representative volume elements (RVE) are obtained for different aspect ratio (l/d) of the fibres from short to long fibres The studied microstructures include different fibre orientations mainly (0, +/-45 and 90 degree) as well as a random fibre orientation. The generation of the RVE were done using DIGIMAT software [9]. A periodic boundary condition was assumed on the RVE with a computation of numerical results in Abaqus CAE.

From an analytical modelling, a Mori-Tanaka homogenisation scheme is used to derive the effective thermo-mechanical properties. As a material nonlinearity, rate independent constitutive equations are written for the matrix through the J2 plasticity. Results obtained for a fibre volume fraction of 20% validate the effective properties of the composite reinforced with random fibres which was priorly investigated experimentally and analytically by Barteau et al, [2].

Finally, a multiscale application at the macroscale led to the design of a quadcopter (drone) and established the elasto-plastic structural response of the structure at different fibre volume fractions. The established thermo-mechanical properties for the flax fibre-reinforced composite were adopted for writing a constitutive model for application in numerical macroscale analysis and design of a quadcopter (drone) to establish the elasto-plastic structural response of the structure under varying fibre volume fraction. The obtained thermo-mechanical properties were validated analytically using the Mori-Tanaka homogenization scheme. Further, the numerical models validated the previous results obtained for the random state of fibres through experimental analysis and analytical analysis of the four natural fibres. The previous research is published and titled "Recycling of wood-reinforced poly-(propylene) composites: a numerical and experimental approach, Industrial Crops and The previous research is published and titled "Recycling of wood-reinforced poly-(propylene) composites: a numerical and experimental approach, Industrial Crops and Products"[2]. Further, Barteau et. al. [2] evaluated the effect of degradation, which was modelled and discussed in their work; however, such a phenomenon was not studied in this work; hence, the work only considered the virgin state of the natural fibres. It is worth nothing that, due to computational cost, this study was limited to one-site modelling; therefore, the interactions between the fibres were not studied.

This research report has been structured in the following sequence: Chapter one is an introduction that provides a brief insight into the whole research process. Chapter two is a literature review that provides a state-of-the art review of research work on natural fibres using a multiscale modelling approach (homogenization and de-homogenization). Chapter three is research materials and methodology, which provides full insight into the material properties and numerical and analytical approaches adopted in this research, while Chapter four (results presentation and discussion) provides pedagogical presentation of results and logical interpretation and discussion of the results. Chapter five (conclusion and recommendations) is the concluding chapter of the work

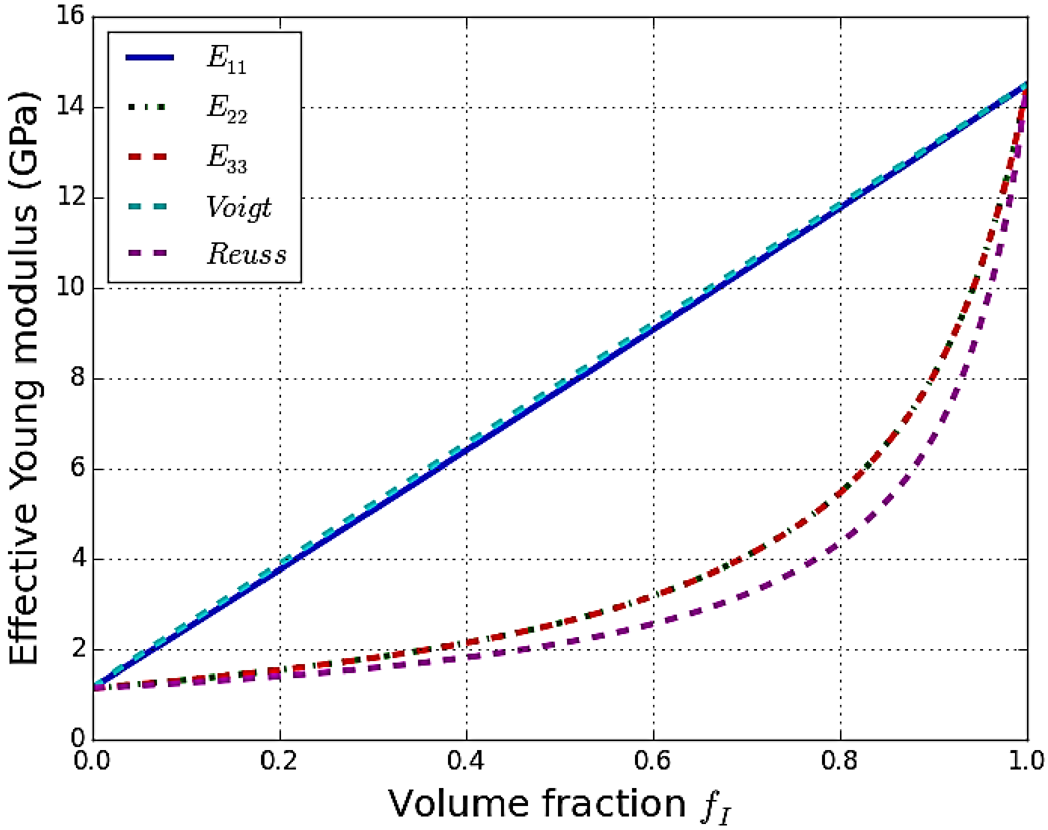

Figure 1-3:The resultant of Voigt and Reuss approximation of effective properties. Source: [10]

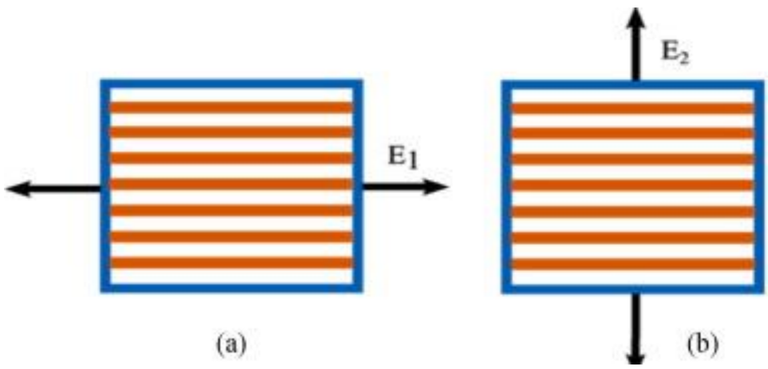

Figure 1-4: Rule of mixture model s- Voigt (a) and the Reuss (b) models. Source [1].

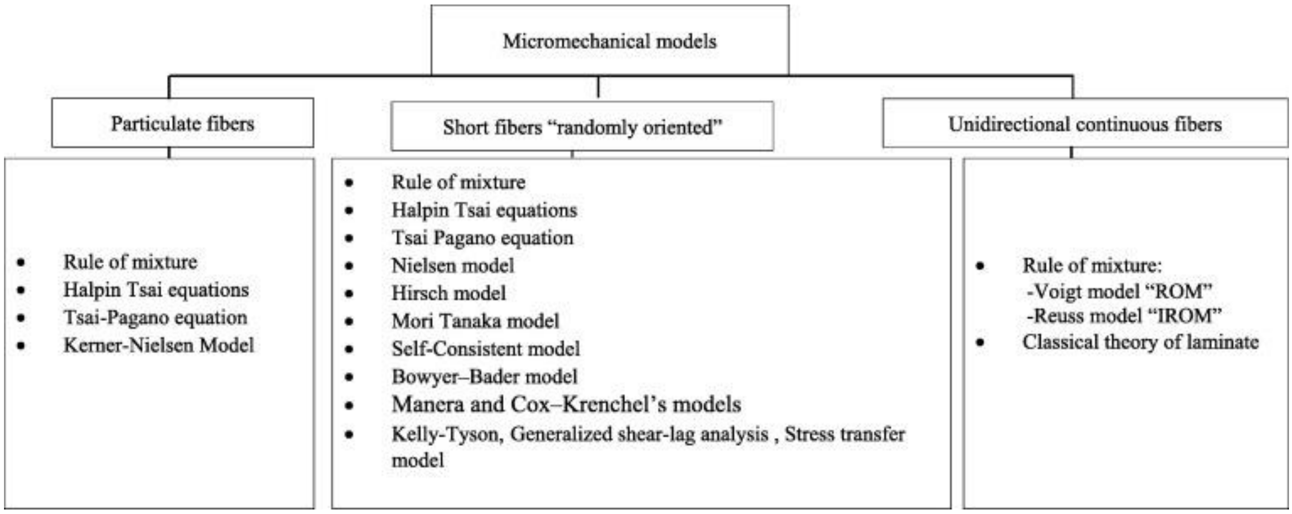

Figure 1-5: Micromechanical model classified. Source [1].

THIS PAGE WAS INTENTIONALLY LEFT BLANK

.

2. LITERATURE REVIEW

2.1. Overview of thermoplastic composite reinforced with natural fibres

A composite material can be simply defined as a material made up of two or more materials in different material phases. A composite material is formed by combining two or more distinct components that do not have the ability to mix or dissolve into each other [2]. These distinct materials combine to form a material with superior properties when compared to the properties of each of the constitutive materials. A composite material is comprised of a continuous phase called the matrix, which serves to maintain the reinforcing elements known as fibres and facilitate charge transfer. The matrix phase plays a crucial role by encompassing and binding the reinforcing component, ensuring its cohesion, and maintaining the desired shape [11].

The fibre is considered to be in a discontinuous phase with is stronger and stiffer than the matrix [1] Due to their desirable properties such as low density, excellent shock absorption, and ease of manufacturing, composite materials have become a popular alternative to traditional metallic materials across various industries [12]. It is therefore important to understand the properties of the constitutive materials (matrices and fibres) and the various homogenization techniques. These are discussed extensively in the subsequent sub-sections.

2.2. Reinforcement: Natural Fibre Review

Fibres or reinforcements in composite materials can be classified in terms of origin and geometry. As evident in figure 2-1, in terms of origin or type, it can be classified as either synthetic fibre (inorganic) or natural fibre (organic). Geometrically, it has been classified as either a continuous (long) fibre or a discontinuous fibre. The discontinuous fibres can be further classified into short fibres (random and aligned), particulate fibres, and platelet fibres. The most significant classification of fibre is in terms of its origin; the geometry adopted is dependent on the purpose of the composite. Long fibres (discontinuous) are mostly considered for components exposed to high structural loads.

The variations in properties of natural fibres arise from their biochemical composition and the ultrastructure, specifically the microfibrillar angle [2]. The microfibrillar angle (MFA) in wood science represents the angle between the long axis of the cell wall and the direction of the helical windings of cellulose microfibrils in the secondary cell wall of fibres [13] and [14]. [15] reported that MFA is the main factor that determines the strength of plant natural fibres.

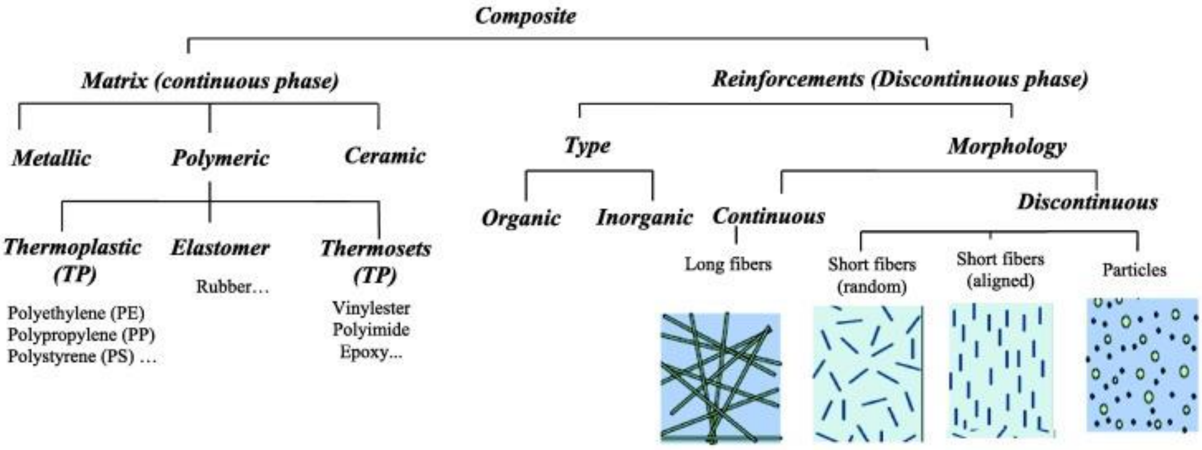

Figure 2-1: Classification of constituent of composite. Source [1]

As shown in figure 2-2 by Dimple et al. [16], plant fibre structure is a multi-layer structure which include both primary cell wall and secondary cell walls. The constituent of the primary cell wall is reported to be hemicellulose, cellulose and pectins. It was further reported that the secondary cell wall is in itself a multilayer structure which contains S_1, S_2 and S_3. S_1 is made up of cellulose, lignin, hemicellulose, and pectins while both S_2 and S_3 contain same contents as S_1 excluding the lignin. Dimple et al. [16] and Kabir et al. [17] reported that the MFA of the S2 is the main determinant of the mechanical properties of wood.

It is widely reported that cellulose, hemicellulose, and lignin are the key components of natural fibres, [1] reported that natural fibres are composed of lignin, waxes, cellulose, pectin, and hemicelluloses. The main structural component of natural plant fibres is cellulose, which is responsible for its stability under temperature effect [18]. These fibres mechanical performance is mostly determined by the amount of cellulose and micro fibrillary angles [19]. Mohanty et. al, [20] further reported that high strength fibre is characterized by a higher cellulose content and a very small MFA angle which was similarly demonstrated in the work of Mukherjee and Satyanarayana [21]. Which is quite reasonable, because it has been shown in numerous research that misaligned fibres are significantly vulnerable to fibre kinking failure. Barteau et al. [2] has reported as shown in table 2, the cellulose content of the studied fibres - flax, vegetal technic, wood-force and the hybrid of flax + vegetal-technic which was measured in terms of the glucose content. It is at least in agreement for the cellulose content reported for flax in the work of Dimple et al. [15]. Various factors, including age, species, climate conditions, and extraction methods, influence the chemical composition of natural components

[1]. These presence of the influence of these complex variables put natural fibres at disadvantage against synthetic fibres, otherwise, natural fibres would confidently compete with synthetic fibres as shown in figure 2-3, Flax and hemp can compete with glass fibre in terms of mechanical strength [22].

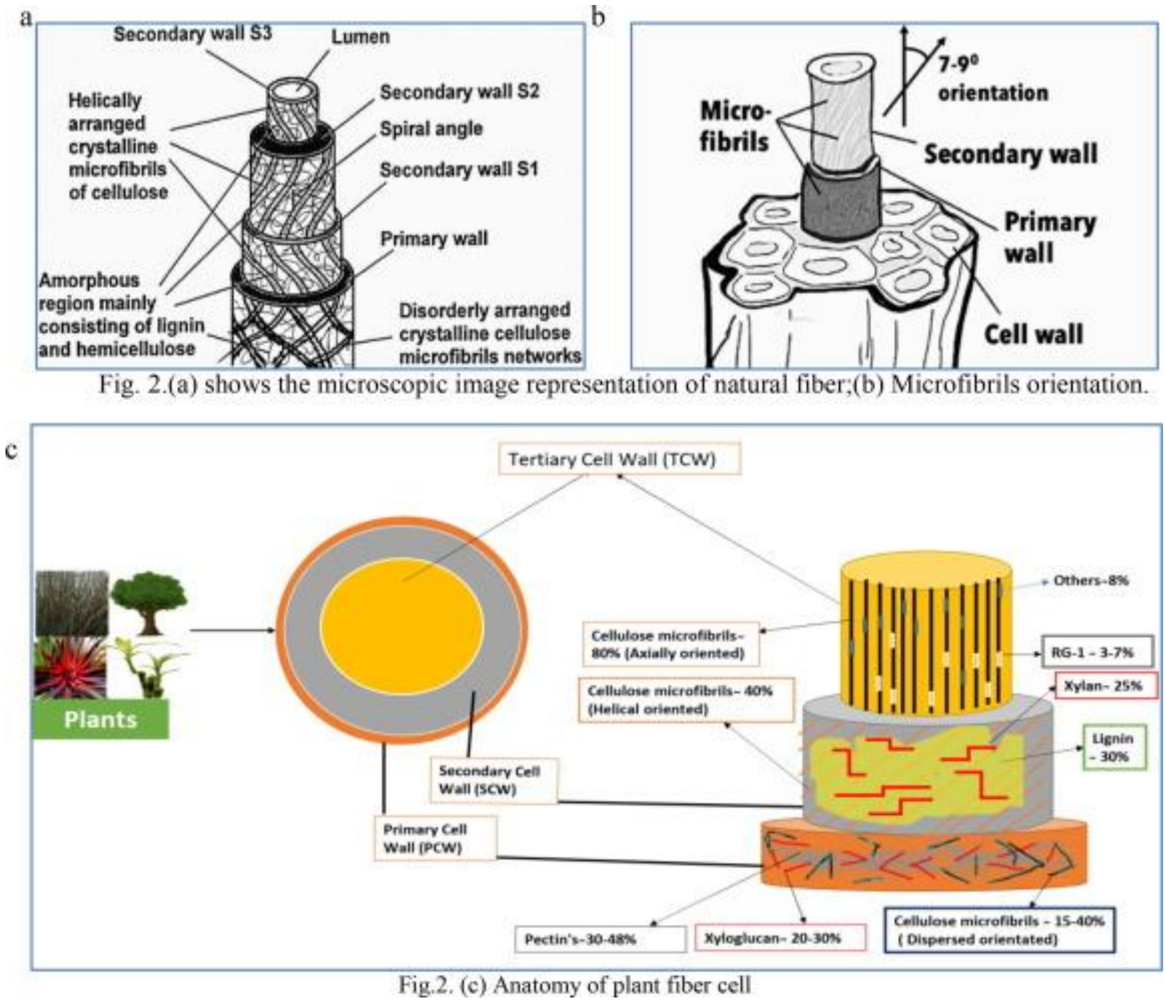

Figure 2-2: Plant internal structures. Source: [16]

It worth nothing that there is a possibility to mix different fibres of different origins. This is known as hybridization. Hybridization involves creating a combination that is specifically engineered to generate improved and enhanced functionalities beyond what the individual components can achieve on their own[1]. There have been different forms of hybridization: composite laminates with steel or different fibres; composites made with fibres of different origins (for example, a combination of synthetic and natural fibres); composites made with fibres of the same origin (all synthetic or all-natural fibres) but different fibres of the same kind. One of the samples studied in this research is a hybrid of Flax and vegetal-technic, which is an example of a hybrid composite made with fibres of the same origin—all-natural fibres but different fibres of the same kind. Another example of a hybrid composite made of composites of the same origin (synthetic) is a combination of glass fibre and carbon. The ultimate gain of having a hybrid composite is having a better performing property, which could not have been achieved by using a single type of fibre.

A recent work by Mahmud et al. [23] demonstrated how hybridization of natural fibres and synthetic fibres (carbon fibre, glass fibre, and natural jute fibre) was able to lead to a 550% increase in the flexural strength of the composites made of fully natural fibres and around 14 % and 34 % higher flexural strength fibres. The idea represented in this paper shows a good use of hybridization and how to mazimize its properties; see figure 2-4. Instead of providing these synthetic and natural fibres haphazardly, it is very good, as shown in the paper, to use each of the materials at the region of most significance where their properties are mostly needed. For example, the synthetic fibre is used on the outermost layer of a structure subjected to high bending stress to take full advantage of the high strength capacity of the fibre.

Table 2-1: Morphological, mechanical properties and biochemical composition of flax and wood single fibres. Source [2]

Fibres	Length (mm)	Diameter (mm)	Density (g/cm^3)	Young Modulus (GPa)	Strength (MPa)	Strain at break (%)
Flax (Linum Usitatissimum L.)	6 – 80	12.4 – 23.9	1.53 – 1.54	37.2 – 75.1	595 – 1,510	1.6 – 3.6
Wood (Different species)	1 – 8	10 – 60	1.44 – 1.50	15.4 – 27.5	553 – 1,300	3 - 7
	Number of points		Indentation modulus (GPa)		Indentation hardness (MPa)	
Flax	32		19.5 ± 1.5		387 ± 28	
WoodForce	35		14.8 ± 1.6		362 ± 37	
Vegetal Technic	31		14.5 ± 1.3		323 ± 32	
	Flax		WoodForce		Vegetal technic	
Lignin content	1.95 ± 0.48		27.50 ± 0.72		28.80 ± 0.95	
Arabinose	0.74 ± 0.06		1.29 ± 0.16		0.46 ± 0.06	
Rhamnose	0.63 ± 0.11		0.58 ± 0.16		0.37 ± 0.17	
Galactose	2.75 ± 0.25		2.07 ± 0.08		0.85 ± 0.22	
Glucose	69.66 ± 3.66		47.23 ± 2.80		51.39 ± 2.39	
Xylose	1.01 ± 0.17		3.97 ± 0.11		8.14 ± 0.31	
	Flax		WoodForce		Vegetal technic	
Mannose	3.52 ± 0.35		12.08 ± 0.73		1.73 ± 0.24	
Uronic acid	1.92 ± 0.01		0.00 ± 0.00		0.00 ± 0.00	

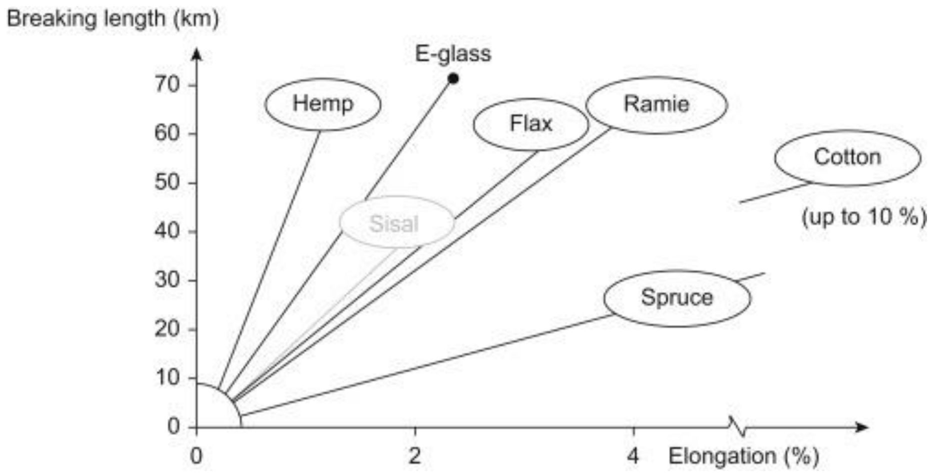

Figure 2-3:Mechanical performance of biofibres and their corresponding composites. Source: [22]

Table 2-2: Chemical Composition of Some Common Natural Plant Fibres. Source [18]

Fibre	Cellulose (%)	Hemicellulose	Lignin (wt%)	Waxes (wt%)
Bagasse	55.2	16.8	25.3	-
Bamboo	26-43	30	21 – 31	-
Flax	71	18.6 – 20.6	2.2	1.5
Kenaf	72	20.3	9	-
Jute	61 - 71	14 - 20	12 - 13	0.5
Hemp	68	15	10	0.8
Ramie	68.6 – 76.2	13 - 16	0.6 – 0.7	0.3
Abaca	56 - 63	13 - 16	0.6 – 0.7	0.3
Sisal	65	12	9.9	2
Coir	32 - 43	0.15 – 0.25	40 - 45	-
Oil palm	65	-	29	-
Pineapple	81	-	12.7	-
Curaua	73.6	9.9	7.5	-
Wheat straw	38 - 45	15 - 31	12 – 20	-
Rice husk	35 - 45	19 - 25	20	14 – 17
Rice straw	41 - 57	33	8 - 19	8 - 28

Figure 2-4: Gradient hybrid composite. Source: [23]

The yearning for sustainable and eco-friendly structures, which are possible through eco-friendly materials, is responsible for the growing demand for natural fibres. Natural reinforcements refer to substances derived from animal or vegetable sources that are incorporated into a matrix in the form of particles, threads, filaments, or cords. Examples of organic animal reinforcements include silk, wool from sheep, and hair from alpacas. These natural reinforcements have wide-ranging applications, including but not limited to wall and floor coverings, electrical and thermal insulation, paper manufacturing, and packaging [1].

Numerous researchers have conducted studies on various reinforcements like alfalfa, coir, coconut sheath, date palm, flax, and the Juncus plant. The objective of these studies was to assess the potential of green bio-composites by analysing different factors that affect the mechanical and thermal properties of these composites. The desire for natural materials in the composite industry has been increasing since about 15 years ago. As reported by Chichane et al. [1], 20 papers were published on natural fibres between 2005 and 2018, with 18 of the 20 published between 2010 and 2018. This simply shows the growth in demand for natural fibres in the composite world. To better reflect the current development in natural fibres, in addition to the research directions reported in [1], a review of recently published research papers on natural fibres are briefly highlighted in table 2-3.

The work of Jino et al. [24] showed a different dimension to the hybridization. The work applies mixture of nanocomposite to the micro-composite of natural fibres. As reported by different researchers that nanocomposite have positive impact on the mechanical behaviour of composite, similarly, this work reported same but also unravel the direct application of this form of hybrid composite. It also worth highlighting the emerging idea of using natural fibre in 3D and 4D printing of composites currently been discussed by researcher. A recent work by [3] highlighted this potential natuiral fibre has in additive manufacturing. Clearly, the potential of natural fibres is yet to be fully explored, therefore, it is safe to say its industrial applications will continue to grow in the foreseeable future.

Therefore, it is more than relevant to establish its properties to enhance the wide acceptance and encourage industrial adoption of these materials for design and manufacturing of reliable composite structures that is as well eco-friendly. This work did not only seek to provide thermos-mechanical properties of different natural fibres, but also using the least expensive yet reliable and accurate approach - multiscale modelling enhanced by computational mechanics which was validated by analytical approach. The capacity of these microstructural models to determine the material properties was first established by implementing it determine the properties of the random fibres that have been previously established experimentally and analytically which was reported by Barteau et. al, [2]. It was upon confirming the capacity of the model to accurate determine the thermo-mechanical properties of the fibres in random orientation that the models were extended to determine the thermo-mechanical properties of the long aligned oriented fibres. The numerically determined properties for the long aligned natural fibres were analytically validated. There is strong agreement between these results.

It is interesting to note the potential of natural fibres in the production of ballistic protection and safety gadgets. The work of Doddamani et. al, [25] provided extensive review of its application in this regard. It is important to recognize that natural fibres need to be treated to reduce its vulnerability to moisture. Therefore, chemical treatments have been established and used to improve its hydrophobic properties. It was reported that this chemical treatment also increases its interlocking capacity because of the altered surface of the natural fibres[3].

Table 2-3: Recent papers on natural fibres published in 2023.

Year	Summary of latest research on natural fibres	Reference
July 2023	This study developed an energy-efficient manufacturing method for natural fibre-reinforced composites using a conductive biopolymer nanocomposite film. The smart nanocomposite layer acts as a self-regulating heating element to cure the laminates at the desired temperature, achieving a 95% reduction in energy consumption compared to traditional oven curing. The embedded nanocomposite surface film on the cured laminate provides integrated real-time deformation and damage sensing capabilities with enhanced water barrier properties, prolonging the service life of natural fibre composites. This approach addresses challenges and concerns in natural fibre-reinforced plastics, such as high moisture absorption and high energy consumption during manufacturing.	[26]
July, 2023	Sustainable development in the construction sector is crucial to reduce environmental impact. Geopolymer materials offer lower CO_2 emissions and excellent thermal properties. Natural fibres, like bamboo and hemp, can reinforce geopolymer composites, enhancing strength and insulation. This review explores geopolymer materials' properties, manufacturing conditions, and the impact of natural fibre reinforcement, providing insights for future research.	[27]
June 2023	In this paper, a gradient hybrid fibre reinforcement was designed using carbon, glass, and natural jute fibres in a self-healable shape memory polymer. Performance tests showed the gradient composites had competitive mechanical properties compared to fully carbon or glass fibre composites. They exhibited up to 550% higher flexural strength than fully natural fibre composites and higher strength than pure glass or carbon fibre composites. Additionally, the gradient composites retained self-healing, shape-recovery, and fibre-recycling properties.	[23]

Table 2-4: Recent papers on natural fibres published in 2023 (cont"d)

Year	Summary of latest research on natural fibres	Reference
May 2023	Over the past few decades, the extensive research and growth in Natural Fibre Reinforced Composites (NFRCs) have significantly influenced their utilization in research and innovation. NFRCs possess remarkable properties compared to synthetic fibre composites, including biodegradability, renewable resources, abundance, and improved performance. Modifications in natural fibres have been made to enhance the capabilities of NFRCs, with a need for further investigation. This review article focuses on recent developments in application-based NFRCs, highlighting their thermo-mechanical properties, challenges, and future research trends.	[28]
May 2023	This study focuses on evaluating the mechanical properties of a composite comprising kenaf, hemp fibre, and epoxy polymer to determine its specific strength. The environmental impact has spurred the quest for natural composites as substitutes for conventional materials. Natural fibres possess desirable properties like thermal insulation, low density, and favourable mechanical and acoustic characteristics, driving their use in diverse industrial applications for enhanced efficiency. Natural fibre composites exhibit durability, affordability, lightweight, high specific strength, non-abrasiveness, commendable mechanical properties, eco-friendliness, and biodegradability.	[29]
May, 2023	Eco-friendly natural fibre reinforced composites (NFRC) have gained significant interest due to their advantages such as abundance, low cost, and biodegradability. NFRC finds applications in various industries, but machining them poses challenges. Abrasive waterjet machining (AWJM) is an efficient technique for machining NFRC. This review examines different natural fibres, their mechanical properties, and explores the effect of AWJM parameters on the machinability of NFRC. Optimum process parameters for achieving better machining quality are discussed.	[30]

Table 2-5: Recent papers on natural fibres published in 2023 (cont"d)

Year	Summary of latest research on natural fibres	Reference
May, 2023	This study explores the use of chemically treated kenaf and coconut fibres to reinforce a sustainable cementitious composite. The mechanical, microstructural, and durability properties of the composite were investigated, and a 3D finite element model was developed to assess its performance in railway infrastructure. The results show that incorporating 1.5% wt of kenaf fibre improves the mechanical behaviour and durability of the composite. This research highlights the potential of natural fibres in developing affordable and reliable cementitious composites for various infrastructure applications.	[19]
May, 2023	Researchers are actively seeking environmentally friendly alternatives to synthetic fibres, such as natural fibres derived from plants and animals. Natural fibres like bamboo, hemp, jute, and oil palm offer the potential to create lightweight and biodegradable composites with improved mechanical properties. Chemical modifications and treatments can further enhance these properties by modifying the fibre morphology. This review highlights the properties and applications of natural fibres, emphasizing the importance of sustainable choices over non-biodegradable synthetic fibres. The study aims to promote the use of natural fibres in various industries to replace synthetic fibres and improve environmental sustainability.	[3]
April 2023	The objective of this research is to create an eco-friendly composite brake friction material to replace hazardous asbestos and non-asbestos materials. The study utilizes a hybrid composite of jute, coir, and glass fibre with vinyl ester resin to measure the shear strength and wear rate of the brake pads. The effectiveness and application of the composite material depend on its thickness and wear resistance	[31]

Table 2-6: Recent papers on natural fibres published in 2023 (cont''d)

Year	Summary of latest research on natural fibres	Reference
April 2023	Natural polymer composites offer an eco-friendly alternative for the automotive, railway, and aerospace industries. Areca fibre is a promising natural fibre option for developing polymer composites that can reduce carbon emissions by decreasing the weight of automotive systems. This study explores the mechanical behaviour of areca fibre-based polymer composites under various conditions, including untreated, treated, and hybrid approaches.	[32]
April 2023	Industries are shifting towards green composite materials to obtain carbon credits by reducing air pollution. Natural fibre-reinforced composite materials offer exceptional properties and environmental benefits, making them popular in various industries. This study analyses the mechanical and thermal properties of natural cellulosic fibre-reinforced composites and natural fibres, which are widely used in contemporary industrial sectors, including sports, automotive, medicine, aerospace, electronics, food packaging, and energy storage.	[16]
April 2023	In the pursuit of sustainable development, researchers are focusing on developing environmentally-friendly materials. Natural fibres are being explored as potential reinforcements in polymer composites, offering biodegradability and reducing the greenhouse effect. These materials show promising physical, mechanical, and tribological properties, making them viable alternatives to traditional structural materials. This review paper highlights the experimental studies on the physical, mechanical, and tribological behaviour of natural fibre-reinforced polymer composites, as well as discussing their diverse applications resulting from their tailored properties.	[33]

Table 2-7: Recent papers on natural fibres published in 2023 (cont''d)

Year	Summary of latest research on natural fibres	Reference
March 2023	This study investigates the feasibility of developing a tribo-material by incorporating chemically treated plant fibres (sisal, banana, and bagasse) into a Poly-lactic acid (PLA) matrix at 10% and 20% fibre concentrations using the injection moulding process. The wear properties of the composites were studied under dry sliding conditions, and the results showed that the incorporation of natural fibres improved the tribological properties of the PLA matrix. The worn surfaces of the composites were examined using a scanning electron microscope to study the wear.	[34]
March, 2023	This paper focuses on the flexural characteristics of epoxy composites fabricated using different fibres, including emu bird feather, kusha grass, and copper wire. The composites were prepared using the hand layup technique, varying fibre lengths (10-50 mm) and fibre weight percentages (1-5%). The results indicate that the flexural strength of emu fibre-reinforced composites decreases with increasing fibre length and loading. Conversely, kusha grass and copper fibre composites exhibit increased flexural strength with longer fibres and higher fibre weight percentages. These findings have practical implications in thermal structure engineering applications.	[30]
February, 2023	This review analyzes the factors affecting the performance of natural fibre composites in armor systems, including material composition, fibre/matrix type, and projectile parameters. The study explores various research approaches to improve the composites' ballistic efficiency and highlights the economic cost analysis of using natural fibres instead of synthetic ones in ballistic composites.	[35]

Table 2-8: Recent papers on natural fibres published in 2023 (cont''d)

Year	Summary of latest research on natural fibres	Reference
February 2023	The automotive industry is increasingly utilizing natural fibre reinforced composite materials due to their beneficial qualities. Natural-fibre composites (NFC) offer advantages in sound absorption and thermal properties, making them suitable for applications in noise management. This paper presents a comprehensive analysis of the applications and acoustic properties of polymer composites reinforced with natural fibres. Natural fibre reinforcement is proven to be an efficient substitute for synthetic fibres in various sectors including construction, automotive, geotextiles, railway, electrical, defence, and packaging.	[8]
February 2023	This review explores the potential impact of adding nanoparticles to natural fibres in altering the physical and chemical properties of natural fibre composites. It investigates whether nanoparticles can enhance the fibre by modifying its properties and structure. The review covers an introduction to natural fibres and nanoparticles, including their types and classifications. It also examines the interaction between nanoparticles and natural fibres, explores applications, and concludes with insights into the subject matter.	[24]

2.3.Polymer Matrix - Review

As shown in figure 2-5, matrix can be classified as metallic; polymeric or ceramic in nature. These kind of matrices are different in terms of temperature, specific strength and specific modulus. Polymer matrix is considered the most common matrix owing to their great characteristics such as ease of processing, good mechanical performance and low density. The affordability and ease of production contribute to the widespread acceptance of polymer matrix composites (PMCs) [11]. In the fields of construction, aerospace, automotive, and medical applications, polymers have replaced metals and ceramics. The fundamental properties and sustainability potential of polymers ensure that this transition will continue [11]. This is corroborated by the idea of biodegradable polymeric composite which is recently gaining traction. Avcu et al. [36] reported acceptance of biodegradable polymer composite in some industries including biomedical engineering and plastic industry. With advancements in technology and expertise, polymer-based materials have emerged as promising options for various applications. However, the inherent low mechanical properties and strength of non-reinforced polymers limit their potential uses [11] The mechanical properties of the matrix material are vital for the load-bearing performance of the reinforcing components in composite structures.

In a polymer matrix composite, reinforcement is incorporated to enhance the strength and stiffness of the matrix, as opposed to solely improving fracture toughness, which is more common in ceramic matrix composites. The presence of reinforcement enables the composite to withstand mechanical loads experienced during service. Examples of thermoset polymer matrix include vinyl esters, epoxies and polyamides. They are highly favoured in fibre-reinforced composites applications due to their excellent dimensional stability and high heat resistance, which can be attributed to their robust three-dimensional crosslinked structure. Over the years, significant progress has been made in enhancing the toughness and expanding the working temperature range of thermosetting composites. These advanced composites surpass metals in terms of specific strength and stiffness, making them a preferred choice in many industries [11].

Thermoplastic polymer matrix is the second class of polymeric matrix and it is considered to unfavourable at a high temperature where thermoset polymer shine. This quite limit its usage despite its great characteristics which include high toughness, flexibility and recyclability. Examples of thermoplastic matrix are polyetheretherketone (PEEK), polyethylene (PE), polypropylene(PP), polycarbonate (PC) and polyphenylene sulphide (PPS). PP was used in this study,

Ceramic materials excel in multiple aspects compared to traditional steel, plastic, or non-ferrous materials. They boast high hardness, exceptional wear resistance, impressive compressive strength, substantial electrical resistance, and robust corrosion resistance [37] and at high temperature as conspicuously shown in figure 2-6.

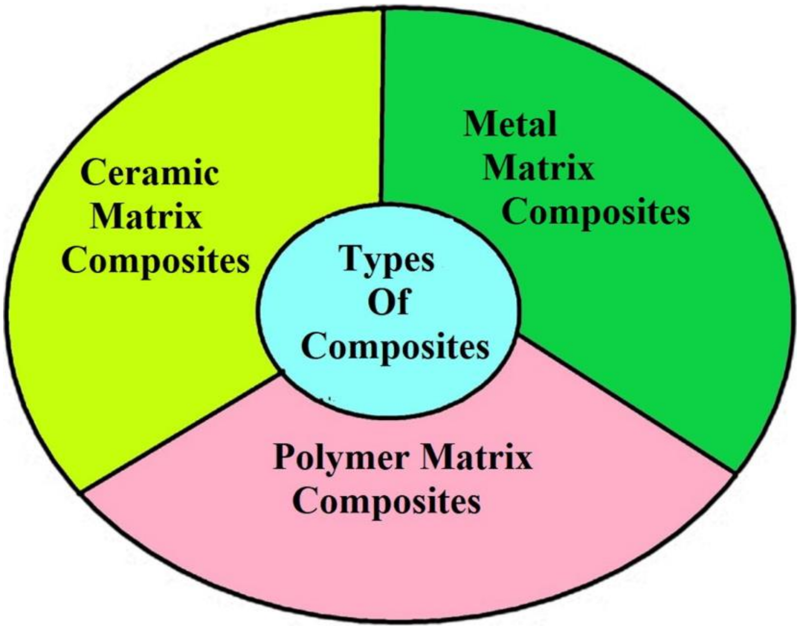

Figure 2-5: Type of composites. Source: [11]

To overcome the brittle fracture behaviour and lack of toughness in monolithic ceramics, advanced ceramic matrix composites (CMCs) have been developed. These composites incorporate high-performance fibres and optimise the fibre-matrix interface. As a result, they exhibit improved fracture strength, toughness, high-temperature resistance, flame retardancy, enhanced friction and wear performance, and reduced mass density. Figure 2-6 shows its dominance at high temperatures above metallic matrix composite and polymeric composite. CMCs can be categorised into two material systems: oxide-based and non-oxide-based. Oxide-based CMCs consist of an oxide fibre and an oxide matrix. On the other hand, non-oxide CMCs can be composed of carbon fibres (CFs) with a carbon matrix, CFs with a silicon carbide (SiC) matrix, or SiC fibres with a SiC matrix. Non-oxide.

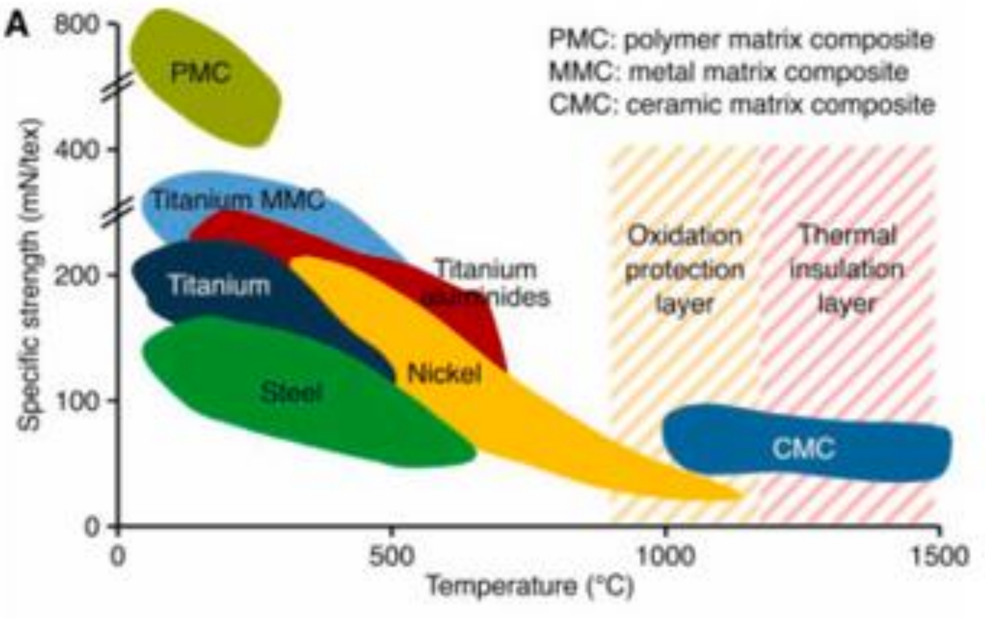

Figure 2-6:Thermo-mechanical properties of different classes of composite. Source: [37]

2.4.Micromechanics Modelling Framework

Homogenization techniques facilitate the characterization of a heterogeneous elastic material at the microscale by approximating it to an equivalent homogeneous elastic material at the macroscale. This simplification allows for a more manageable analysis and understanding of the material's behaviour [38].While conventional homogenization is essential, it falls short of accurately describing the mechanical response when the material's heterogeneity is comparable to the scale being analysed. In such cases, conventional homogenization methods struggle to capture the intricate behaviour of the material at the macroscale. When the microstructure contains small levels of heterogeneity or the macroscopic length scale is infinitely large, classical homogenization techniques provide a satisfactory estimation of the average macroscopic properties. In such cases, the conventional homogenization approach effectively captures the overall behaviour of the material at the macroscale. The conventional homogenization technique is inadequate when the size of the heterogeneity is comparable to the scale of the macroscopic problem. In such cases, the traditional homogenization approach fails to accurately capture the behaviour of the material at the macroscale [38].

Homogenization, a key issue in the mechanics of materials, pertains to determining the effective response within a representative volume element (RVE) [39]. It was reported that homogenization can be done using different approaches, one is the use of finite element to simulate the RVE while another approach is asymptotic homogenization. Mean field homogenization (MFH) methods are also a viable method [39]. In this study, the homogenization approach adopted was the simulation of the microstructure using RVE of the materials studied, which was done using FE. When conducting calculations and analysis exclusively at the representative volume element (RVE) level within the linear elastic domain, some arguments, such as approximate stress localizations, may criticise the use of mean-field homogenization (MFH) methods. However, one crucial advantage that is often overlooked is the ease with which microstructure generation, including the setup of the RVE, can be accomplished using MFH methods. These methods excel in accounting for specific fibre orientation distributions (FOD), even at high fibre volume fractions (sometimes exceeding 50%). In contrast, alternative methods often encounter difficulties in generating and meshing the microstructure, making the application of MFH methods significantly more convenient in such cases [39]. MFH formulations provide a wide range of opportunities for modelling damage, defects, and non-linear behaviour. It must be noted that despite the increase in computational resources, techniques such as the Fast Fourier Transform or model order reduction have made linear homogenization more affordable in terms of computation. However, when it comes to full-field simulations in the nonlinear regime, the computational cost remains considerably high [39]. Elmasry et al. [40] has summarised the different methods in multi-scale modelling in figure 2-7, classifying them into ease of modelling and accuracy. Figure 2-8 summarises the processes involved in homogenization.

However, these formulations enable the analysis of composites with varying fibre architectures and offer insights into the behaviour of materials with damage and defects [39]. Eshelby assumed the inclusion is ellipsoidal which more often not the situation for most fibres. Consequently, a transformation of the fibre into an equivalent ellipsoidal inclusion(s) is required when applying MFH methods. It is however important to note that selecting the appropriate MFH scheme is a non-trivial task and depends on various factors, including the suitability for specific fibre parameters (architecture, length, and volume fraction), adherence to physical admissibility requirements, and consideration for accuracy. With a wide array of MFH formulations available, each variant is based on specific simplifications regarding interactions between different inclusions. The understanding of the fibre orientation distribution (FOD) is important before the Eshelby transformation is done [39] Usually, this is experimentally established. Elmasry et al. [41] reported to have used SEM (scanning electron microscope) to determine the FOD for glass fibre while Raman spectrometry was used to obtain the FOD for graphene platelet (GPLs).

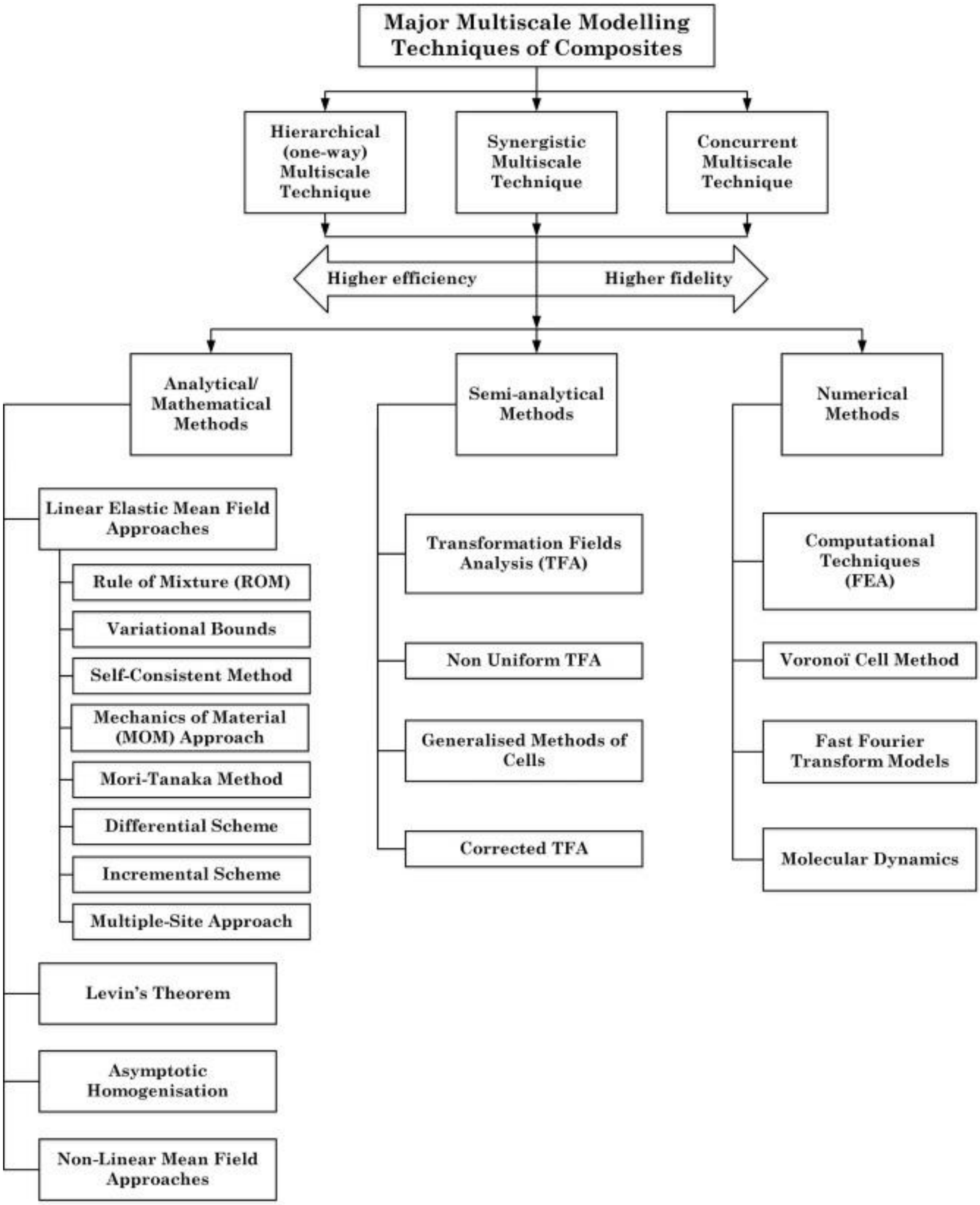

Figure 2-7: Illustration of the major multiscale approaches of composite. Source[40]

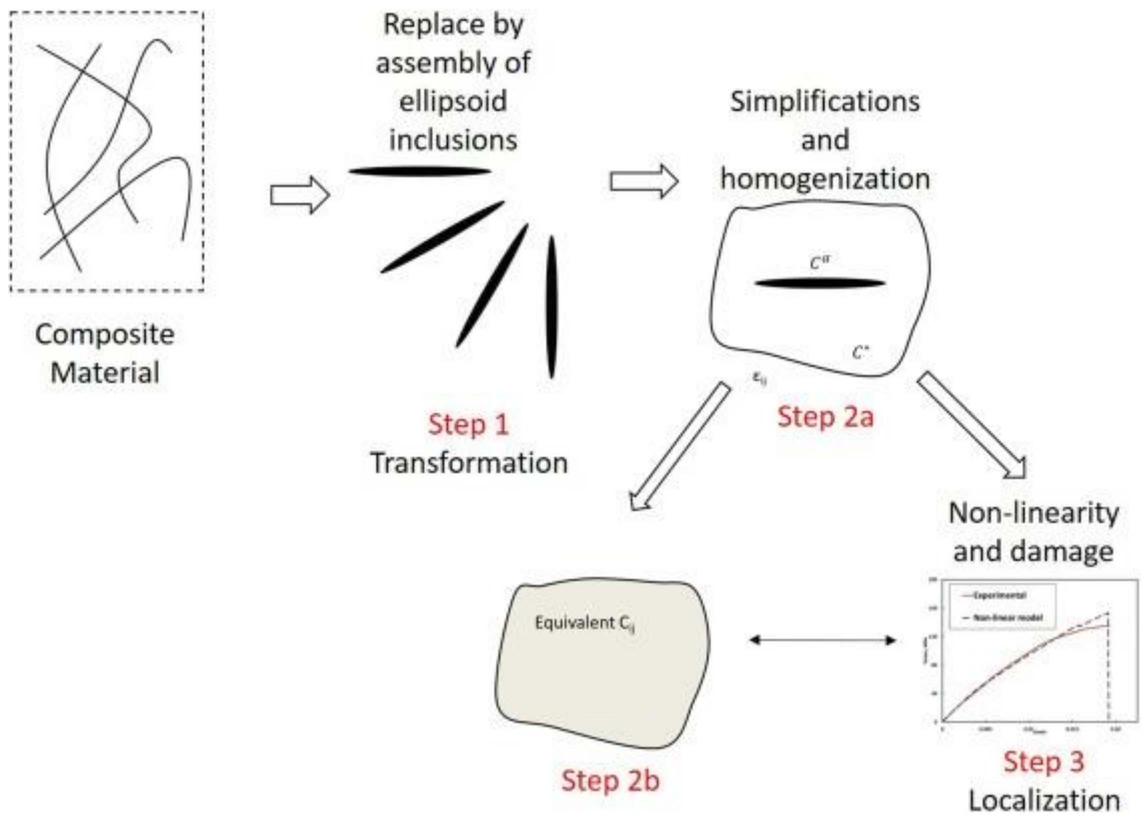

Figure 2-8: Summary of homogenization process. Source [39]

Similarly, Barteau et al. [2] used SEM to determine the randomness of the investigated fibres shown in figure 2-9. However, it was reported to be commonly assumed to be random in the absence of the experimental understanding of the FOD.

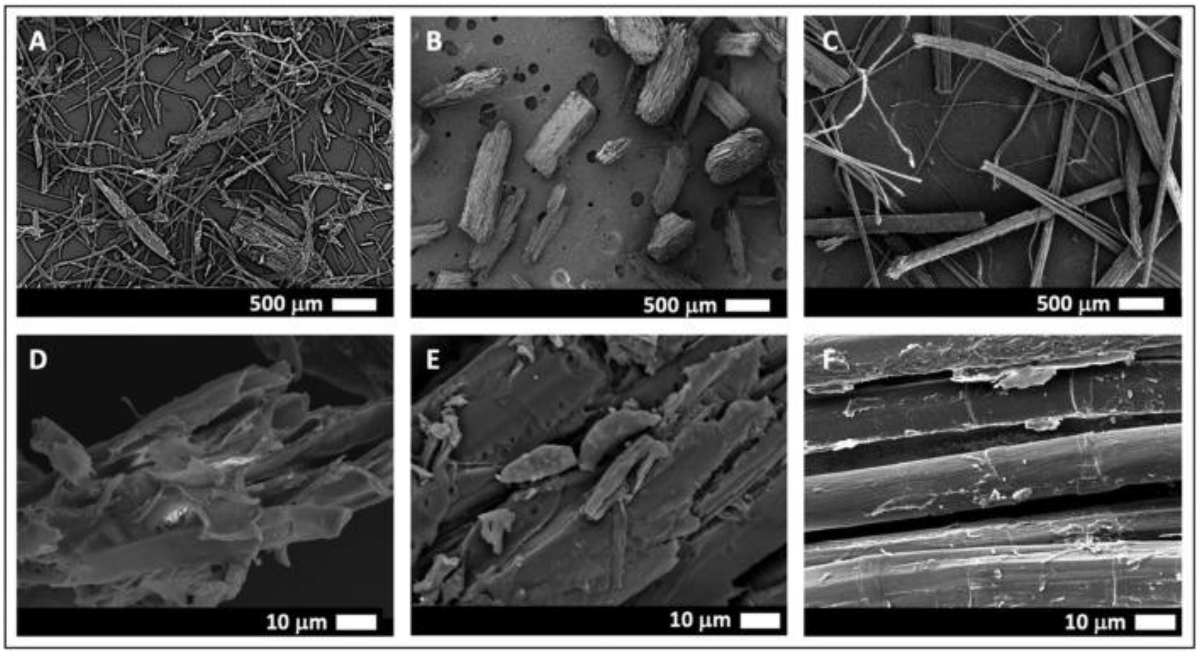

Figure 2-9: Scanning electron microscopy (SEM) of WoodForce (A, D), Vegetal Technic (B, E) and Flax fibres (C, F). Source [2]

The linear distribution function (LDF) which gives information about the aspect ratio of the fibre is also necessary [39] but it is usually ignored, hence, the average length is often adopted. A comprehensive investigation of the length distribution function (LDF) demonstrated that disregarding length distributions can result in notable errors in the effective stiffness. Likewise, [39] and [42] conducted a study where carbon nanotubes were modelled as straight inclusions, and it was found that averaging the length of the nanotubes led to errors exceeding 30%.
The fibre volume fraction (V_f) is computed using equation (2.1)

$$V_f = \frac{1}{V_f}\sum_{i=1}^{N} l_i \frac{\pi d^2}{4} \tag{2.1}$$

As highlighted earlier that natural fibres are vulnerable to moisture, which chemical treatment has been reported to be efficient. It is necessary to note that the presence of the coating needs to be modelled to better capture its influence on the properties of the composite. Jain [39] reported similar thing, and suggested a simplifying assumption which is to treat coatings as individual inclusions and apply MFH methods to analyse their effect. Cherkaoui et al. [43] proposed multilevel and multistep homogenization approach to capture this effect. Homogenization typically involves establishing a relationship between the effective stiffness (C^{eff}) of the composite material and the strain concentration tensor, A^{α}, associated with the inclusions [39] computed with equation 2.2.

$$C^{eff} = C^m + \sum_{\alpha=1}^{M} C_{\alpha}(C^{\alpha} - C^m)A^{\alpha} \tag{2.2}$$

Where C^m is the stiffness of the matrix and C_{α} is the inclusion stiffness. The analytical formulation adopted for the analytical validation was based on the Mori-Tanaka Homogenization scheme. The adopted formation is briefly highlighted. It is common to describe a composite as a bi-phase material or a multi-phase material. Where the matrix is known to be one phase and is regarded as the continuous phase, while the inclusions or fibres are another phase and are regarded as a discontinuous phase. The major differences between the bi-phase and the multi-phase are that the bi-phase is when the composite comprises just one type of matrix and fibre, while the multi-phase is when there is more than one matrix and/or more than one fibre. Although having more than one matrix is quite rare, there is more than one fibre in the case of hybrid composites.
Elmasry et al.[41] indicated that at the microscopic scale, individual constituents within a material undergo localised strain, which is represented by the variable a(r) was first echoed by Eshelby [7]. To find the stress in both the inclusion and fibre, Eshelby [7] assumed that the matrix is under uniform microstrain (thermal, kinematic perturbation) such that when a portion

of the matrix is cut and removed from the composite, the microstrain disappears and the shape distortion is allowed. When the matrix is returned back into the opening with surface traction applied, the stress in the matrix is annulled and remains constant in the inclusion. This is mathematically described by Elmasry et al. [41] in equation 2.3 where the total strain in RVE is said to be summation of elastic strain and thermal strain at each local point in the composite.

$$\epsilon(r) = \epsilon^E(r) + \varepsilon^T(r) \qquad (2.3)$$

To obtain total stress of the RVE, the constitutive law (hook's law) which relate the strain at each local point to stress at the point is defined mathematically by equation 2.4 where the coefficient of thermal expansivity relate the thermal strain and the thermal stress $\beta(r)$ was defined in equation 2.5.

$$\sigma(r) = c(r) : \varepsilon(r) - \beta(r)\Delta T \qquad (2.4)$$

$$\beta(r) = c(r) : \alpha(r) \qquad (5)$$

The process of transitioning from the macroscopic to the micromechanical scale involves the localization of the macroscopic strain tensor E using fourth-order global strain concentration tensors A(r) and second-order global strain concentration tensors a(r). Further, the homogenization process involves using the average method to predict the macroscopic response. These conversion factors, A (r) and a (r), are said to be unknown [41]. The RVE thermo-mechanical properties can be obtained based on average theorem. Hill [44] and Mandel 1971 definition for the effective thermo-mechanical properties of RVE based on average theorem are defined in equations 2.6 and 2.7.

$$C^{eff} = \frac{1}{V}\int_V C(r) : A(r)dV \qquad (2.6)$$

$$\beta^{eff} = \frac{1}{V}\int_V \beta(r) - c(r) : a(r)dV \qquad (2.7)$$

On the basis that the global strain concentration tensor A(r) relate the local strain to the macro/global strain of the RVE, therefore, the local in equation 1 above is substituted into equations 2.8 and 2.9.

$$\sigma(r) = c(r) : \varepsilon(r) - \beta(r)\Delta T \qquad (2.8)$$

$$\varepsilon(r) = A(r) : \mathrm{E} + \Delta T a(r) \qquad (2.9)$$

Just as every structural system can be said to have a steady state and fluctuating state the local thermo-mechanical properties have these two components are as described by Elmasry et al [41] described in equation 2.10 and 2.12.

$$c(r) = c^R - \delta c(r) \qquad (2.10)$$

$$\beta(r) = \beta^R - \delta\beta(r) \qquad (2.11)$$

To solve these problems, some ingredients are needed, which are the static equilibrium equations and the equation of kinematic equilibrium (compatibility of deformation). Ahaouari [45] and Ahaouari et al. [46] has previously established solution to the equation shown in equation 2.12

$$\varepsilon(r) = E^R - \int_V \Gamma(r - r') : \; [\delta c(r') : \varepsilon(r') - \Delta T \delta\beta(r')] dV' \tag{2.12}$$

where the strain field within the infinite medium is subjected to the same boundary conditions as the RVE and $\Gamma(r - r')$ is reported as the modified Green tensor. Since the importance of the yet unknown global strain concentration tensor to the determination of the RVE global stress from the local stress in the RVE has been highlighted, therefore it is very relevant to understand it. Kpobie et al.[47] identified that the global strain concentration tensor A (r) and second-order global strain concentration tensor is computed as follows 2.13 - 2.20:

$$\mathrm{A}' = \zeta' : (\overline{\zeta'})^{-1} \tag{13}$$

$$\mathrm{A}' = \mathrm{I} \quad) \tag{14}$$

$$\mathrm{a}' = \beth' - \mathrm{A}' : \overline{\beth'} \tag{15}$$

$$\overline{\mathrm{a}'} = 0 \tag{16}$$

$$\beth'_{(0)} = (\mathrm{I} + \mathrm{T}'' : (\mathrm{c}' - \mathrm{c}^{\mathrm{R}}))^{-1} \tag{17}$$

$$\beth'_{(0)} = \beth'_{(0)} : \mathrm{T}'' : \Delta\beta' \tag{18}$$

$$\zeta'_{(\mathrm{i}+1)} = (\mathrm{I} + \mathrm{T}'' : (\mathrm{c}' - \mathrm{c}^{\mathrm{R}}))^{-1} \tag{19}$$

$$: \left(\mathrm{I} - \sum_{\substack{\mathrm{i}=0 \\ \mathrm{j}\neq 1}}^{\mathrm{N}} \mathrm{T}^{\mathrm{IJ}} : (\mathrm{c}^{\mathrm{J}} - \mathrm{c}^{\mathrm{R}}) : \zeta'_{(\mathrm{i})} \right)$$

$$\beth'_{(\mathrm{i}+1)} = \left(\mathrm{I} + \mathrm{T}'' : (\mathrm{c}' - \mathrm{c}^{\mathrm{R}})\right)^{-1} : [\mathrm{T}^{\mathrm{IJ}} \tag{20}$$

$$: \Delta\beta' + \sum_{\substack{\mathrm{i}=0 \\ \mathrm{j}\neq 1}}^{\mathrm{N}} \mathrm{T}^{\mathrm{IJ}} : (\Delta\beta') - (\mathrm{c}^{\mathrm{J}} - \mathrm{c}^{\mathrm{R}}) : \beth'_{(\mathrm{i})}) \,]$$

$$\mathrm{I} = 0, 1, 2, \ldots.\mathrm{N}$$

Elmasry [41] reported that T^{ii} and T^{ij} represent the interaction tensor between matrix and inclusion (one-site) and interaction between individual inclusion (multi-site), respectively. Recall that one site is when the interaction between the discontinuous phase and the continuous phase is studied, while multi-site includes the study of the interactions between the discontinuous phases. As said earlier, the one-site situation is less computationally expensive, which makes it preferred by several researchers. Even when multi-site is recognised as significantly relevant for hybrid composites like the hybrid of flax and vegetal technology being studied, the computational cost informed the decision to ignore it for one-site modelling. The equation to compute multisite and one-site computation is 2.21 and 2.22 respectively.

$$T^{ij}(c') = \frac{1}{V^{I}}\int_{v^{I}} \int_{v^{J}} \Gamma(r - r^{J})\, dV'dV \quad (21)$$

$$T^{II}(c') = \frac{1}{V^{I}}\int_{v^{I}} \int_{v^{I}} \Gamma(r - r^{J})\, dV'dV \quad (22)$$

Elmasry et al.[41] re-echoed that aligned long inclusions in an isotropic matrix result in a transversely isotropic composite. An isotropic fourth order tensor can be averaged to an isotropic tensor, as shown below by Doghri and Ouaar [48]; Torquato [49] and Torquato et al. [50] using equations 2.23 – 2.27.

$$\Gamma_{ijkl}^{iso} = \left(\frac{1}{3}\Gamma_{iijj}^{ani}\right)\left(\frac{1}{3}\delta_{ij}\delta_{kl}\right) + \frac{1}{5}(\Gamma_{ijji}^{ani} - \frac{1}{3}\Gamma_{iijj}^{ani})(\frac{1}{2}(\delta_{ik}\delta_{jl} + \delta_{il}\delta_{jk}) - \frac{1}{2}\delta_{ij}\delta_{kl}) \quad (23)$$

$$\Gamma_{ij}^{iso} = \frac{1}{3}\Gamma_{ii}^{ani}\delta_{ij} \quad (24)$$

$$C^{MMT} = \sum_{I=0}^{N} V_I C^I : A^I = C^0 + \sum_{I=1}^{N} v_I (c^J - c^R) : A^I \quad (25)$$

$$\beta^{MMT} = \sum_{I=0}^{N} V_I [\beta^I - (c^I - c^0) : a^I] \quad (26)$$

$$= \beta^0 + \sum_{I=1}^{N} v_I [(\Delta\beta^I) - (c^J - c^0) : a^I$$

$$\alpha^{MMT} = (C^{MMT})^{-1} : \beta^{MMT} \quad (27)$$

The nonlinear behaviour of the composite was evaluated using the classical J2 plasticity model described in equations 2.28, 2.29, 2.30 and 2.31.

$$\sigma = (1 - D)C^{vl} : (\varepsilon - \varepsilon^{r}) \quad (28)$$

$$f(\sigma, R, D) = J_2\left(\bar{\sigma} - R(r) - \sigma_{\gamma}\right) \quad (29)$$

$$\mathrm{r} = \dot{p}\widehat{N}.\dot{p}\sqrt[2]{\left(\frac{2}{3}\, p : p\right)} \quad (30)$$

$$\dot{D} = (\frac{Y}{S_0})^{s}\, \dot{p}ip \geq p_e \; and\; D \leq D_e \quad (31)$$

3. MATERIALS AND METHODS

The focus of this research is to study the mechanical and thermal properties of thermoplastic composites reinforced with four different natural fibres: flax, Vegetal-technic, Wood-force, and a hybrid of Flax and Vegetal-technic. The thermoplastic matrix used is polypropylene (PP). Both the properties of the fibres, including the volume fraction and aspect ratio, are shown in Table 3.1, while Table 3.2 shows the properties of the thermoplastic matrix (PP).

Table 3-1: Equivalent fibres length LEFI, equivalent fibres diameter DIFI and aspect ratio of three not injected samples (Virgin WF, virgin VT, virgin Flax) and four samples after the first injection cycle (PP-Flax, PP-VT, PP-WF, PP-VT/Flax. Source [2]

Sample	Fibre length LEFI (μm)	Fibres diameter DIFI (μm)	Aspect ratio L/D
Virgin Flax	2.060 ± 626	64.3 ± 33.9	37.5
Virgin VT	1,054 ± 402	87.5 ± 33.2	9.1
Virgin WF	1,386 ± 893	30.8 ± 14.6	17.5
PP-Flax cycle 0	1,021 ± 737	27.2 ± 14.6	37.5
PP-VT cycle 0	979 ± 322	107.4 ± 38.0	9.1
PP-WF cycle 0	727 ± 572	42.0 ± 42.1	17.5
PP-VT/Flax cycle 0	745 ± 625	40.4 ± 32.6	18.5

Table 3-2: Flax and polypropylene (PP) matrix properties. Source (1)

<table>
<tr><th colspan="6">Matrix (Polypropylene)</th><th colspan="3">Inclusions (flax)</th></tr>
<tr><th rowspan="2">Youngs modulus E (MPa)</th><th colspan="2">Hardening parameters</th><th colspan="2">Damage parameters</th><th rowspan="2">Yield stress σ_Y (MPa)</th><th rowspan="2">Young modulus E (MPa)</th><th rowspan="2">Poisson’s ratio ν</th><th rowspan="2">Aspect ratio AR</th></tr>
<tr><th>k (MPa)</th><th>m</th><th>So</th><th>s</th></tr>
<tr><td>1576</td><td>135</td><td>0.51</td><td>4</td><td>0.1</td><td>7</td><td>52500</td><td>0.498</td><td>37.5</td></tr>
</table>

The flax fibre adopted is botanically described as Linum usitassinum L., Aliz´e variety. The vegetal-technic (VT) fibre is a fibre made from logs of hardwood from France, while the woodforce fibre is a fibre from softwood produced by Sonae Arauco (Maia, Portugal) [2]. In this study, the study of the thermo-mechanical properties was done numerically and analytically. For the numerical study, a cubic RVE was developed using DIGIMAT [10] (commercial software). Different RVEs were generated for long fibres in different orientations (axes) and random orientations (see figures 3-1, 3-2, 3-3 and 3-4 for a typical RVE model) in accordance with the aspect ratios and volume fractions summarised in table 4. DIGIMAT [9] automatically applied periodic boundary conditions to constrain the opposite faces of the RVE; boundary conditions were applied, and traction was applied in the form of displacement with respect to whether a shear or normal stress is of interest. See plates 1 for the RVE with boundary conditions and loads applied. The boundary condition is defined in detail in tables 6–11. The generated model from DIGIMAT [9] was imported into Abaqus software (a commercial software developed by Dassault Systems). Then the simulations were run on the different models. A Python script was used for post-processing to obtain properties of interest.

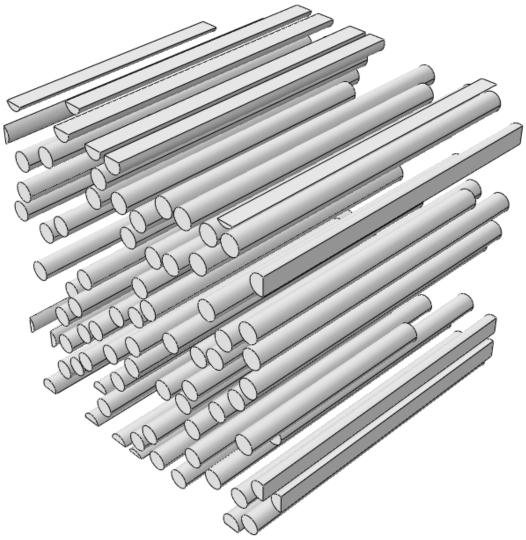

Figure 3-1: Isolated long aligned flax fibre from the thermoplastic composite RVE.

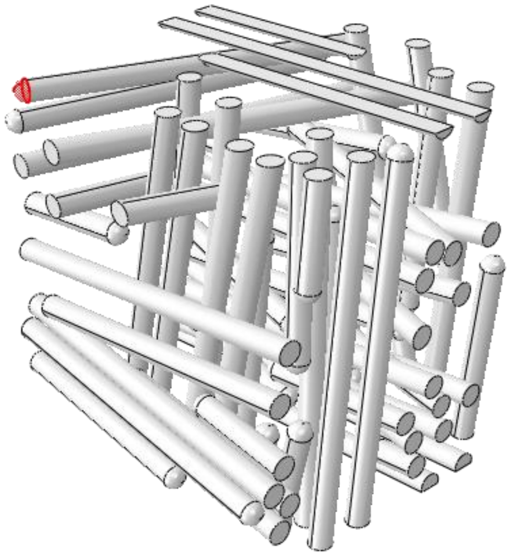

Figure 3-2: Isolated long random flax fibre from the thermoplastic composite RVE.

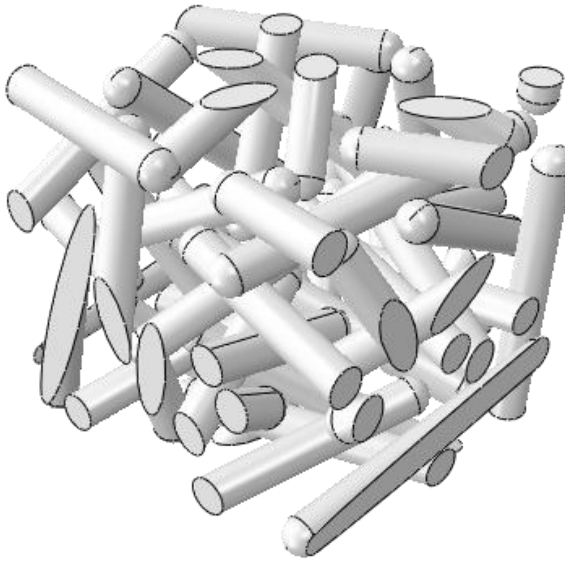

Figure 3-3: Isolated short random vegetal-technic fibre from the thermoplastic composite RVE.

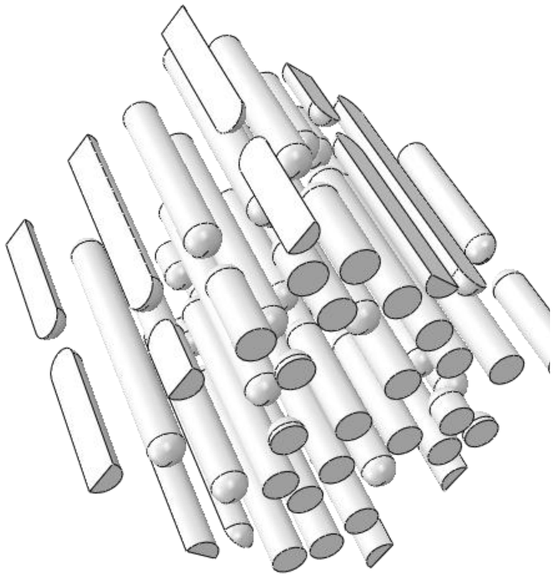

Figure 3-4: Isolated long aligned wood-force fibre from the thermoplastic composite RVE.

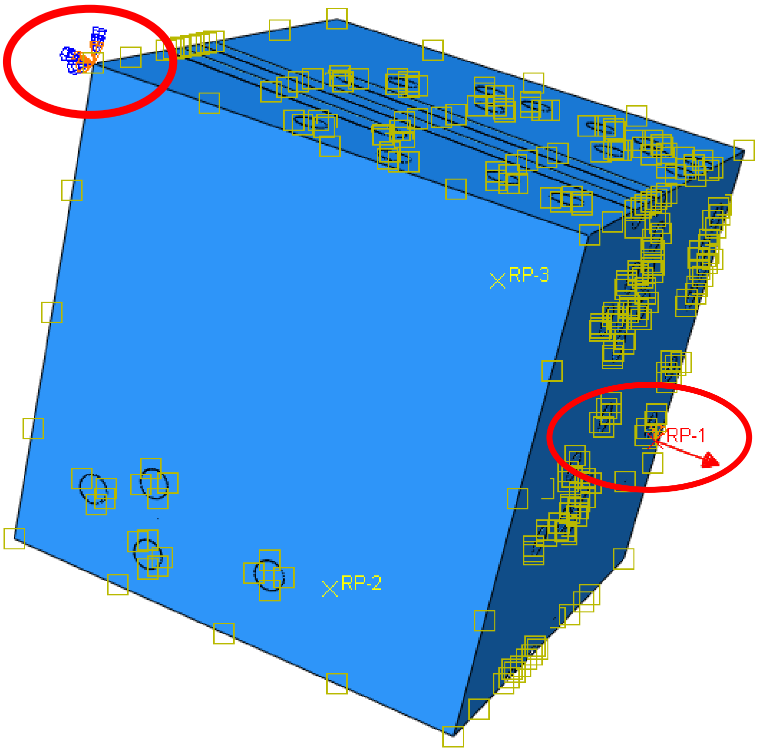

Plate 3-1:Typical RVE model with boundary condion and load

3.1.Boundary condition

As previously stated above, different loading conditions were applied depending on the properties of interest; therefore, it is necessary to explicitly highlight how they were applied. It is necessary to highlight that the axes of the DIGIMAT [9] differ from those of the Abaqus software; the axes (1(X), 2(Y), and 3(Z)) of the DIGIMAT [10] correspond with the Abaqus axes (Z(3), Y(2), and X(1)), respectively. The fibre in the 0 direction aligns with the Z(3) axis in Abaqus. As mentioned earlier, DIGIMAT [9] was used to model the RVE, and DIGIMAT [9] constricted each face by creating one reference point on one of the two opposite faces named RP1, RP2, and RP3. The summary of the load applied and the corresponding boundary condition is provided in tables 3-3, 3-4, 3-5, 3-6, 3-7, and 3-8.

Table 3-3:Summary of boundary conditions applied - Traction XX – direction on Abaqus

Boundary condition name	DIGIMAT notation	Abaqus notation	Displacement
BC-1	BC-1	Point 1	Fixed (U1=U2=U3=0)
BC-2	RP 4	RP1	U1 = 0.18
BC-3	RP 4	RP1	U2 = 0
BC-7	RP5	RP2	U3 = 0
BC-8	RP6	RP3	U1 = 0

Table 3-4:Summary of boundary conditions applied - Traction YY – direction on Abaqus

Boundary condition name	DIGIMAT notation	Abaqus notation	Displacement
BC-1	BC-1	Point 1	Fixed (U1=U2=U3=0)
BC-3	RP 4	RP1	U2 = 0
BC-6	RP 5	RP2	U2 = 0.18
BC-7	RP5	RP2	U3 = 0
BC-8	RP6	RP3	U1 = 0

Table 3-5: Summary of boundary conditions applied - traction ZZ – direction on Abaqus

Boundary condition name	DIGIMAT	Abaqus	Displacement
BC-1	BC-1	Point 1	Fixed (U1=U2=U3=0)
BC-3	RP 4	RP 1	U1 = 0
BC-10	RP 6	RP 3	U2 = 0.18
BC-7	RP 5	RP 2	U3 = 0
BC-8	RP 6	RP 3	U1 = 0

Table 3-6:Summary of boundary conditions applied - shear XY – direction on Abaqus

Boundary condition name	DIGIMAT	Abaqus	Displacement
BC-1	BC-1	Point 1	Fixed (U1=U2=U3=0)
BC-3	RP 4	RP 1	U2 = 0
BC-5	RP 5	RP 2	U1 = 0.18
BC-7	RP 5	RP 2	U3 = 0
BC-8	RP 6	RP 3	U1 = 0

Table 3-7: Summary of boundary conditions applied - shear YZ – direction on Abaqus

Boundary condition name	DIGIMAT	Abaqus	Displacement
BC-1	BC-1	Point 1	Fixed (U1=U2=U3=0)
BC-3	RP 4	RP 1	U2 = 0
BC-7	RP 5	RP 2	U3 = 0
BC-8	RP 5	RP 2	U1 = 0
BC-9	RP 6	RP 3	U1 = 0.18

Table 3-8: Summary of boundary conditions applied - shear XZ – direction on Abaqus

Boundary condition name	DIGIMAT notation	Abaqus notation	Displacement
BC-1	BC-1	Point 1	Fixed (U1=U2=U3=0)
BC-3	RP 4	RP 1	U2 = 0
BC-4	RP 4	RP 1	U3 = 0.18
BC-7	RP 5	RP 2	U3 = 0
BC-8	RP 6	RP 3	U1 = 0

3.2.Post-processing

To obtain the effective properties from the Abaqus model, a python script was used to post-process the result contained in the Abaqus Output Database (ODB) to compute properties such as elastic modulus in the three directions (E_{11}, E_{22}, and E_{33}), shear modulus (G_{13}, G_{23}, and G_{12}), Poisson ratio (ν_{12}, ν_{23}, ν_{13}), and coefficient of thermal expansion (CTE) of each of the materials. Numerically, the properties were computed from the RVE model. Recall that the RVE of the composite consists of matrix and fibre. The formula operated in the script to obtain the highlighted properties is stated below, which operated on each of the gauss points in the volume element of the meshed RVE. The composite's effective properties are computed as an aggregate of the properties of the fibres and the matrix. The formula is similar to the equations used in [41]. The average stress in the matrix is computed using equation 32.

$$\text{Average stress in matrix } [\text{Av\_S\_M}] = \frac{\sum_{i=1}^{N_M} \text{IVOL(i) x S (i)}}{(\sum_{i=1}^{N_M} \text{IVOL(i)} + \sum_{j=1}^{N_f} \text{IVOL(j)})} \qquad (32)$$

A typical stress in matrix obtained from the isolated matrix from the whole RVEis shown in figures 3-5, 3-9 and 3-10 which is based on the assumption of volume average theorem. The average stress in fibre is computed using equation 33 and a typical stress in fibre shown in the isolated fibre from the

$$\text{Average stress in fibre } [\text{Av\_S\_F}] = \frac{\sum_{i=1}^{N_f} \text{IVOL(i) x S (i)}}{(\sum_{i=1}^{N_M} \text{IVOL(i)} + \sum_{j=1}^{N_f} \text{IVOL(j)})} \qquad (33)$$

whole RVE is shown in figures 3-6, 3-7 and 3-11 on the assumption of volume average theorem. For a RVE subjected to only perturbation, the global stress is computed using equation 34.

$$[\text{Glo\_P\_Stress}] = [\text{Av\_S\_F}] + [\text{Av\_S\_M}] \qquad (34)$$

while total global stress in the RVE with both thermal load and perturbation are computed using equation 35. A typical example of RVE to compute a global stress is shown in figure 3-7 and 3-12 which are a RVE that contain both fibre and matrix.

$$[\text{T\_Glo\_Stress}] = [\text{Glo\_P\_Stress}] + [\text{Ther\_S\_Stress}] \qquad (35)$$

where [Ther_S_Stress] is computed as stated in equation 36.

Ditto approach was followed to obtain the global strain in the RVE also the stress and strain caused by temperature load termed thermal global stress [Ther_S_Stress] and strain [Ther_E_Strain] in RVE respectively. The thermal global stress in the RVE is computed using equation 36:

$$[\text{Ther\_S\_Stress}] = [\text{Av\_Ther\_S\_F}] + [\text{Av\_ Ther\_S\_M}] \qquad (36)$$

The global strain [Glo_E_Strain] was computed with equation 37:

$$[\text{Glo\_E\_Strain}] = [\text{Av\_E\_F}] + [\text{Av\_E\_M}] \qquad (37)$$

While the thermal strain in the RVE is computed using equation 38

$$[\text{Ther\_E\_Strain}] = [\text{Av\_Ther\_E\_F}] + [\text{Av\_ Ther\_E\_M}] \qquad (38)$$

Recall that different boundary conditions and loading (displacement) were applied to obtain different properties of the RVE. To obtain the elastic modulus in the X-X axis, the boundary condition in table was used and equation 39 was used to compute the elastic modulus in X-X axis which was ran in a python script that operated on the Abaqus ODB for the analysis. was used and equation 39 was used to compute the elastic modulus in X-X axis which was ran in a python script that operated on the Abaqus ODB for the analysis. The Poisson ratios and the coefficient of thermal expansion ν_{xy} , ν_{xz} and α_{ct} were computed using equations 40, 41 and 42 respectively.

$$E_{xx} = \frac{\sum \sigma_{xx}}{\sum \varepsilon_{xx}} = \frac{S\_[Glo\_Stress]\ [0,0]_{xx}}{E\_[Glo\_E\_Strain]\ [0,0]_{xx}} \tag{39}$$

$$\nu_{xy} \quad -\frac{\sum \varepsilon_{yy}}{\sum \varepsilon_{xx}} = -\left(\frac{E\_[Glo\_E\_Strain]\ [1,1]_{yy}}{E\_[Glo\_E\_Strain]\ [0,0]_{xx}}\right) \tag{40}$$

$$\nu_{xz} \quad -\frac{\sum \varepsilon_{zz}}{\sum \varepsilon_{xx}} = -\left(\frac{E\_[Glo\_E\_Strain]\ [2,2]_{zz}}{E\_[Glo\_E\_Strain]\ [0,0]_{xx}}\right) \tag{41}$$

$$\alpha_{ct} = \frac{\sum \varepsilon^{T}}{\triangle T} = \left(\frac{The\_E\_Strain\ [3,3]}{Temp\_Glo}\right) \tag{42}$$

The determination of the shear response of the composite is as important as other previously highlighted properties, therefore, equation 43 was used to compute the shear responses of the RVE. Similarly, the other properties in other directions were established.

$$\mu_{xy} = \frac{1}{2}\left(\frac{S\_[Glo\_Stress]\ [0,1]_{xy}}{E\_[Glo\_E\_Strain]\ [0,1]_{xy} + E\_[Glo\_E\_Strain]\ [1,0]_{yx}}\right) \tag{43}$$

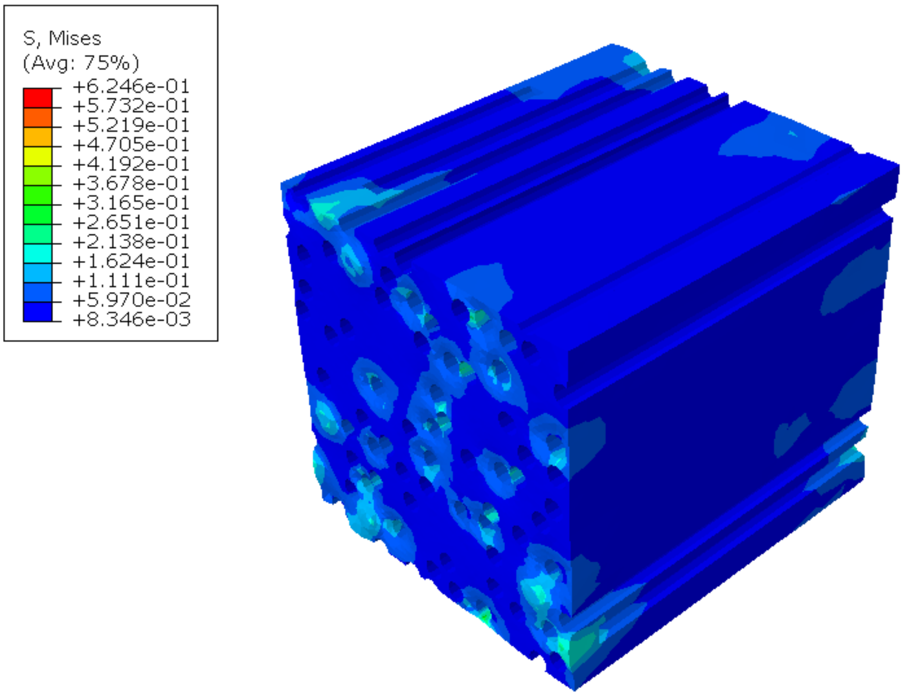

Figure 3-5:Typical contribution of matrix only (isolated) to the total stress of a RVE

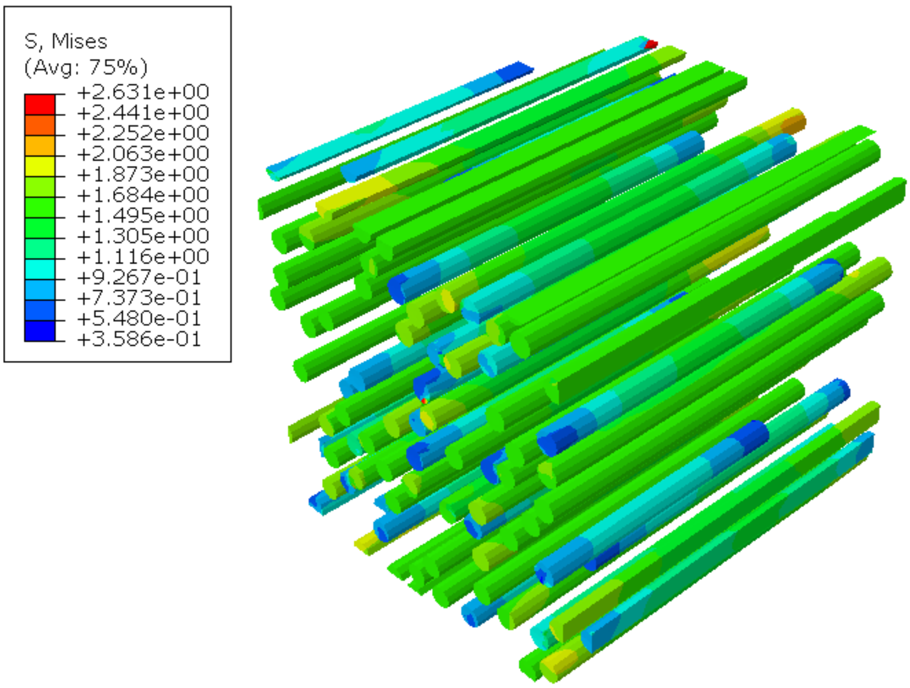

Figure 3-6: Typical contribution of fibres only (isolated) for an aligned orientation to the global stress of a RVE

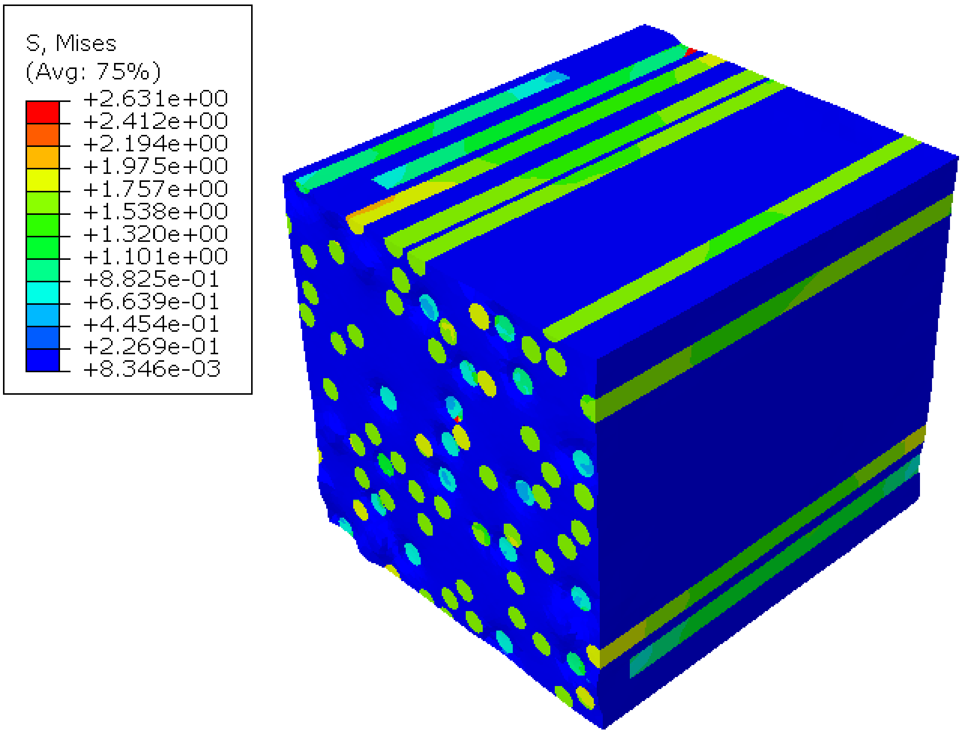

Figure 3-7: Typical total stress of an RVE (fibre + matrix)

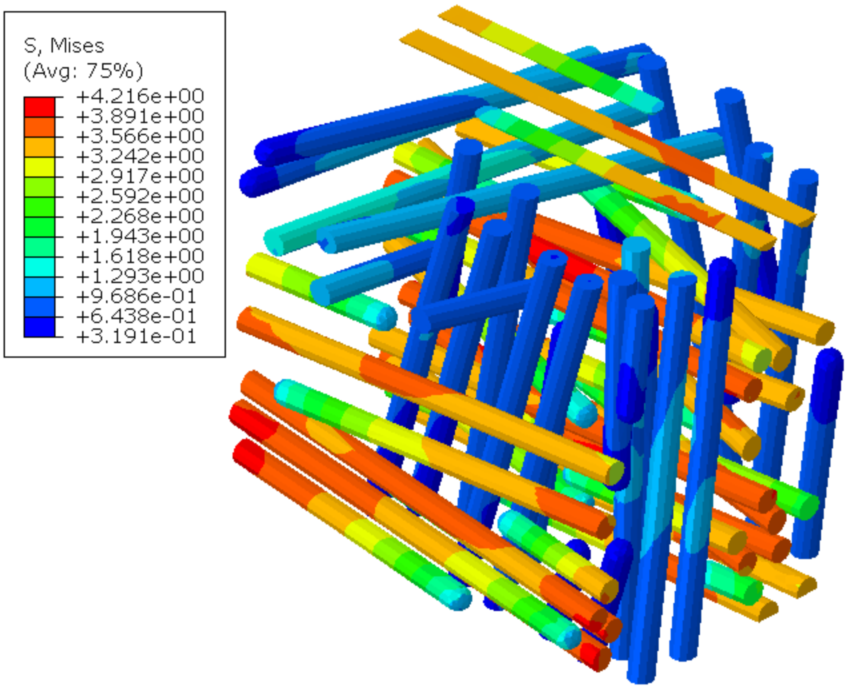

Figure 3-8: Typical contribution of fibres only (isolated) for a random orientation to the global stress of a RVE

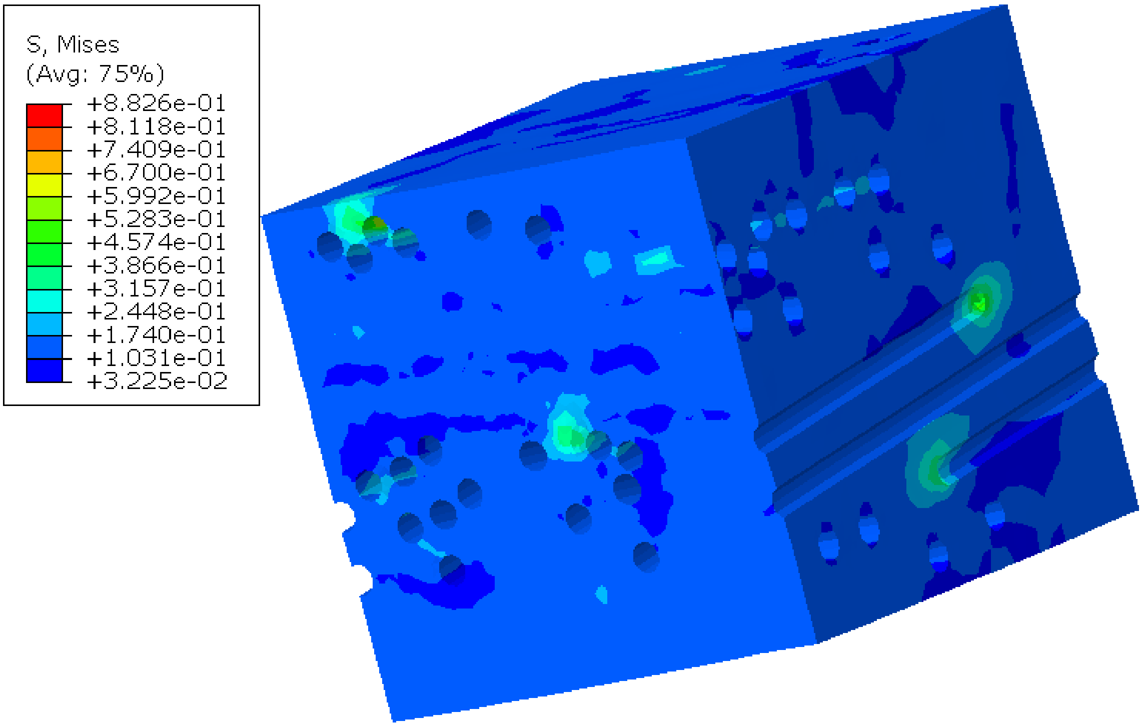

Figure 3-9:Typical contribution of matrix only (isolated) in a random composite to the total stress of a RVE

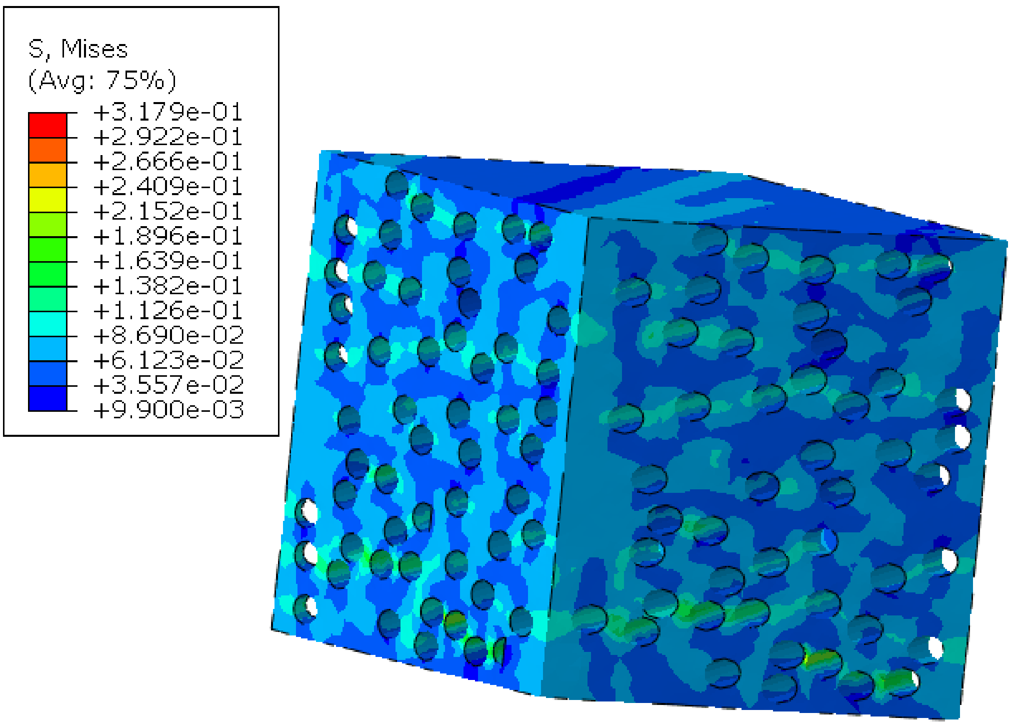

Figure 3-10: Typical contribution of matrix only (isolated) at a 45 orientation to the total stress of a RVE

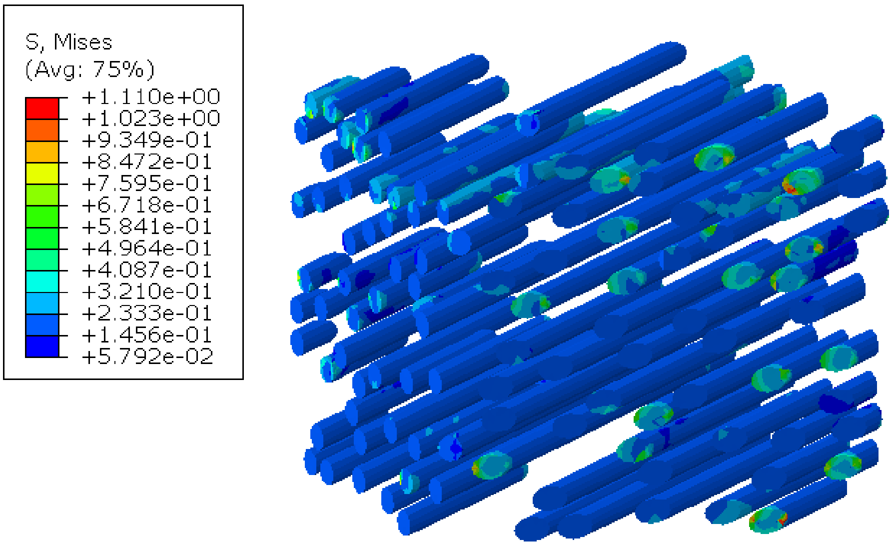

Figure 3-11: Typical contribution of fibres only (isolated) for a 45 degree orientation to the global stress of a RVE

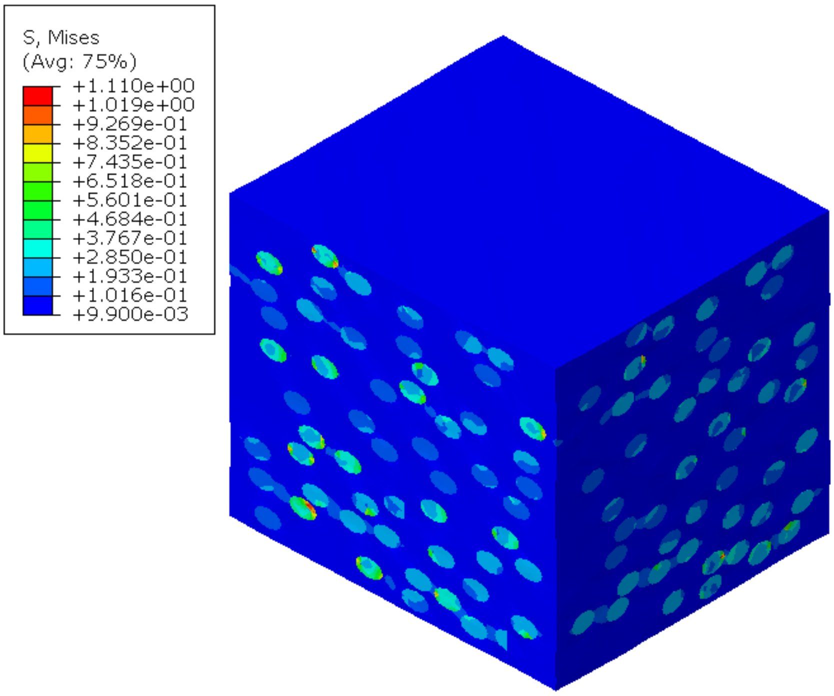

Figure 3-12: Typical total stress of an RVE (fibre + matrix) for a 45 degree oriented fibre

3.3. Application of material properties

Upon obtaining the effective thermo-mechanical properties of the studied materials, the Flax properties were used in the design of the quadcopter design shown in figures 3-13 to obtain its yield strength, strain, and acumulated plastic strain. The CAD file of the drone was imported into Abaqus CAE, and it was meshed using the C3D10 mesh type (see figures 3-14 for the meshed quadcopter). A UMAT (user defined material) was written and ran on Abaqus to determine the elasto-plastic behaviour of the composite of flax (reinforcement) and polypropylene (matrix) at varying fibre volume fractions to determine the optimum fibre volume fraction. The plastic behaviour of composites is known to be wholly contributed by the matrix, while the elastic behaviour is contributed by both the fibre and the matrix; however, flax contributes the majority of the elastic behaviour. Therefore, the plastic properties of the matrix provided in the work of Barteau et al. [2] were included in the UMAT; see table 5 (reproduced below) An isotropic hardening power law was used to model the plasticity of the composite. It is worth highlighting that this study was limited to an undamaged situation.

In the UMAT, some variables of interest were declared state variables; the accumulated plastic strain obtained is an example. The UMAT provided contains the constitutive model, while Abaqus provides the displacement incrementally in the analysis to include the different mechanical parameters such as stress, force, and strain, amongst others.

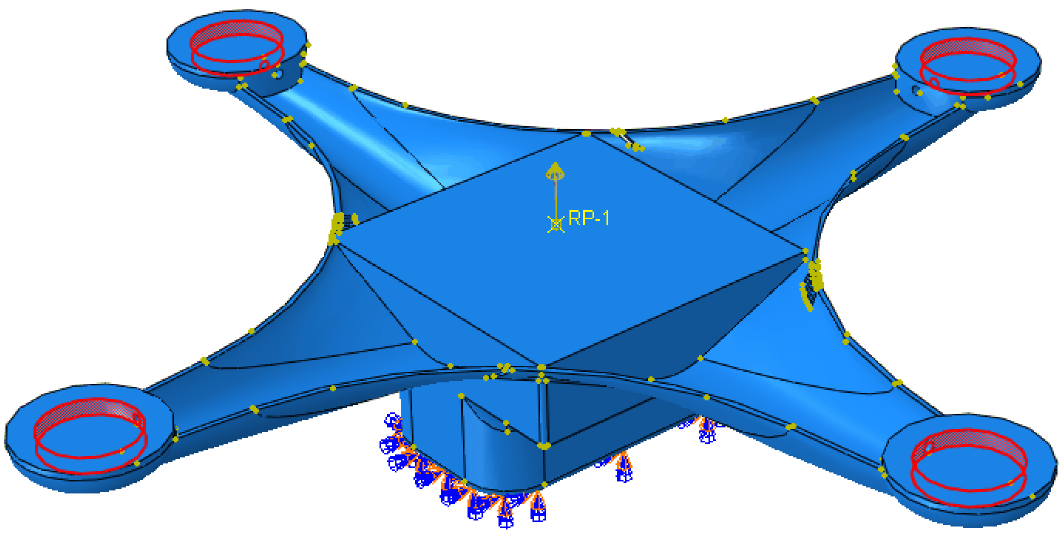

Figure 3-13:Quadcopter CAD model

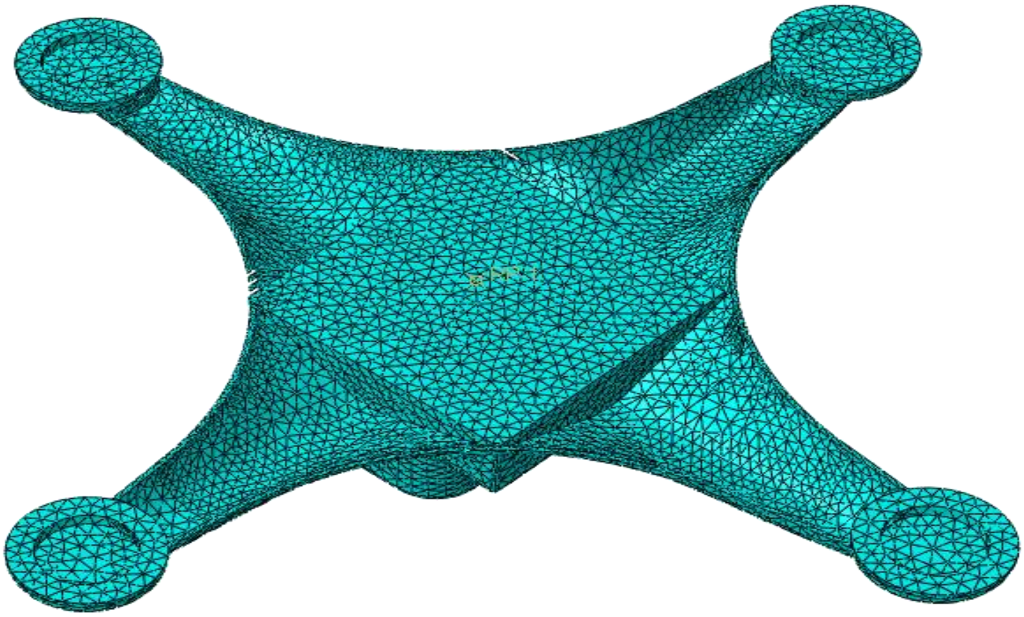

Figure 3-14:The meshed quadcopter

The classical J_2 plasticity model described in equations 28, 29, 30 and 31 reported in Barteau et al. [2] were adopted to determine the nonlinear behaviour of the polypropylene thermoplastic composite reinforced with flax fibres at different fibre volume fractions – 0.1, 0.2, 0.3, 04 and 0.5. Figure 3-15 summarise the multi-scale modelling operation.

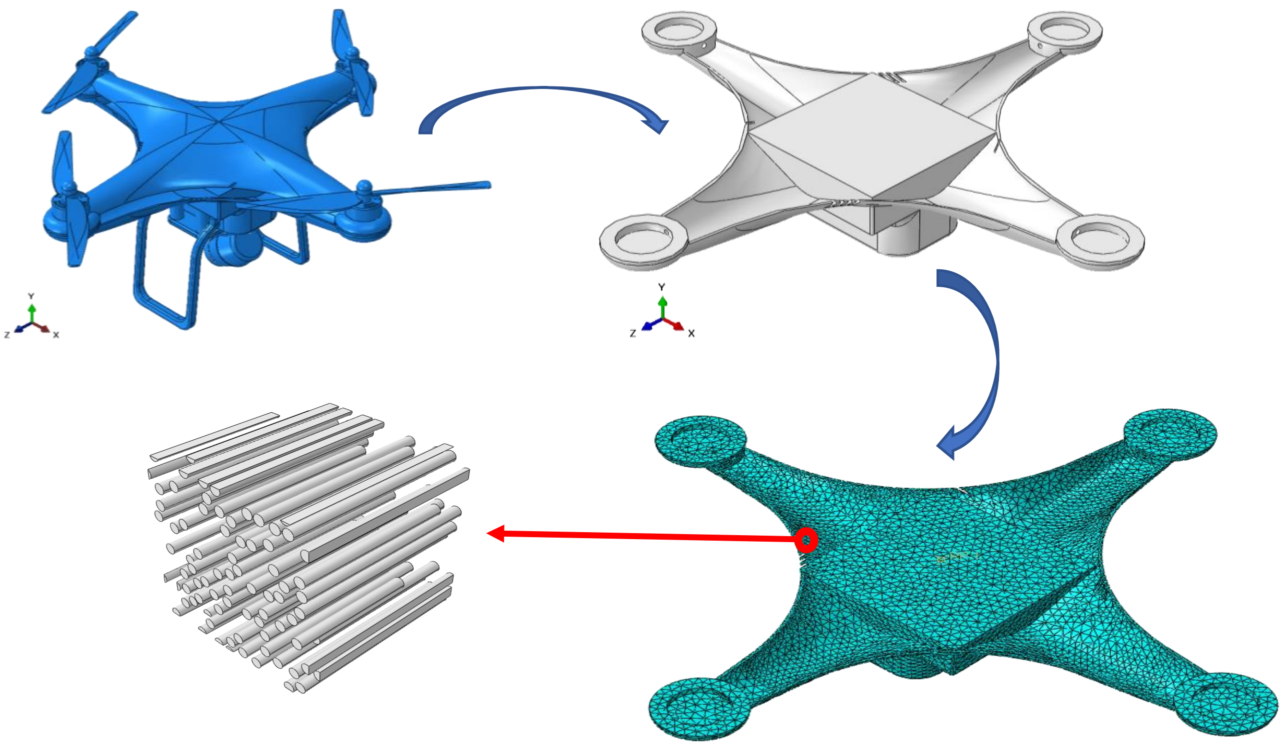

Figure 3-15: Multi-scale modelling

Table 3-9: Flax and polypropylene (PP) matrix properties. Source (1)

Matrix (Polypropylene)						**Inclusions (flax)**		
Youngs modulus E (MPa)	**Hardening parameters**		**Damage parameters**		**Yield stress σ_Y (MPa)**	**Young modulus E (MPa)**	**Poisson's ratio ν**	**Aspect ratio AR**
	k **(MPa)**	**m**	**So**	s				
1576	135	0.51	4	0.1	7	52500	0.498	37.5

4. RESULTS AND DISCUSSIONS

As established, the thermo-mechanical properties of the thermoplastic composite reinforced with natural fibres (such as Flax, Vegetal-technic, Wood-force and hybrid of Flax and Vegetal-Technic) were intended to be determined to enhance the adoption of the natural materials for practical application. This research provides numerical results which were analytically validated for the long fibre and random short fibres. While, the result of the random short fibres of were further validated the experimental results obtained in Barteau et al. [2]. The results are presented and discussed in the following sequence- flax, vegetal-technic, wood-force and hybrid of flax and vegetal-technic

4.1.Flax – PP Composite Engineering Properties

The results of the elastic modulus obtained from the numerical analysis performed on the random short flax fibre RVE model are shown in Table 4-1 and Figures 4-1. The result showed great agreement with the experimental and analytical results reported in the work of Barteau et al. [2]. The relative error in the results has been computed with reference to the mean and is therefore described as the relative mean error expressed in equation 44. The difference in the numerical result between the analytical and experimental results can be attributed to the temperature load included in the numerical analysis as well as the complexity of the properties included in the analysis. For instance, temperature load was not reported in the experimental study by Barteau et al. [2]. In addition, phenomena such as viscosity and friction were not defined in the numerical analysis, which could possibly have had an influence on the study. Further, the variation in the effective elastic modulus results obtained from numerical analysis and the previously established results from experimental and analytical results could possibly be caused by the relative variation in the degree of randomness of the RVE and the experimental sample. Knowing that it is practically impossible to numerically replicate in the RVE the degree of randomness captured experimentally through SEM analysis as shown in Figure 2-9, These differences in randomness between the macroscale sample (Figure 2-9) and the composite RVE model are shown in Figures 3-1 and 3-2. Apparently, it could impact the result.

However, the agreement in the elastic modulus results obtained analytically and numerically is strong enough to conclude that the numerical model is good enough to determine the thermo-mechanical properties of the composite.

Table 4-1: Elastic modulus result of PP composite reinforced with random flax fibre with VF=0.2 & AR = 37.5

	Numerical	**Analytical**	**Experimental**
Elastic Modulus GPa	3.874	3.616	3.606
Relative mean error %	4.759	-2.217	-2.487

$$\text{Relative mean error \%} = \frac{x_i - \bar{x}}{\bar{x}} * 100\% \quad (44)$$

Where $\bar{x}$ *is the mean of the properties and* x_i *is the individual property.*

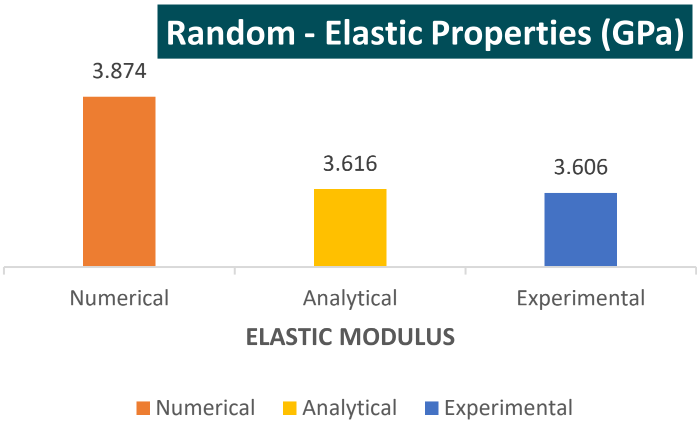

Figure 4-1: Histogram of elastic modulus of random short flax fibre reinforced thermoplastic composite with VF=0.2 & AR = 37.5

Upon the establishment of the performance of the RVE model to predict the properties of the composite, carried out through the analysis of the random flax fibre thermoplastic plastic, the numerical and analytical analysis of the long flax fibre thermoplastic composite was carried out, where the fibre volume fraction was 0.2 and the aspect ratio was 37.5. The RVE is of a transversely isotropic composite because all the fibres are aligned in one direction, and this is conspicuous in the results of the elastic modulus shown in Table 4-2 and figure 4-2, as E_{11} is significantly greater than the elastic E_{22} and E33, while the results of E_{22} and E_{33} are approximately the same. Which means a higher stiffness along the fibre direction than the two transverse directions (unreinforced), whose behaviour is largely governed by the matrix behaviour. The numerical and analytical results shown in figure 4-2 behave as expected.

The interesting thing to note is that the numerically obtained result shows great agreement with the analytical result, but this does not mean there is no variation in the results, as shown by the relative error. However, the variation, as previously suggested, is caused by the complexity of the material properties defined in the simulation and also by the fibre distribution in the RVE,

Table 4-2:Elastic modulus result of PP composite reinforced with aligned flax fibre with VF=0.2 & AR = 37.5

	E_{11} (GPa)		E_{22} (GPa)		E_{33} (GPa)	
	Numerical	Analytical	Numerical	Analytical	Numerical	Analytical
Value	10.537	11.752	2.656	2.407	2.656	2.407
Relative mean error %	-5.541	5.441	4.918	-4.918	4.918	-4.918

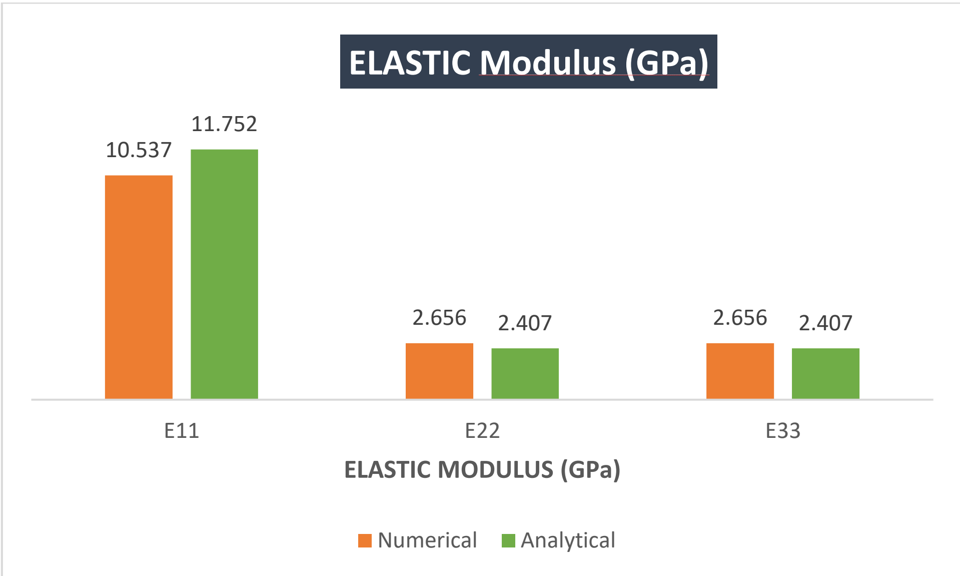

Figure 4-2: Histogram display of elastic modulus of aligned flax fibre reinforced thermoplastic composite with VF=0.2 & AR = 37.5

which has been noted to be exact with the analytical equation. Therefore, the elastic modulus results are considered to be within an acceptable limit.

Shear modulus is a valuable material property to design a reliable structure and significantly influences the tortional rigidity of a structure; hence, this property was numerically and analytically computed for a flax-PP composite. The shear modulus of the flax-PP composite computed numerically and analytically for G_{13}, G_{23}, and G12 is shown in table 4-3 and figure 4-3.

Overall, the numerical model predicted a higher shear response for the composite than the analytical model. This deviation may be attributed to the mesh size used. To avoid overestimating the shear capacity of the structure, the average shear modulus of both analytical and numerical results is recommended as follows: G_{13} is 0.4495 GPa; G_{23} is 0.4435 GPa; and G_{12} is 0.4355 GPa.

Table 4-3:Shear modulus result of PP composite reinforced with aligned flax fibre with VF=0.2 & AR = 37.5

	G_{13} (GPa)		**G_{23} (GPa)**		**G_{12} (GPa)**	
	Numerical	Analytical	Numerical	Analytical	Numerical	Analytical
Value	0.47	0.429	0.464	0.423	0.47	0.401
Relative mean error %	4.5606	-4.561	4.622	4.622	7.921	-7.921

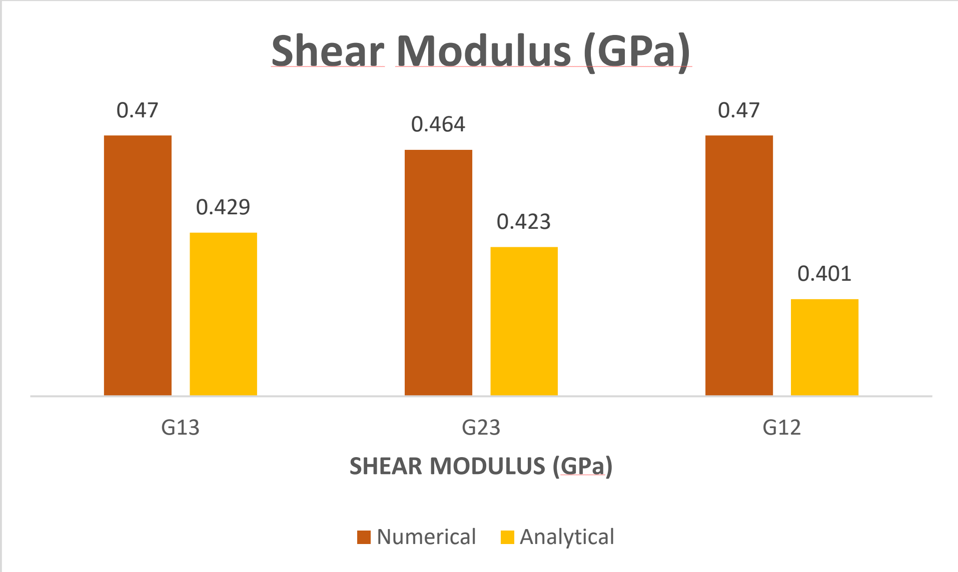

Figure 4-3: Histogram of shear modulus of aligned flax fibre reinforced thermoplastic composite with VF=0.2 & AR =37.5

The Poisson ratio of a material is another important property needed to properly characterise the behaviour of the material and for its application in the structural design of components and structures. Table 4-4 and figure 4-4 show the numerical and analytical results for a Flax-PP composite with a volume fraction of 0.2 and an aspect ratio of 37.5. There is great agreement in the results obtained from the two approaches.

The coefficient of thermal expansion of the flax-pp composite was found to be 1.76043e-05 (1/°C); this suggests that flax is stable under thermal load as small volumetric changes are expected due to its low thermal coefficient.

Table 4-4:Poisson ratio result of PP composite reinforced with aligned flax fibre with VF=0.2 & AR = 37.5

	ν_{12}		ν_{23}		ν_{13}	
	Numerical	Analytical	Numerical	Analytical	Numerical	Analytical
Value	0.425	0.499	0.346	0.369	0.0874	0.0757
Relative mean error %	-8.01	8.01	-3.217	3.217	7.174	-7.174

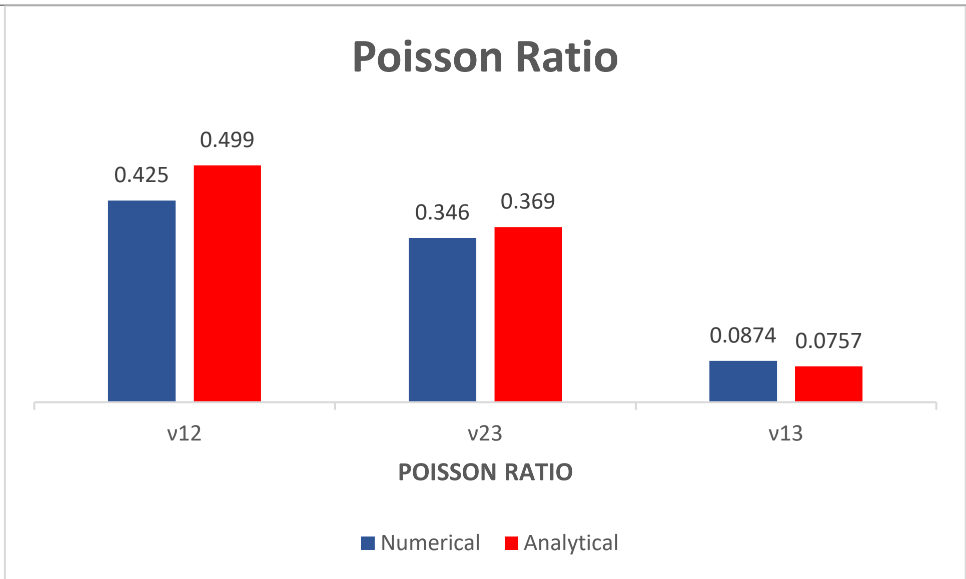

Figure 4-4: Histogram of Poisson ratio for long flax fibre reinforced thermoplastic composite with VF=0.2 & AR = 37.5

4.2. Vegetal Technic - PP Composite Engineering Properties

As previously established in the case of the flax-pp composite in Section 4.1, the random fibre composite was similarly analysed on the RVE with the properties of vegetal-technic. The elastic modulus result computed from various approaches—numerical, analytical, and experimental—is described in Table 4-5 and Figure 4-5. It is obvious that the numerical result agrees with the results previously obtained experimentally and analytically, but this does not mean it is without variance, which has been described as relative mean error. However, the possible causes of the variation have been previously explained as the complexity of the material properties included in the analysis, the differences in the level of randomness of the RVE used in the simulation, and the randomness of the real sample tested. Overall, the result obtained in the simulation is considered considerably correct.

Table 4-5:Elastic modulus result of PP composite reinforced with random vegetal-technic fibre with VF=0.2 & AR = 9.1

	Numerical	Analytical	Experimental
Elastic Modulus GPa	3.825	3.346	3.629
Relative mean error %	6.25	-7.06	0.806

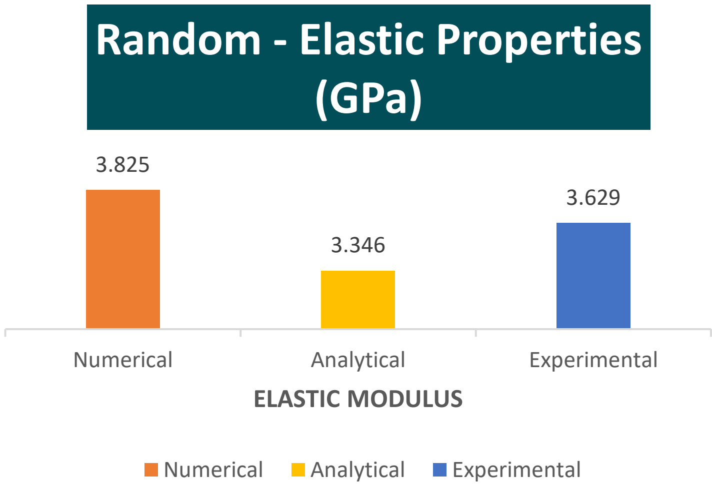

Figure 4-5: Histogram of elastic modulus of random short vegetal-technic reinforced thermoplastic composite with VF=0.2 & AR = 9.1

Similarly analysis was performed for a composite RVE of the long vegetal-technic fibre of volume fraction 0.21 and an aspect ratio of 9.1. The elastic modulus predicted by the numerical model is considered representative of the material behaviour as the analytical result shows good agreement in all the three directions, as shown in table 4-6 and figure 4-6.

Table 4-6:Elastic modulus result of PP composite reinforced with aligned vegetal-technic fibre with VF=0.2 & AR = 9.1

	E_{11} (GPa)		**E_{22} (GPa)**		**E_{33} (GPa)**	
	Numerical	Analytical	Numerical	Analytical	Numerical	Analytical
Value	7.253	7.235	2.825	2.37	2.825	2.37
Relative mean error %	0.124	-0.124	8.758	-8.758	8.758	-8.758

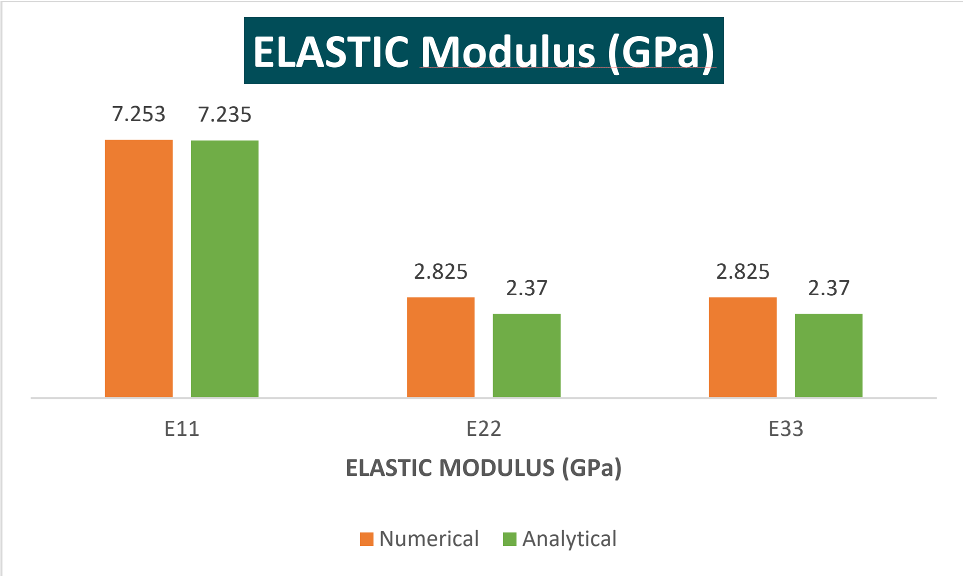

Figure 4-6: Histogram of elastic modulus of long vegetal-technic fibre reinforced thermoplastic composite with VF=0.2 & AR = 9.1

The shear moduli of vegetal-technic and PP composites computed numerically and analytically for G_{13}, G_{23}, and G_{12} are shown in table 4-7 and figure 4-7. Overall, the numerical model predicted a higher shear response for the composite than the analytical model. This deviation may be attributed to the mesh size used. To avoid overestimating the shear capacity of the structure, the average shear modulus of both analytical and numerical results is recommended as follows: G_{13} is 0.4495 GPa; G_{23} is 0.4435 GPa; and G_{12} is 0.4355 GPa.

Table 4-7:Shear modulus result of PP composite reinforced with aligned vegetal-technic fibre with VF=0.2 & AR = 9.1

	G_{13} (GPa)		**G_{23} (GPa)**		**G_{12} (GPa)**	
	Numerical	Analytical	Numerical	Analytical	Numerical	Analytical
Value	0.507	0.424	0.504	0.424	0.501	0.4007
Relative mean error %	8.915	-8.915	8.620	-8.621	11.123	-11.123

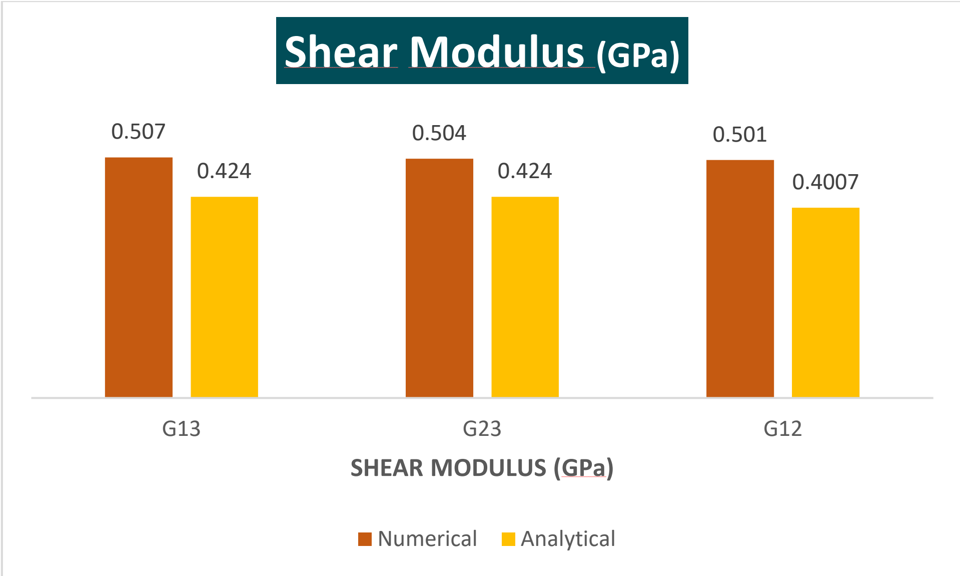

Figure 4-7: Histogram of shear modulus of long wood-force fibre reinforced thermoplastic composite with VF=0.2 & AR = 9.1

The Poisson ratio is an important property needed to properly characterise the behaviour of the material and for its application in the structural design of components and structures. Table 4-8 and Figure 4-8 show the numerical and analytical results for a Vegetal-Technic-PP composite with a volume fraction of 0.2 and an aspect ratio of 9.1. There is a great deal of agreement in the results obtained from the two approaches, as the relative mean error is considerably small. Further, the coefficient of thermal expansion of the vegetal-technic-PP composite was estimated at 1.7521086E-05 (1/°C), and it is isotropic. It is considerably stable under thermal load.

Table 4-8:Poisson ratio result of PP composite reinforced with aligned vegetal-technic fibre with VF=0.2 & AR = 9.1

	ν_{12}		ν_{23}		ν_{13}	
	Numerical	Analytical	Numerical	Analytical	Numerical	Analytical
Value	0.317	0.342	0.406	0.478	0.323	0.342
Relative mean error %	-3.794	3.794	-8.145	8.145	-3.003	3.084

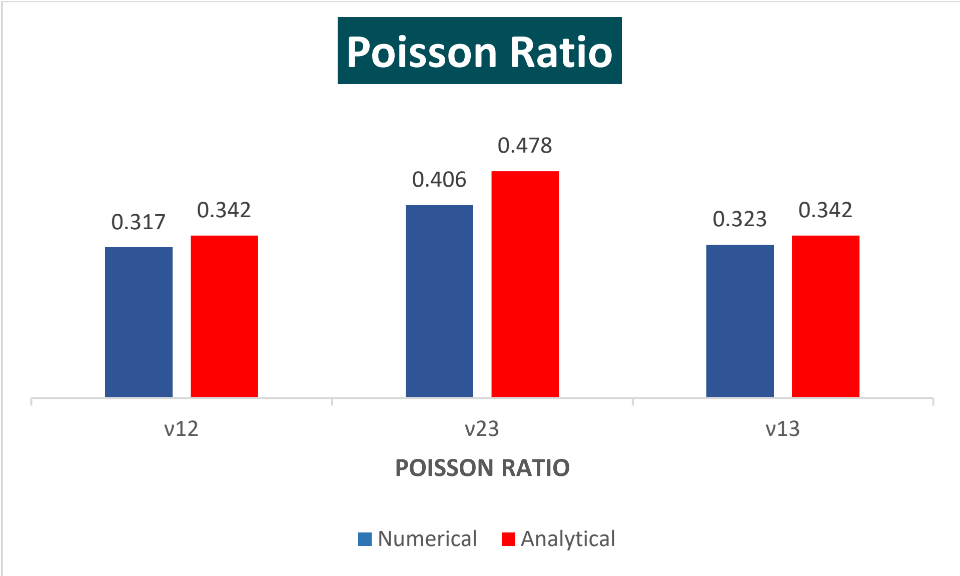

Figure 4-8:Histogram of Poisson ratio result of PP composite reinforced with aligned vegetal-technic fibre with VF=0.2 & AR = 9.1

4.3. Wood-Force Composite Engineering Properties

The elastic modulus of the polypropylene thermoplastic composite reinforced with random wood-force fibre estimated through finite element similation was computed to be 2.987 GPa, which is in close agreement with the results obtained analytically and experimentally previously reported in Barteau et al. [2] as 2.717 GPa and 2.906 GPa, respectively. These results are shown in table 4-9 and tigure 4-9. It is evident that the results are in close agreement with one another as the relative mean error is reasonably small; therefore, the modelling approach was extended to determine the mechanical properties of composite reinforced with long fibres of wood. The elastic modulus results are shown in table 4-10 and figure 4-10. The numerical and analytical results for the wood-force long fibre-reinforced polypropyleen thermoplastic composites for E_{11}, E_{22}, and E_{33} are 5.589 GPa and 4.817 GPa; 2.694 GPa and 2.561 GPa; 2.719 GPa and 2.356 GPa, respectively.

Table 4-9:Elastic modulus result of PP composite reinforced with random wood-force fibre with VF=0.2 & AR = 17.5

	Numerical	**Analytical**	**Experimental**
Elastic Modulus (GPa)	2.987	2.717	2.906
Relative mean error %	4.076	-5.331	1.254

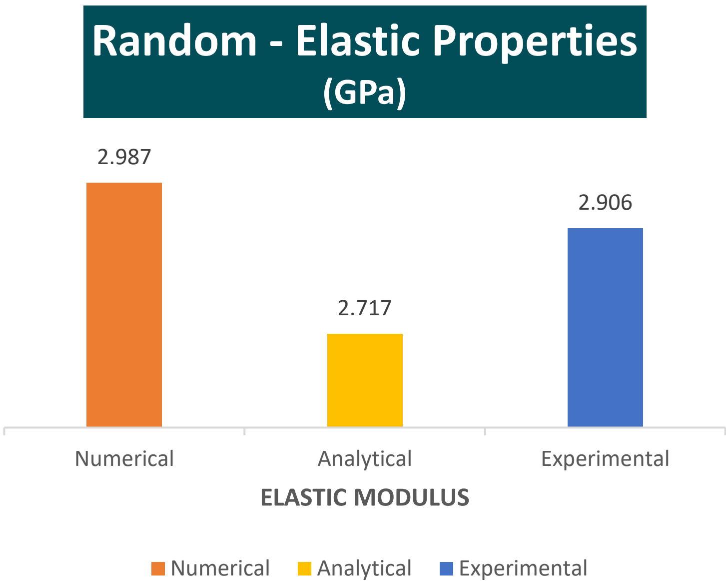

Figure 4-9: Histogram of elastic modulus of random short vegetal-technic fibre reinforced thermoplastic composite with VF=0.2 & AR = 17.5

Table 4-10:Elastic modulus result of PP composite reinforced with aligned wood-force fibre with VF=0.2 & AR = 17.5

	E_{11} (GPa)		E_{22} (GPa)		E_{33} (GPa)	
	Numerical	Analytical	Numerical	Analytical	Numerical	Analytical
Value	5.589	4.817	2.694	2.561	2.719	2.356
Relative mean error %	7.418	-7.418	2.5309	-2.5309	7.152	-7.153

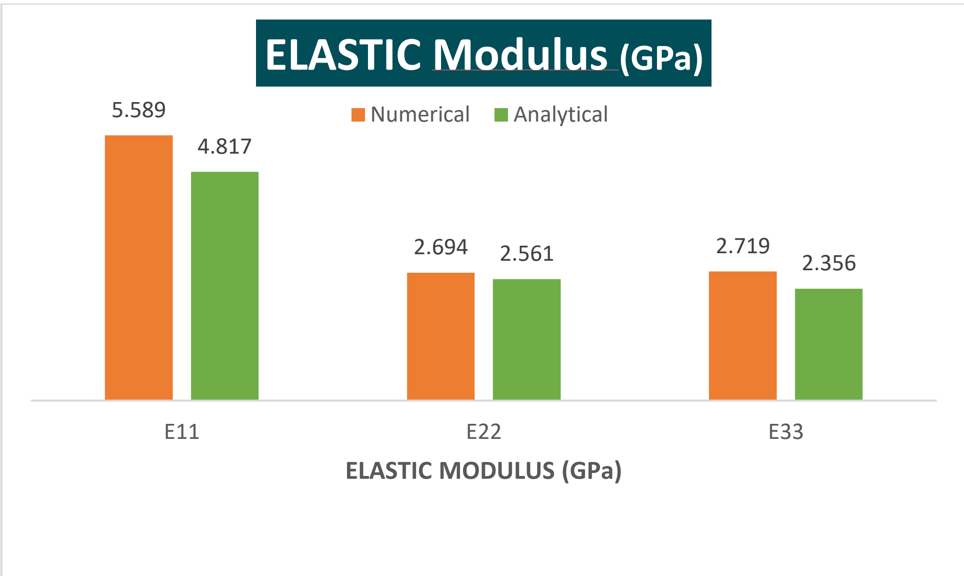

Figure 4-10: Histogram of elastic modulus of long wood-force fibre reinforced thermoplastic composite with VF=0.2 & AR = 17.5

The errors in the computation are approximately 16 %, 5 %, and 15 %, respectively, and the causes of the variation are as previously established in sections 4.1 and 4.2. The average values of the numerical and analytical results are recommended for adoption as E_{11}, E_{22}, and E_{33}: 5.203 GPa, 2.6275 GPa, and 2.5375 GPa, respectively.

Further, the shear modulus was computed from the long fibre RVE as well, and the results are shown in table 4-11 and figure 4-11. The estimated G_{13}, G_{23}, and G_{12} numerically and analytically are 0.488 GPa and 0.422 GPa, 0.483 GPa and 0.482 GPa, and 0.398 GPa, respectively. The average of the two approaches for G_{13}, G_{23}, and G_{12} is 0.455 GPa, 0.4525 GPa, and 0.44 GPa, respectively.

Table 4-11:Shear modulus result of PP composite reinforced with aligned wood-force fibre with VF=0.2 & AR = 17.5

	G_{13} (GPa)		**G_{23} (GPa)**		**G_{12} (GPa)**	
	Numerical	Analytical	Numerical	Analytical	Numerical	Analytical
Value	0.488	0.422	0.483	0.422	0.482	0.398
Relative mean error %	7.252	-7.252	6.740	-6.740	9.545	-9.545

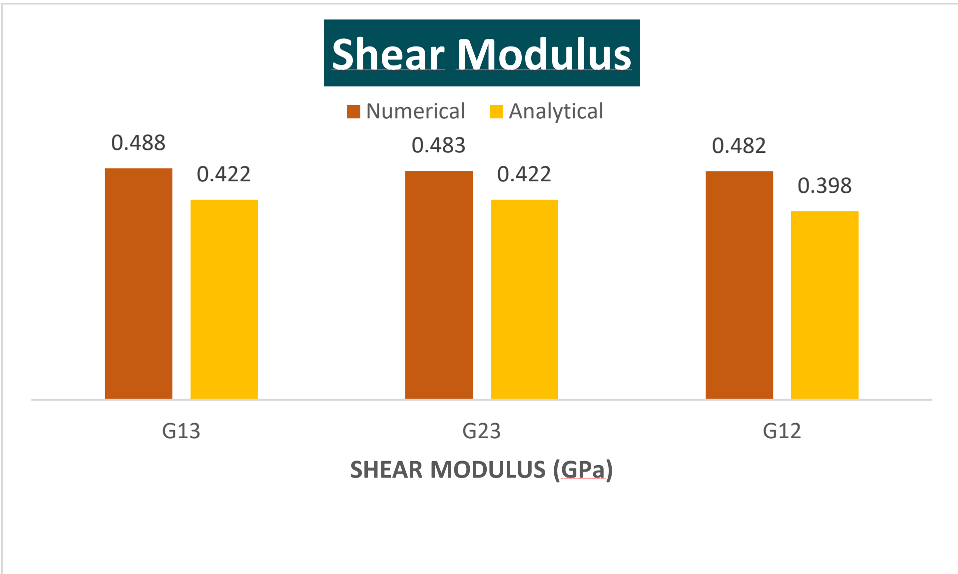

Figure 4-11: Histogram of shear modulus of long wood-force fibre reinforced thermoplastic composite with VF=0.2 & AR = 17.5

The results of the Poisson ratio obtained numerically are in agreement with those obtained by analytical computation. The Poisson ratio results are shown in table 4-12 and figure 4-12. The coefficient of thermal expansion of the wood-force-PP composite was estimated at 1.760437E-05 (1/°C).

Table 4-12:Poisson ratio result of PP composite reinforced with aligned wood-force fibre with VF=0.2 & AR = 17.5

	ν_{12}		ν_{23}		ν_{13}	
	Numerical	Analytical	Numerical	Analytical	Numerical	Analytical
Value	0.354	0.482	0.399	0.448	0.353	0.345
Relative mean error %	-15.31	15.31	-5.785	5.785	1.146	-1.146

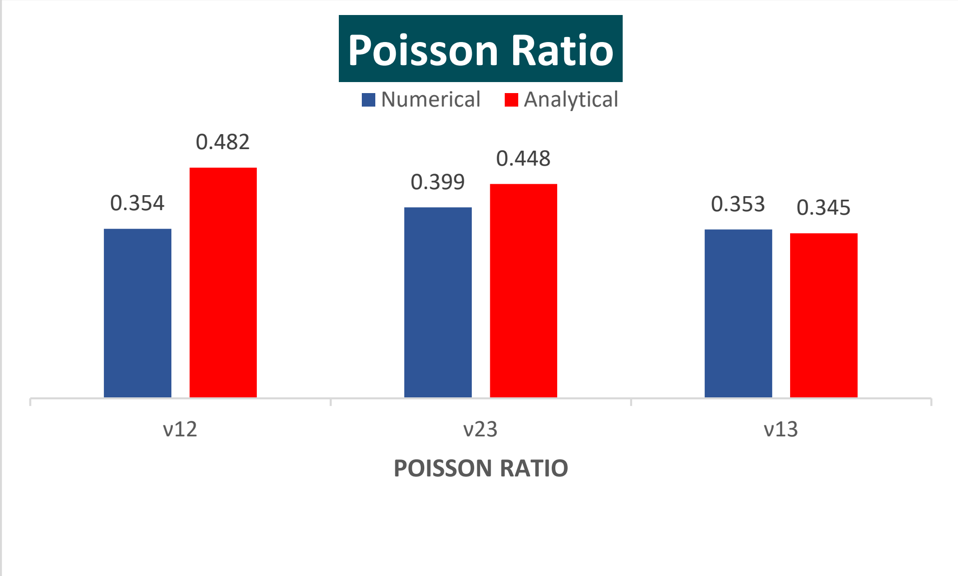

Figure 4-12:Graphical display of Poisson ratio result of PP composite reinforced with aligned wood-force fibre with VF=0.2 & AR = 17.5

4.4.Hybrid of Flax- Vegetal-Technic-PP Composite Engineering Properties

The properties of a hybrid composite made of flax, vegetal-technic reinforcement, and polypropylene matrix were investigated numerically and analytically. Table 4-13 and figure 4-13 show the elastic modulus results predicted by the analytical calculation and the numerical computations. These results are quite close, even though the relative error to the mean is up to approximately ±11% in the transverse directions. The E_{11} results show greater agreement between the two approaches than those obtained for E_{22} and E_{33}.

In addition, the shear modulus predictions for G_{13}, G_{23}, and G_{12} numerically and analytically obtained results are shown in Table 4-14 and Figure 4-14, respectively. The relative error is quite small, at less than 9%, which suggests good agreement between the two approaches. The computed Poisson ratio is shown in Table 4-15 and Figure 4-15. The model showed great agreement in the results obtained and unfortunately shows a weak

Table 4-13:Elastic modulus result of PP composite reinforced with a hybrid of flax and vegetal-technic fibre with VF=0.2 & AR = 18.5

	E_{11} (GPa)		E_{22} (GPa)		E_{33} (GPa)	
	Numerical	Analytical	Numerical	Analytical	Numerical	Analytical
Value	7.554	7.699	2.929	2.363	2.92	2.363
Relative mean error %	-0.9246	0.9771	10.695	-10.7332	10.543	-10.543

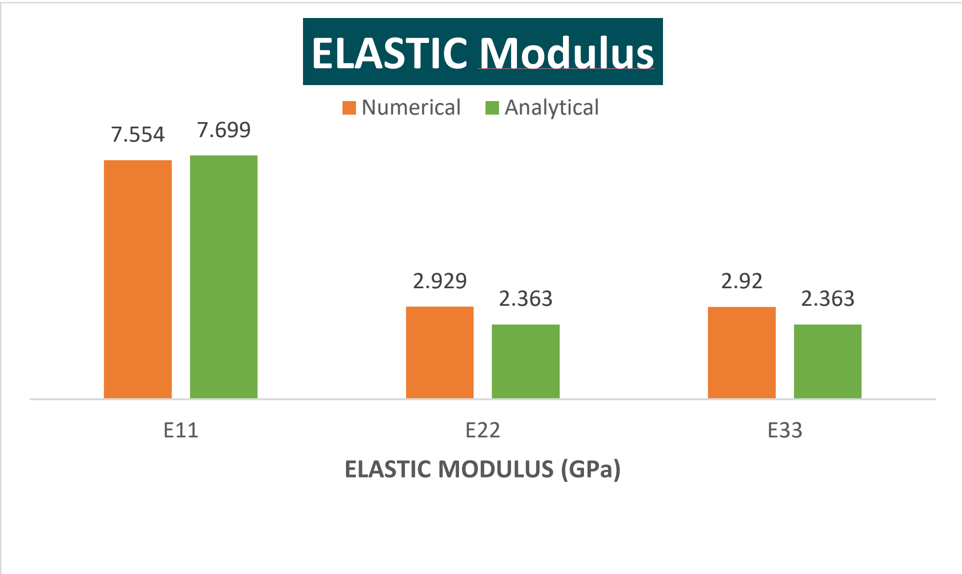

Figure 4-13: Elastic modulus result of PP composite reinforced with aligned hybrid of flax and vegetal-technic with VF=0.2 & AR = 18.5

relation between the mean of both the analytical and numerical results, as the relative mean error is up to 25% for the analytical approach and about -14% for the numerical method.

Table 4-14:Shear modulus result of PP composite reinforced with aligned hybrid of flax and vegetal-technic fibre with VF=0.2 & AR = 18.5

	G_{13} (GPa)		G_{23} (GPa)		G_{12} (GPa)	
	Numerical	Analytical	Numerical	Analytical	Numerical	Analytical
Value	0.356	0.422	0.356	0.422	0.357	0.390
Relative mean error %	-8.483	8.483	-8.483	8.483	-4.417	4.417

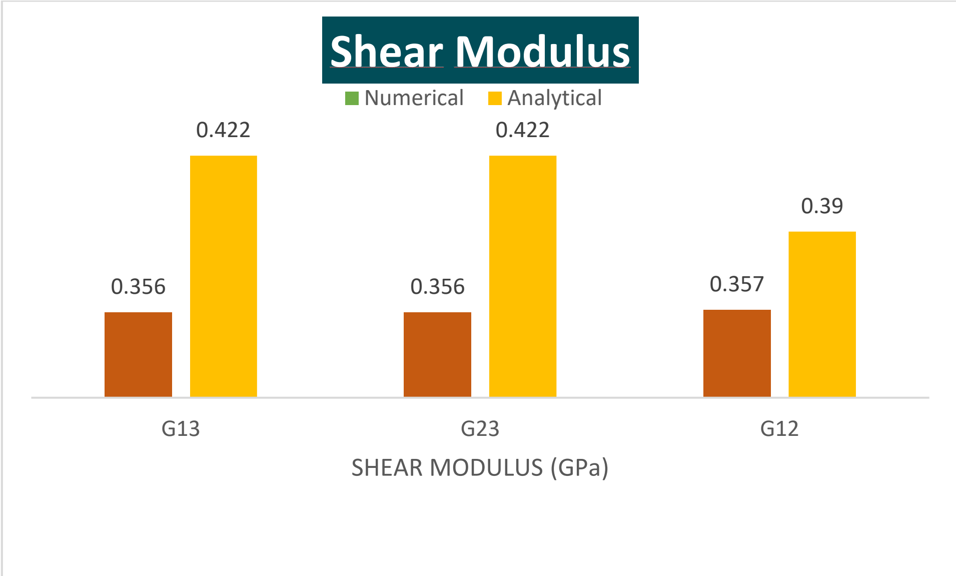

Figure 4-14:Histogram of shear modulus of aligned hybrid of flax and vegetal-technic fibre reinforced thermoplastic composite with VF=0.2 & AR = 18.5

Table 4-15:Poisson ratio result of PP composite reinforced with aligned hybrid of flax and vegetal-technic with VF=0.2 & AR = 18.5

	ν_{12}		ν_{23}		ν_{13}	
	Numerical	Analytical	Numerical	Analytical	Numerical	Analytical
Value	0.354	0.470	0.1318	0.113	0.353	0.370
Relative mean error %	-14.077	25.836	7.679	-7.679	-2.351	2.351

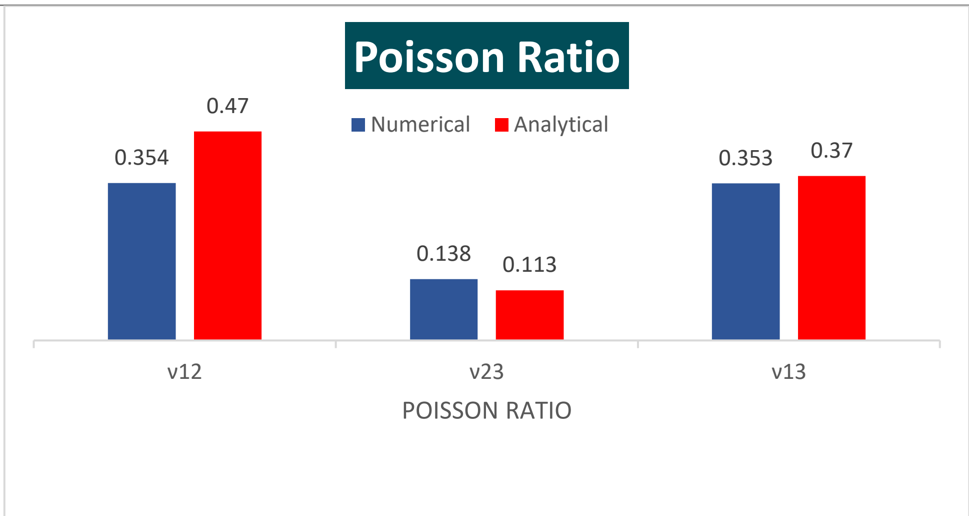

Figure 4-15: Histogram of Poisson ratio for PP composite reinforced with aligned hybrid of flax and vegetal-technic fibre with VF=0.2 & AR = 18.5

The elastic modulus of a composite made with a hybrid of flax and vegetal technology in a random orientation was also computed. The results of the elastic modulus of the random hybrid of flax and vegetal-technic fibre-reinforced composite are shown in table 4-16 and graphically shown in figure 4-16. It is evident that there is strong agreement amongst the results obtained numerically, analytically, and experimentally, even though there is variation in these results. However, the relative error is ±7%, which is considered reasonable. The coefficient of thermal expansion computed is isotropic, and it is 1.762611E-05 (1/°C).

Table 4-16:Elastic modulus result of PP composite reinforced with random hybrid of flax and vegetal-technic with VF=0.2 & AR = 18.5

	Numerical	Analytical	Experimental
Elastic Modulus (GPa)	3.825	3.329	3.586
Relative mean error %	6.843	-7.011	0.1675

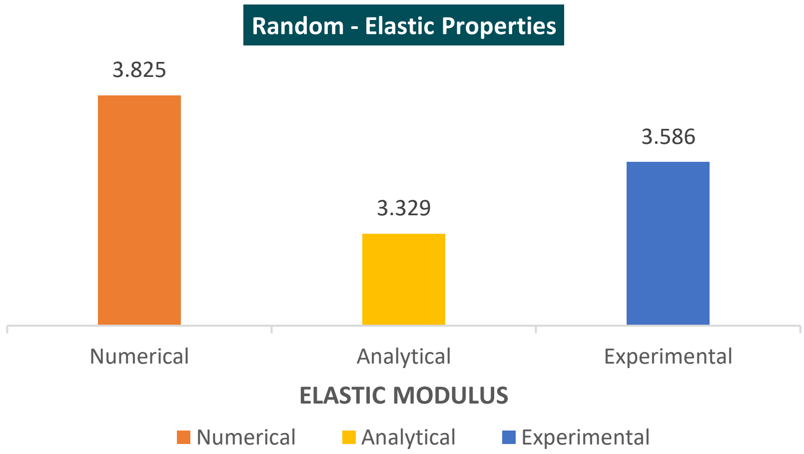

Figure 4-16: Histogram of elastic modulus of random hybrid of flax and vegetal-technic fibre reinforced thermoplastic composite with VF=0.2 & AR = 18.5

4.5. Comparative Analysis of the Thermomechanical Properties of the Four Materials Studied

The thermomechanical properties computed both analytically and numerically for the different natural fibres suggest the good capacity of the micromechanical approach. The obtained results show agreement with the natural composition of the fibres. As established earlier, the mechanical strength of natural fibres is directly proportional to their cellulose content. Although the cellulose contents of the studied materials have been expressed in terms of their glucose content (table 2-1), nevertheless, the results showed agreement with result of flax reported by Bhattacharyya et al. [18] in table 2-2.

For instance, making the elastic properties the property of reference, the average of the elastic properties of the PP-reinforced with random and E_{11} in the fibre-aligned orriented composites are 3.698 GPa and 11.1445 GPa for flax-reinforced composites, respectively. Similarly, the average of the elastic properties of the PP-reinforced with random and the and E_{11} in the fibre-aligned orriented composites for vegetal-technic are 3.60 GPa and 7.244 Gpa; while for wood-force reinforced composite are 2.87 GPa and 5.203 GPa. Comparatively, as shown in table 2-1, the glucose content of flax, vegetal-technic, and wood-force is 69.66 ± 3.66, 51.39 ± 2.39, and 47.23 ± 2.80, respectively. As the glucose content is higher in the flax than vegetal-technic, it is expected that PP-flax fibre-reinforced composite should have a higher elastic modulus than the PP-vegetal-technic reinforced fibre composite and in fact, that is the case which is consistent with the result. Similarly, the higher glucose content in vegetal-technic fibre than wood-force agrees with the numerical model and analytically predicted result to have a better elastic modulus (random and aligned orientation) than the PP-wood-force reinforced composite.

One might be tempted to extrapolate the trend to arrive at a similar conclusion for the hybrid composite (flax and vegetal technology), but it cannot be confirmed as the hybrid does not have experimentally derived glucose or cellulose content. Although the glucose content of the hybrid may be said to be an average of the glucose content of the constituent fibres the two fibres as they are approximately of the same proportion. By extension, the elastic properties may be an average of the two fibres in thecomposite. The predicted elastic modulus for both random and aligned orientation of the hybrid composite (flax & vegetal-technic) are 3.58 GPa and 7.626GPa respectively which seem to agree to the established observations for flax, vegetal-technic and wood-force reinforced composite. However, the high variability of the glucose content in the natural fibres and the adopted modelling strategy, which was the modelling of a single type of fibre in the RVE (rather than a mixture of two different fibre microstructures), and the fact that the average properties of the two materials were assigned as provided in Barteau et al. [2] makes it difficult to conclude so. But such assumption may be advanced.

4.6.Flax – Polypropylene Reinforced Composite: Application

The ultimate goal of the structural design of any component/structure is to ensure that the structure does not fail abruptly and that the deformation of the structure is limited within a tolerable limit. Since it was obvious from the results that the flax-polypropylene composite have the best mechanical properties amongst the four materials study, therefore, its mechanical response under mechanical loading was study to obtain its yield strength, strain, and acumulated plastic strain (SDV 50) as its fibre volume fraction is varied from 10% to 50% under varying loads. These properties were obtained at the most critical part of the drone, which is shown in figures 4-17 and 4-18.

The stress-strain curve (figure 4-19) was plotted for varying fibre volume fractions, and it is evident in that strength increases as the fibre volume fraction increases from 0.1 to 0.5. The accumulated plastic strain (SDV 50) versus stress curve shown in figure 4-20 reflects that, as the fibre volume fraction increases, the stress necessary to cause plasticity in flax-PP composite increases.

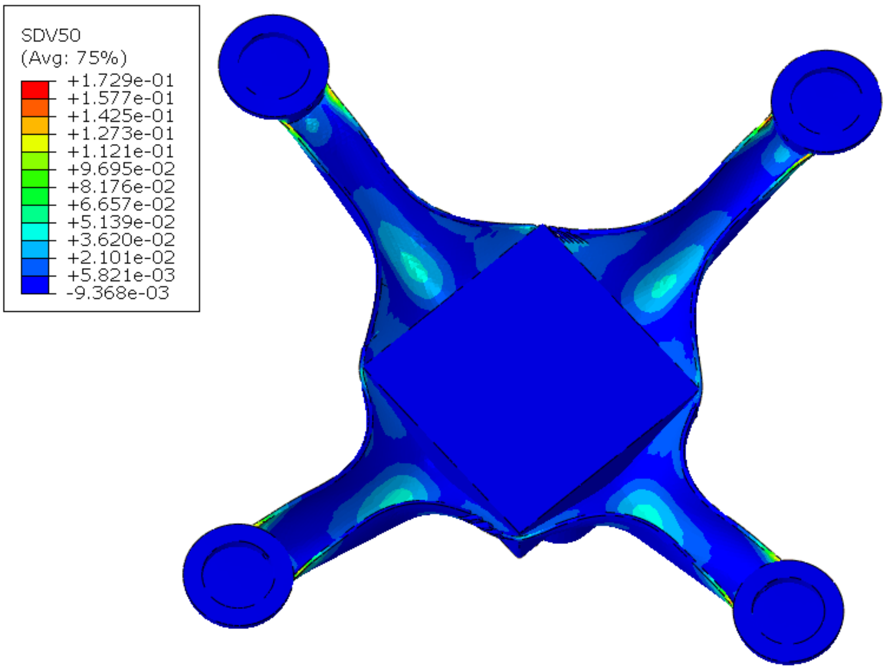

Figure 4-17: Accumulated plastic strain result

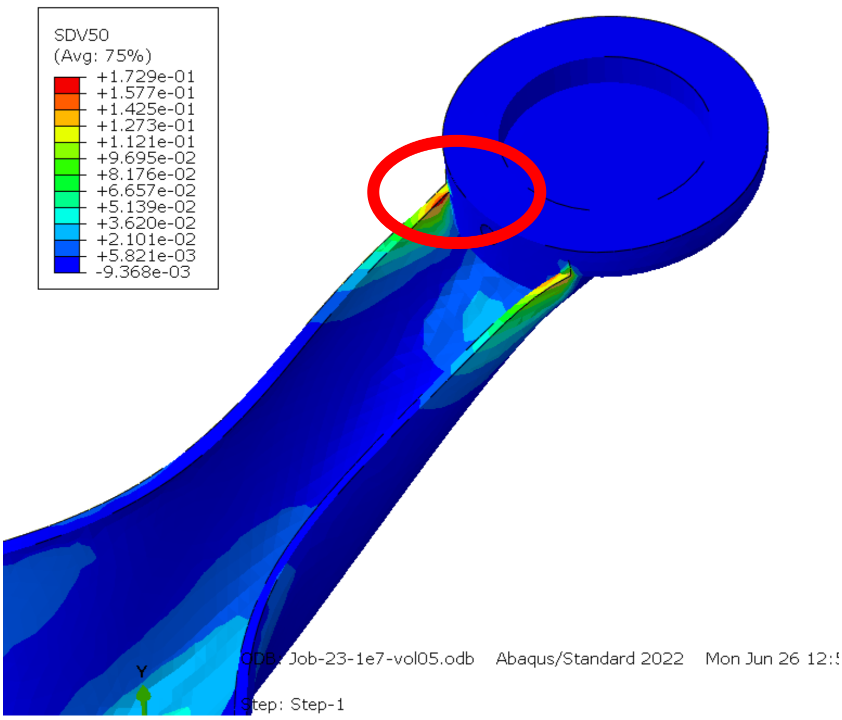

Figure 4-18: Element of interest

This suggests that a high-volume fraction of about 0.4 or 0.5 is recommended for use when the structural component is subjected to a high structural load. The accumulated plastic strain (SDV 50) versus strain curve is shown in figure 4-21. It was observed that, at a certain strain level, the accumulated plastic strain is higher in composite with higher volume fraction than composite with lower fibre volume fraction and this behaviour is consistent from fibre fibre volume fraction of 0.1 to 0.5. This suggests that, as the fibre volume fraction increases from 0.1 to 0.5, the flax-PP composite has increased capacity to withstand a higher load than at a lower fibre fraction. Which is iconsistent in the result plotted in figure 4-19 that the strength capacity of the flax-PP composite increases with an increase in fibre volume fraction.

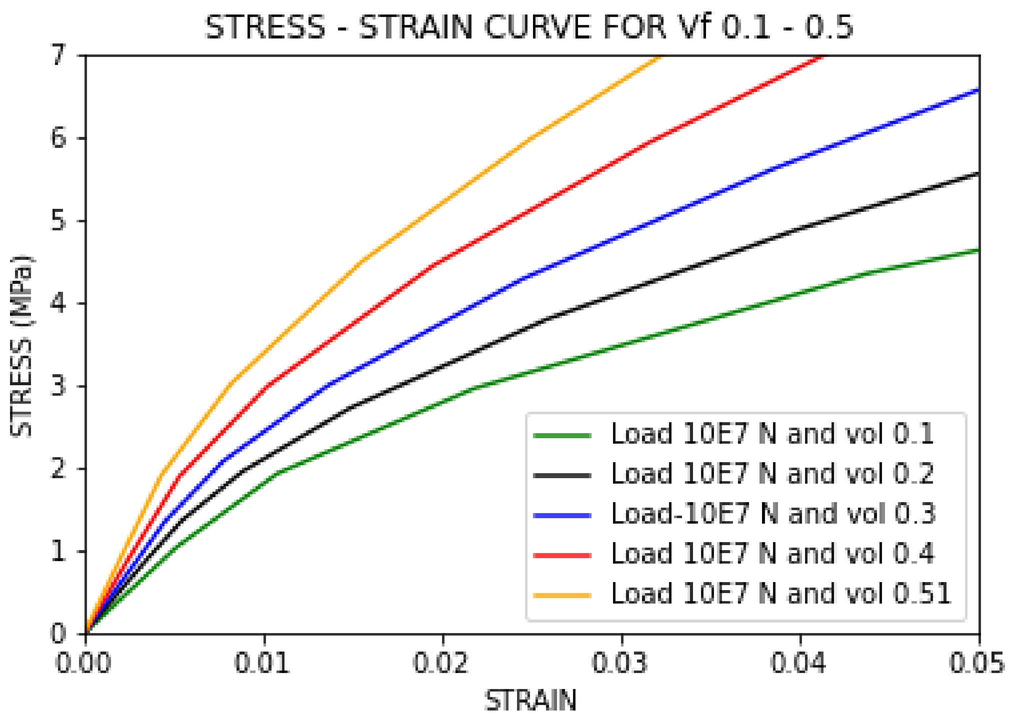

Figure 4-19: Stress - strain curve

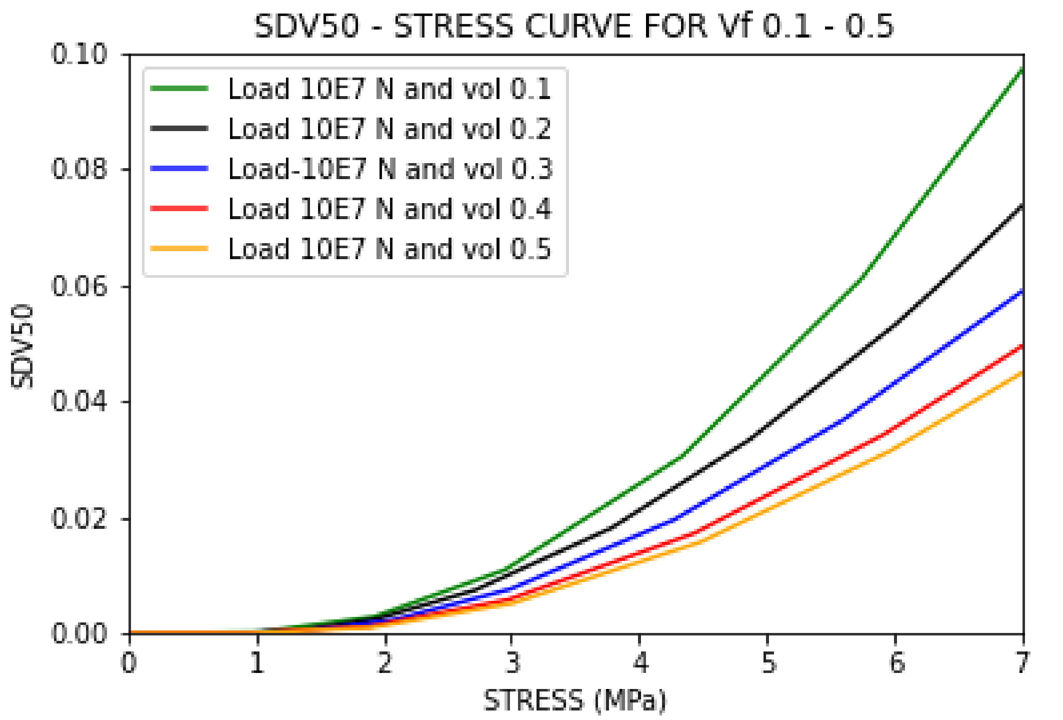

Figure 4-20: Accumulated plastic strain - stress curve

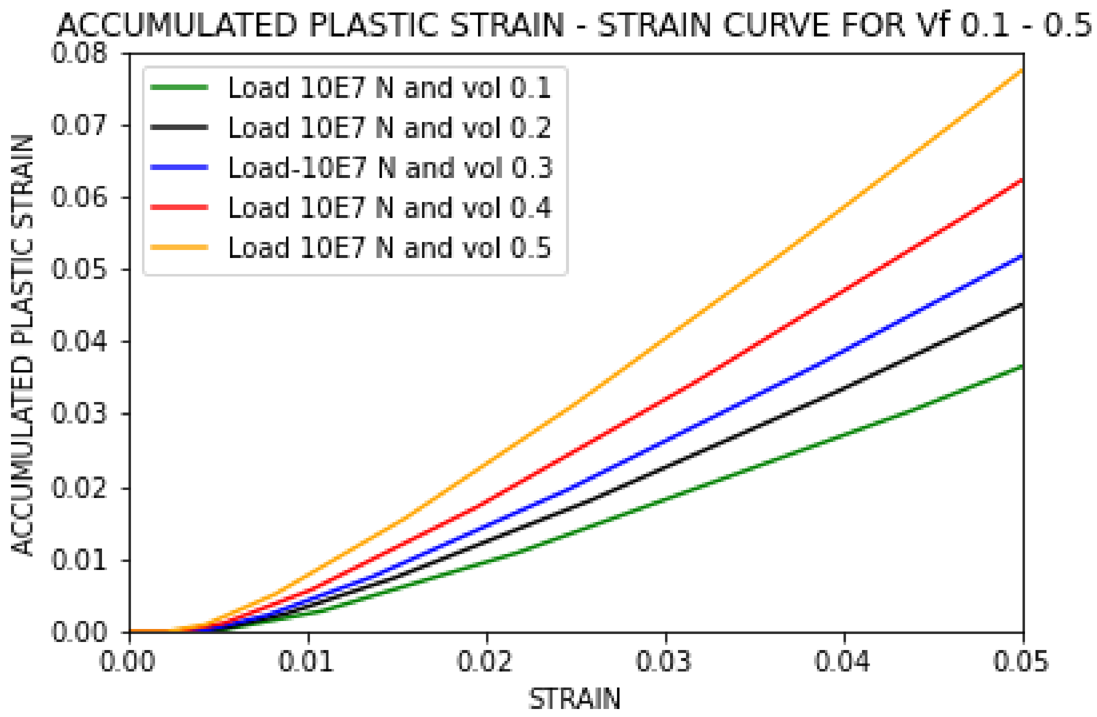

Figure 4-21:Accumulated plastic strain – strain curve

5. CONCLUSION

This research was aimed to use micromechanics numerical approach to establish the thermomechanical properties of thermoplastic composites made with a polypropylene matrix and reinforced with natural fibres: flax, vegetal-technic, wood-force and a hybrid of flax and vegetal-technic for both random and aligned oriented fibres for a fibre volume fraction of 20%. For the aligned fibre-oriented composites, the thermomechanical results established numerically was validated by analytical calculation. The mechanical properties obtained for the random fibres are to validate the results obtained through experimental and analytical study report by Barteau et al. [2]. In addition, to numerically established its mechanical performance under mechanical loading through its application for the design of a quadcopter by determining its stress, strain and accumulated plastic strain.

This research revealed that the properties predicted by the numerical models were in good agreement with the results of the random oriented fibre composite obtained experimentally and analytically. For the composite made with aligned oriented fibres, there is strong agreement between the numerical and the analytical results. It was obvious from the study that, Flax-PP composite has a better mechanical performance than vegetal-technic-PP composite as the glucose content is higher in flax than that of vegetal-technic. Similarly, vegetal-technic-PP composite also has a better mechanical performance than woodforce-PP composite. In addition, the mechanical properties of vegetal-technic-PP composite rival the hybrid composite made with combination of flax and vegetal-technic with polypropylene matrix. Despite the varying degree of anisotropy of the different natural fibre reinforced composites studied, the coefficient of thermal expansion was isotropic.

Finally, it was obvious from this study that for the flax-PP composite, as its strength increases, its fibre volume fraction increases from 10% to 50%. The high strength observed as the fibre volume fraction increases from 10% to 50% was corroborated as the accumulated plastic strain which also increases as the fibre volume fraction increases from 10% to 50%. This suggest its stability under an increasing structural load as its fibre volume fraction increases from 10% to 50%.

Reference

1. CHICHANE, A., BOUJMAL, R., El BARKANY, A.: Bio-composites and bio-hybrid composites reinforced with natural fibers: Review. Mater Today Proc. 72, 3471–3479 (2023). https://doi.org/10.1016/J.MATPR.2022.08.132
2. Barteau, G., Azoti, W., Gautreau, M., Francart, C., Alès, G., Jmal, H., Bouchet, J., Kervoëlen, A., Beaugrand, J., Bahlouli, N., Bourmaud, A.: Recycling of wood-reinforced poly-(propylene) composites: A numerical and experimental approach. Ind Crops Prod. 167, 113518 (2021). https://doi.org/10.1016/J.INDCROP.2021.113518
3. Kurien, R.A., Maria Anil, M., Sharan Mohan, S.L., Anna Thomas, J.: Natural fiber composites as sustainable resources for emerging applications- a review. Mater Today Proc. (2023). https://doi.org/10.1016/J.MATPR.2023.04.363
4. Soyarslan, C., Havinga, J., Abelmann, L., van den Boogaard, T.: Asymptotic homogenization in the determination of effective intrinsic magnetic properties of composites. Results Phys. 44, 106188 (2023). https://doi.org/10.1016/J.RINP.2022.106188
5. Kurien, R.A., Maria Anil, M., Sharan Mohan, S.L., Anna Thomas, J.: Natural fiber composites as sustainable resources for emerging applications- a review. Mater Today Proc. (2023). https://doi.org/10.1016/J.MATPR.2023.04.363
6. Senthil Kumar, P., Jegadheesan, C., Narasimmabharathi, S., Nithiyarasan, R., Manideep, B., Pal Singh, A.: Investigations on tribological behavior of natural fiber hybrid composites for brake friction. Mater Today Proc. (2023). https://doi.org/10.1016/J.MATPR.2023.04.261
7. Eshelby J. D.: The Determination of the Elastic Field of an Ellipsoidal Inclusion, and Related Problems. In: Proceedings Physical and Engineering Sciences. The Royal Society. pp. 376–396 (1957)
8. Choudhary, S., Haloi, J., Kumar Sain, M., Saraswat, P., Kumar, V.: Systematic literature review on thermal and acoustic characteristics of natural fibre polymer composites for automobile applications. Mater Today Proc. (2023). https://doi.org/10.1016/J.MATPR.2023.01.349
9. Hexagon: Digimat 2021.1 - User’s Manual (PDF), (2021)
10. Dr. Wiyao Azoti: Multiscale modelling of rigid tissue applied to biomechanics

11. Kumar Sharma, A., Bhandari, R., Sharma, C., Krishna Dhakad, S., Pinca-Bretotean, C.: Polymer matrix composites: A state of art review. Mater Today Proc. 57, 2330–2333 (2022). https://doi.org/10.1016/J.MATPR.2021.12.592
12. M.A. Laribi: Characterization and micromechanical modeling of the behavior of SMC composites under quasi-static thermo-mechanical loading and fatigue, (2018)
13. CaveI. D: X-Ray Measurement of Microfibril Angle. For. Prod. J. 44374. (1966)
14. Tamer A. Tabet, Fauziah Abdul Aziz: Cellulose Microfibril Angle in Wood and Its Dynamic Mechanical Significance. In: Theo van de Ven and Louis Godbout (eds.) Cellulose - Fundamental Aspects. InTech (2013)
15. Djafari Petroudy, S.R.: Physical and mechanical properties of natural fibers. Advanced High Strength Natural Fibre Composites in Construction. 59–83 (2017). https://doi.org/10.1016/B978-0-08-100411-1.00003-0
16. Dimple, Singh, G.P., Mangal, R.: A comprehensive review of natural fiber reinforced composite and their modern application. Mater Today Proc. (2023). https://doi.org/10.1016/J.MATPR.2023.03.745
17. Kabir, M.M., Wang, H., Lau, K.T., Cardona, F.: Chemical treatments on plant-based natural fibre reinforced polymer composites: An overview. Compos B Eng. 43, 2883–2892 (2012). https://doi.org/10.1016/J.COMPOSITESB.2012.04.053
18. Bhattacharyya, D., Subasinghe, A., Kim, N.K.: Natural fibers: Their composites and flammability characterizations. Multifunctionality of Polymer Composites: Challenges and New Solutions. 102–143 (2015). https://doi.org/10.1016/B978-0-323-26434-1.00004-0
19. Abedi, M., Hassanshahi, O., Rashiddel, A., Ashtari, H., Seddik Meddah, M., Dias, D., Arjomand, M.A., Keong Choong, K.: A sustainable cementitious composite reinforced with natural fibers: An experimental and numerical study. Constr Build Mater. 378, 131093 (2023). https://doi.org/10.1016/J.CONBUILDMAT.2023.131093
20. Mohanty, A.K., Misra, M., Drzal, L.T.: Natural Fibers, Biopolymer and Biocomposites. (2005)
21. Satyanarayana, K.G., Sukumaran, K., Mukherjee, P.S., Pillai, S.G.K.: Materials science of some lignocellulosic fibers. Metallography. 19, 389–400 (1986). https://doi.org/10.1016/0026-0800(86)90073-X
22. Ramamoorthy, S.K., Åkesson, D., Rajan, R., Periyasamy, A.P., Skrifvars, M.: Mechanical performance of biofibers and their corresponding composites. Mechanical

and Physical Testing of Biocomposites, Fibre-Reinforced Composites and Hybrid Composites. 259–292 (2019). https://doi.org/10.1016/B978-0-08-102292-4.00014-X

23. Mahmud, S., Konlan, J., Deicaza, J., Schmidt, R.A., Li, G.: Thermoset polymer composites with gradient natural and synthetic fiber reinforcement: Self-healing, shape-memory, and fiber recyclability. Mater Today Commun. 35, 105950 (2023). https://doi.org/10.1016/J.MTCOMM.2023.105950

24. Jino, L., Dev Prasad, V., Ajay Eswar, M., Manoj, E., Jacob, A., Arockia Suthan, S., Jayaganthan, A., Anderson, A.: Review on natural fibre composites reinforced with nanoparticles. Mater Today Proc. (2023). https://doi.org/10.1016/J.MATPR.2023.01.126

25. Doddamani, S., Kulkarni, S.M., Joladarashi, S., Kumar T S, M., Gurjar, A.K.: Analysis of light weight natural fiber composites against ballistic impact: A review. International Journal of Lightweight Materials and Manufacture. 6, 450–468 (2023). https://doi.org/10.1016/J.IJLMM.2023.01.003

26. Wang, Y., Yao, X., Thorn, T.D.S., Huo, S., Porwal, H., Newton, M., Liu, Y., Papageorgiou, D., Bilotti, E., Zhang, H.: Energy efficient out-of-oven manufacturing of natural fibre composites with integrated sensing capabilities and improved water barrier properties. Compos Sci Technol. 239, 110062 (2023). https://doi.org/10.1016/J.COMPSCITECH.2023.110062

27. Moujoud, Z., Sair, S., Ait Ousaleh, H., Ayouch, I., El Bouari, A., Tanane, O.: Geopolymer composites reinforced with natural Fibers: A review of recent advances in processing and properties. Constr Build Mater. 388, 131666 (2023). https://doi.org/10.1016/J.CONBUILDMAT.2023.131666

28. Ranjan, C., Sarkhel, G., Kumar, K.: Efficacy of natural fibre reinforced biodegradable composite towards industrial products – An extensive review. Mater Today Proc. (2023). https://doi.org/10.1016/J.MATPR.2023.04.689

29. Yamini, P., Rokkala, S., Rishika, S., Meghana Rani, P., Arul Kumar, R.: Mechanical properties of natural fiber reinforced composite structure. Mater Today Proc. (2023). https://doi.org/10.1016/J.MATPR.2023.04.547

30. Chandra Sekhar, V., Dasore, A., Yalamasetti, B., Sudha Madhuri, K., G., N.: Flexural behavior of natural fiber epoxy composites. Mater Today Proc. (2023). https://doi.org/10.1016/J.MATPR.2023.03.429

31. Senthil Kumar, P., Jegadheesan, C., Narasimmabharathi, S., Nithiyarasan, R., Manideep, B., Pal Singh, A.: Investigations on tribological behavior of natural fiber hybrid

composites for brake friction. Mater Today Proc. (2023). https://doi.org/10.1016/J.MATPR.2023.04.261

32. Sathish, S., Aneesh, S., Naveen Vigneshwaran, S., Nithish Kumar, E.K., Ravichandran, M., Anaz Khan, M.: Role of areca fibres on the mechanical behavior of natural fibre reinforced polymer composite. Mater Today Proc. (2023). https://doi.org/10.1016/J.MATPR.2023.03.606
33. Sahu, M., Patnaik, A., Kishor Sharma, Y., Dalai, A.: Physico-mechanical and tribological behaviour of natural fiber reinforced polymer composites: A short review. Mater Today Proc. (2023). https://doi.org/10.1016/J.MATPR.2023.03.822
34. Yadav, V., Singh, S., Chaudhary, N., Garg, M.P., Sharma, S., Kumar, A., Li, C., Tag Eldin, E.M.: Dry sliding wear characteristics of natural fibre reinforced poly-lactic acid composites for engineering applications: Fabrication, properties and characterizations. Journal of Materials Research and Technology. 23, 1189–1203 (2023). https://doi.org/10.1016/J.JMRT.2023.01.006
35. Doddamani, S., Kulkarni, S.M., Joladarashi, S., Kumar T S, M., Gurjar, A.K.: Analysis of light weight natural fiber composites against ballistic impact: A review. International Journal of Lightweight Materials and Manufacture. 6, 450–468 (2023). https://doi.org/10.1016/J.IJLMM.2023.01.003
36. Avcu, E., Bastan, F.E., Guney, M., Yildiran Avcu, Y., Ur Rehman, M.A., Boccaccini, A.R.: Biodegradable Polymer Matrix Composites Containing Graphene-Related Materials for Antibacterial Applications: A Critical Review. Acta Biomater. 151, 1–44 (2022). https://doi.org/10.1016/J.ACTBIO.2022.07.048
37. Zhang, X., Wang, X., Jiao, W., Liu, Y., Yu, J., Ding, B.: Evolution from microfibers to nanofibers toward next-generation ceramic matrix composites: A review. J Eur Ceram Soc. 43, 1255–1269 (2023). https://doi.org/10.1016/J.JEURCERAMSOC.2022.11.033
38. Yang, H., Abali, B.E., Müller, W.H., Barboura, S., Li, J.: Verification of asymptotic homogenization method developed for periodic architected materials in strain gradient continuum. Int J Solids Struct. 238, 111386 (2022). https://doi.org/10.1016/J.IJSOLSTR.2021.111386
39. Jain, A.: Micro and mesomechanics of fibre reinforced composites using mean field homogenization formulations: A review. Mater Today Commun. 21, 100552 (2019). https://doi.org/10.1016/J.MTCOMM.2019.100552

40. Ahmed Elmasry, Wiyao Azoti, Sherif A. El-Safty, Ahmed Elmarakbi: A comparative review of multiscale models for effective properties of nano- and micro-composites - ScienceDirect, https://www.sciencedirect.com/science/article/pii/S0079642522001037

41. Elmasry, A., Azoti, W., Elmarakbi, M., Elmarakbi, A.: Interaction modelling of the thermomechanical behaviour of spatially-oriented graphene platelets (GPLs) reinforced polymer matrix. Int J Solids Struct. 232, 111183 (2021). https://doi.org/10.1016/J.IJSOLSTR.2021.111183

42. Jiang, B., Liu, C., Zhang, C., Wang, B., Wang, Z.: The effect of non-symmetric distribution of fiber orientation and aspect ratio on elastic properties of composites. Compos B Eng. 38, 24–34 (2007). https://doi.org/10.1016/J.COMPOSITESB.2006.05.002

43. Cherkaoui, M., Muller, D., Sabar, H., Berveiller, M.: Thermoelastic behavior of composites with coated reinforcements: a micromechanical approach and applications. Comput Mater Sci. 5, 45–52 (1996). https://doi.org/10.1016/0927-0256(95)00057-7

44. Hill, R.: Elastic properties of reinforced solids: Some theoretical principles. J Mech Phys Solids. 11, 357–372 (1963). https://doi.org/10.1016/0022-5096(63)90036-X

45. Karima Ahaouari: Contribution à la modélisation de la thermoélasticité et de l'acoustoélasticité des matériaux microhétérogènes. Université Paul Verlaine - Metz. France. (1990)

46. Ahaouari, K., Corvasce, F., Lipinski, P., Berveiller, M.: - Détermination des propriétés thermomécaniques des composites à matrice métallique. Revue de Métallurgie. 87, 73–84 (1990)

47. Kpobie, W., Ben Khlifa, S., Bonfoh, N., Fendler, M., Lipinski, P.: Multi-site micromechanical modelling of thermo-elastic properties of heterogeneous materials. Compos Struct. 94, 2068–2077 (2012). https://doi.org/10.1016/J.COMPSTRUCT.2012.01.014

48. Doghri, I., Ouaar, A.: Homogenization of two-phase elasto-plastic composite materials and structures: Study of tangent operators, cyclic plasticity and numerical algorithms. Int J Solids Struct. 40, 1681–1712 (2003). https://doi.org/10.1016/S0020-7683(03)00013-1

49. Torquato, S.: Effective stiffness tensor of composite media—I. Exact series expansions. J Mech Phys Solids. 45, 1421–1448 (1997). https://doi.org/10.1016/S0022-5096(97)00019-7

50. Torquato, S., A., Haslach, , H., Jr,: Random Heterogeneous Materials: Microstructure and Macroscopic Properties. ASME. Appl. Mech. Rev. . 55(4): B62–B63., (2002)